

**Application of hydrogel for plant cultivation in
contaminated soil**

(汚染土壌における植物栽培へのハイドロゲルの応用)

2024年3月

広島大学大学院工学研究科

HUANG JIN

**Application of Hydrogel for plant cultivation in
contaminated soil**

(汚染土壌における植物栽培へのハイドロゲルの応用)

HUANG JIN

In partial fulfillment of the requirements for the degree of
Doctor of Engineering

Hiroshima University Graduate School of Engineering
1-4-1 Kagamiyama Higashihiroshima Hiroshima 739-8527
Japan

March 2024

Abstract

In the current society, due to the rapid advancement of agriculture and industry, the excessive buildup of heavy metal ions, particularly cadmium, in the soil poses a severe threat to plant growth environments. The highly toxic nature of cadmium heavy metal negatively impacts plant absorption and growth, with potential repercussions on human health through the food chain. Consequently, effectively tackling the issue of cadmium ion pollution in soil has become an urgent concern within the environmental science field.

We successfully synthesized DMAPAA (N-(3- (Dimethyl amino) propyl) acrylamide)/DMAPAAQ (N, N-Dimethyl amino propyl acrylamide, methyl chloride quaternary) hydrogels via free radical polymerization and assessed their capacity to capture cadmium under various cadmium ion concentrations and pH values using inductively coupled plasma emission spectroscopy (ICP). Findings reveal that under pH 7.3 conditions, DMAPAA/DMAPAAQ hydrogels demonstrate optimal cadmium capture performance, fitting well with the Langmuir model. The application of this hydrogel fosters vegetable growth in cadmium stress conditions, particularly at a 4% hydrogel addition, resulting in the highest dry weight of vegetables. Overall, the successfully synthesized hydrogel proves effective in immobilizing cadmium ions in soil, positively influencing vegetable growth and yield, and offering practical significance in mitigating heavy metal ion pollution.

The noteworthy promotional effect exhibited by DMAPAA/DMAPAAQ hydrogels has had an exceedingly positive impact on vegetable growth. Its internal tertiary amine protonation characteristics in aqueous solutions, along with the formation of hydroxyl (OH⁻) characteristics on the surface, efficiently encapsulate cadmium ions internally, resulting in insoluble cadmium hydroxide precipitates. This mechanism successfully alleviates cadmium pollution in the soil, providing a cleaner and more favorable growth environment for vegetables. In our study, we applied two distinct types of hydrogels, DMAPAA/DMAPAAQ ion-type hydrogel and DMAA (N, N-Dimethylacrylamide) non-ion-type hydrogel, for vegetable cultivation in uncontaminated soil. DMAPAAQ promotes nitrate ion adsorption through ion exchange mechanisms, releasing nitrate ions for plant absorption. This combined effect not only further enhances the hydrogel's ability

to alleviate soil cadmium pollution but also supplies necessary nutrient support for plants. Conversely, the promoting effect of DMAA non-ion-type hydrogel on vegetables is relatively limited, underscoring the critical role of hydrogel composition in its interaction with plants under cadmium stress conditions.

Finally, we successfully synthesized potassium polyacrylate (KMAA) hydrogel through free radical polymerization to address high concentrations of sodium ions in industrial wastewater and saline-alkali soil. Experimental results demonstrate that KMAA hydrogel exhibits outstanding performance in removing sodium ions from aqueous solutions and providing potassium ions. At pH 7, the maximum adsorption capacity of sodium ions reaches 70.7 mg/g, while at pH 4, the maximum exchange capacity for potassium ions is 243.7 mg/g. This successfully synthesized hydrogel provides valuable practical insights for addressing high sodium ion concentrations in water sources and promoting potassium fertilizer supply. In summary, the three hydrogels studied in this research present feasible technical solutions for addressing heavy metal and ion pollution in different environments.

Table of Contents

Abstract.....	I
Chapter 1 Introduction	1
1.1 Current Situation of Heavy Metal Pollution	1
1.2 Causes of Heavy Metal Pollution in Soil	3
1.3 Methods for Remediation of Heavy Metal Contaminated Soil.....	4
1.31 Physical remediation.....	4
1.32 Chemical remediation.....	5
1.33 Biological remediation	6
1.4 Soil Heavy Metal Pollution Remediation Materials	7
1.41 Carbon-based materials	7
1.42 Mineral materials.....	8
1.43 Metal oxide materials	8
1.44 Resin materials	9
1.5 Adsorption Model	10
1.51 Langmuir isothermal adsorption.....	10
1.52 Freundlich isothermal adsorption	10
1.53 The first-order adsorption Kinetics.....	11
1.54 The second-order adsorption kinetic	11
1.55 Adsorption thermodynamics.....	12
1.6 Types of Hydrogels	13
1.61 Natural polymer hydrogels	13
1.62 Synthetic polymer hydrogels.....	14
1.7 Synthesis Methods of Hydrogels	14
1.71 Physical synthesis method.....	14
1.72 Chemical synthesis method	15
1.8 Hydrogel Functional Groups.....	16
1.81 Nitrogen-containing functional groups.....	16
1.82 Oxygen-containing functional groups	17
1.83 Sulfur-containing functional groups.....	19
1.84 Phosphorus-containing functional groups	19
1.85 Other functional groups	20
1.9 The Adsorption Mechanism of Superabsorbent Hydrogels	21

References.....	22
Chapter 2 Dual benefits of hydrogel remediation of cadmium-contaminated water or soil and promotion of vegetable growth under cadmium Stress.....	33
2.1 Introduction	33
2.2 Experimental Methods	35
2.21 materials.....	35
2.22 synthesis of hydrogel	35
2.3 Swelling Properties of Hydrogels	36
2.31 Swelling degree of hydrogel in water solutions	36
2.32 Soil water holding rate.....	36
2.4 Adsorption Experiment	37
2.41 Adsorption thermodynamic experiments with different pH values.....	37
2.42 pH effect experiment	37
2.43 Adsorption kinetic experiment	38
2.44 Adsorption thermodynamics at different temperatures	38
2.5 Vegetable Planting Experiment.....	38
2.51 Experimental design	38
2.52 Dry weight of swiss chard	39
2.53 Plant digestion	39
2.54 Characterization.....	39
2.6 Result.....	40
2.61 Swelling degree of hydrogel.....	40
2.62 Effect of pH on gel adsorption	41
2.63 Isothermal adsorption	42
2.64 Adsorption kinetics.....	44
2.65 Adsorption kinetics.....	45
2.66 Characterization of hydrogel structure	46
2.67 Physical picture of vegetable growth.....	47
2.68 Shoot dry Weight.....	48
2.69 Cadmium uptake in swiss chard	49
2.7 Other Elements	50
2.8 Discussion	53
2.9 Conclusion.....	54

References.....	55
Chapter 3 Functional hydrogel promotes vegetable growth in cadmium-contaminated soil.	61
3.1 Introduction	61
3.2 Materials and Methods	64
3.21 materials.....	64
3.22 Synthesis of DMAPAA/DMAPAAQ hydrogel.....	64
3.23 Synthesis of DMAA hydrogel	65
3.24. Experimental design	66
3.25 Dry weight of vegetables.....	66
3.26 Plant digestion	67
3.27 Experiment on cadmium precipitation from soil.....	67
3.28 Characterization.....	67
3.3 Result and Discussion	68
3.31 Detection of elements in soils.....	68
3.32 Soil pH.....	69
3.33 Cadmium precipitation experiments in soils.	69
3.34 Growth state of vegetable under cadmium stress	70
3.35 vegetables growth status under two types of hydrogels	71
3.36 Cadmium element in vegetable	72
3.37 vegetable uptake of elements.....	73
3.38. Dry weight of vegetable	76
3.39. Hydrogel repair cadmium soil mechanism.....	76
3.4 Conclusions	78
Reference	79
Chapter 4 A novel composite hydrogel material for sodium removal and potassium provision	83
4.1Introduction	83
4.2 Experimental Methods	85
4.21 materials.....	85
4.22 Synthesis of hydrogel	86
4.3 Swelling Properties of Hydrogels	87
4.31 Swelling degree of hydrogel in sodium chloride solution.....	87

4.32 Soil water holding rate.....	87
4.4. Adsorption Experiment	87
4.41 Adsorption thermodynamic experiments with different pH values.....	87
4.42 pH effect experiment	88
4.43 Adsorption kinetic experiment	88
4.44 Adsorption thermodynamics at different temperatures	88
4.45 Adsorbent dosage experiment	89
4.5 Soil Experiment.....	89
4.51 Preparation of soil containing NaCl	89
4.52 pH value affects the precipitation of sodium and potassium ions in soil.	89
4.53 Amount of hydrogel affects precipitation of sodium and potassium ions in soil	90
4.6 Result and Discussion	90
4.61 Swelling degree of hydrogel.....	90
4.62 pH affects the adsorption of the gel.....	91
4.63 Isothermal adsorption	92
4.64 Adsorption thermodynamic	95
4.65 Adsorption kinetics.....	98
4.66 The effect of hydrogel dosage	100
4.7 Hydrogel Applied Soil Experiments.	101
4.71 Soil precipitation liquid experiment	101
4.72. Effect of different gel amounts on precipitate.	102
4.8 Structural Characteristics of Hydrogel.....	103
4.9 Mechanism of KMAA Hydrogel Adsorbing Sodium and Exchanging Potassium	104
4.10 Conclusions	105
Reference	105
Chapter 5 Conclusion.....	109
List of publications	111
List of Figures	112
List of Tables	115
Acknowledgments.....	116

Chapter 1 Introduction

1.1 Current Situation of Heavy Metal Pollution

As global industrialization continues to progress, the severity of soil pollution, encompassing heavy metal contamination and soil salinization, has escalated. These changes exert a detrimental impact on the human living environment [1]. Cadmium (Cd), a non-essential and toxic heavy metal element for animals and plants, naturally occurs in ores, often coexisting with zinc, lead, and other minerals. The cadmium content in the Earth's crust is approximately 18 milligrams per kilogram, while the fluctuation in soil ranges from 0.01 to 0.7. In China, the presence of heavy metal elements such as cadmium (Cd), mercury (Hg), arsenic (As), lead (Pb), chromium (Cr), and copper (Cu) in soil has garnered significant attention, as indicated in Table 1 for their threshold values [2]. Exceeding these thresholds may pose potential hazards to agricultural production and human health [3].

Table 1.1 Agricultural land soil pollution risk screening

number	Pollutant Project		risk screening value			
			$\text{pH} \leq 5.5$	$5.5 < \text{pH} \leq 6.5$	$6.5 < \text{pH} \leq 7.5$	$\text{pH} \geq 7.5$
1	Cd	paddy	0.3	0.4	0.6	0.8
		others	0.3	0.3	0.3	0.6
2	Hg	paddy	0.5	0.5	0.6	1.0
		others	1.3	1.8	2.4	3.4
3	As	paddy	30	30	25	20
		others	40	40	30	25
4	Pb	paddy	80	100	140	240
		others	70	90	120	170
5	Cr	paddy	250	250	300	350
		others	150	150	200	250
6	Cu	orchard	150	150	200	200
		others	50	50	100	100
7	Ni		60	70	100	190
8	Zn		200	200	250	300

Table 2 provides a detailed description of heavy metal pollution in key Chinese cities, such as Beijing, Guangzhou, and Hainan. Other city heavy metal pollution in China sees Figure 1.1. In these urban centers, the problem of heavy metal pollution is

notably severe, exerting considerable repercussions on the environment and human health, demanding careful consideration.

Table 1.2 Heavy metal pollution in China(mg·kg⁻¹)

agricultural soil	Place	As	Pb	Cd	Zn	Cr	Ni	Cu	Hg	Reference
	Beijing	-	18.48	0.18	81.10	75.74	-	28.05	-	[4]
	Guangzhou	4.5	60.4	0.16	146.3	-	-	17.5	0.45	[5]
	Yangzhou	10.2	35.70	0.30	98.10	77.20	38.50	33.90	0.20	[6]
	Wuxi	14.3	46.7	0.14	112.9	58.6	-	40.4	0.16	[7]
	Gansu	11.5	31.4	-	-	12.8	-	16.4	0.02	[8]
	Tai hang	6.16	18.80	0.15	69.96	57.77	25.04	21.22	0.08	[9]
	Zhengzhou	6.69	17.11	0.12	-	60.67	-	-	0.08	[10]
	Kunshan	12.0	28.63	0.16	98.57	67.41	35.83	26.0	0.21	[11]
	Xuzhou	11.11	21.68	0.59	74.34	61.64	-	27.34	0.06	[12]
	Shanghai	7.47	23.8	0.11	-	41	-	28.3	0.13	[13]
Hainan	5.64	21.28	0.06	40.93	47.96	8.67	14.89	0.05	[14]	

Table 3 comprehensively outlines the state of heavy metal pollution in several countries globally, encompassing nations such as India and South Korea in Asia, the United States and Canada in North America, and the United Kingdom and Poland in Europe. This demonstrates that heavy metal pollution has deeply permeated every corner of the world, becoming a global environmental challenge.

Table 1.3 Mean concentrations of major heavy metals in road dust of all over the world (mg·kg⁻¹)

	Pb	Zn	Cu	Ni	Cd	Cr	reference
Delhi, India	1899	370.5	1016	-	19.35	-	[15]
Shiraz, Iran	36.8	160.9	49.81	39.4	0.31	31.6	[16]
Ulsan, Korea	117.55	226.85	135.85	23.2	2.35	-	[17]
Paris, France	1450	840	1075	25	1.7	50	[18]
Aviles, Northern	514	4892	-	-	22.3	-	[19]
Birmingham, UK	48	534	466.9	411	1.62	-	[20]
Oslo, Norway	180	412	123	41	1.4	-	[21]
Lublin, E Poland	44.1	241.1	81.6	16.5	5.1	86.4	[22]
Delta, Egypt	308	1840	102	38.5	2.98	85.7	[23]
Benin city, Nigeria	189	-	21.525	22.125	5.775	61.52	[24]
Ottawa, Canada	39.05	112.5	65.84	15.2	0.37	43.3	[25]
Bogota, Colombia	29.2	152	32.4	8.23	0.25	20.7	[26]

Due to the ongoing increase in industrial and agricultural activities, a significant release of heavy metal elements into the soil surpasses the natural environment resilience, giving rise to a global environmental issue. These heavy metals present potential risks to both plant growth and human health, entering the human body through the food chain [27]. Conversely, alkali soil pollution primarily results from improper fertilizer use, causing the excessive accumulation of salts and heavy metals in the soil, hindering normal crop growth. As the global population expands rapidly, soil, being essential for human survival, is paramount. Widespread soil salinization and heavy metal contamination threaten the cultivability of land, ultimately endangering humanity itself. In various regions, soil heavy metal and alkali soil pollution have become urgent environmental problems, demanding prompt, and effective measures to control and restore affected land, ensuring environmental protection and preserving human health [28].

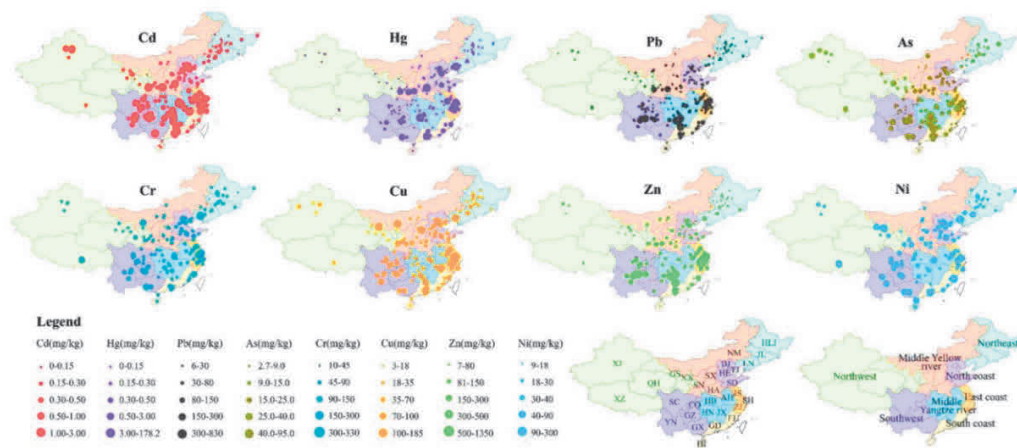


Figure 1.1 Distribution data map of heavy metal content in agricultural soil in China [29].

1.2 Causes of Heavy Metal Pollution in Soil

During industrial production, various activities release wastewater containing heavy metals. Elements like mercury, cadmium, and lead are inherent in coal and oil. When these fossil fuels undergo combustion, these heavy metals are emitted into the atmosphere and subsequently deposited in soil and water through particles in the exhaust gas [30]. Additionally, fertilizers and pesticides used in agriculture may carry certain heavy metal

elements. These substances can leach into the soil during application, eventually finding their way into water bodies or crops [31]. Landfills may contain waste materials with heavy metals, and as these materials decompose or leach, heavy metals can be released into the soil and water [32]. The extraction and smelting processes of ores may discharge a substantial amount of heavy metal pollutants, infiltrating the surrounding soil and water bodies. Medical waste may also contain heavy metal substances, and improper handling can lead to heavy metal pollution [33]. Acid rain contributes to soil acidification, facilitating the transformation of heavy metals from insoluble forms to soluble forms, making it easier for them to enter water bodies and organisms. Due to the adverse effects of heavy metal pollution on the environment and human health, it is imperative to implement measures to reduce the emission of heavy metals and enhance the regulation and control of heavy metal pollution [34].

1.3 Methods for Remediation of Heavy Metal Contaminated Soil

1.31 Physical remediation

At present, the remediation of contaminated soil predominantly relies on physical methods (see Figure 1.2). These approaches encompass soil replacement, soil amendment, deep ploughing, thermal desorption, and electrochemical remediation. The primary aim of these techniques is to diminish or eradicate pollutants in the soil, lowering their concentrations to safe levels. This restoration process is crucial for reinstating the ecological functions of the soil and establishing a secure soil environment [35, 36]. Soil replacement involves substituting the contaminated soil with clean soil, swiftly reducing harmful substance levels, and enhancing soil quality. Soil amendment introduces treated high-quality soil, mixed with the contaminated soil, thereby boosting soil fertility, and improving its structure. Deep ploughing entails thorough tilling to intermingle the contaminated soil layer with clean soil, dispersing and degrading harmful substances. Thermal desorption employs elevated temperatures to eliminate volatile organic compounds, mitigating their environmental impact. Electrochemical remediation utilizes electrochemical reactions to eliminate or diminish pollutants in the soil, ensuring the health of the soil ecosystem. These physical methods share the common objective of

reducing pollutant concentrations to safe levels or minimizing contact between pollutants and plant roots, thereby safeguarding the health of the soil ecosystem.

1.32 Chemical remediation

Chemical remediation methods aim to address heavy metal pollutants in soil by utilizing chemical reactions to reduce, stabilize, or eliminate them. Various additives, surfactants, and metal chelating agents are commonly employed in soil remediation. Phosphates, lime, and silicates are widely recognized substances for treating soil cadmium contamination. The incorporation of phosphates facilitates the formation of insoluble cadmium phosphate precipitates, diminishing the bioavailability of cadmium [37]. Lime, alternatively, adjusts soil pH, influencing the solubility and adsorption of cadmium, thus mitigating its toxic effects on plants [38]. Additionally, the introduction of silicates can react with cadmium, forming insoluble silicates that restrict the migration of cadmium [39]. Other frequently used amendments, such as steel slag and furnace slag, have found application in soil remediation. These substances not only enhance soil structure and foster plant growth but also exhibit adsorption and precipitation effects on heavy metals like cadmium, contributing to the improvement of environmental quality in contaminated soils [40]. This integrated approach, incorporating various chemical substances, provides a diverse array of options for remediating heavy metal-contaminated soil, effectively reducing pollution levels, and safeguarding the health of soil ecosystems.

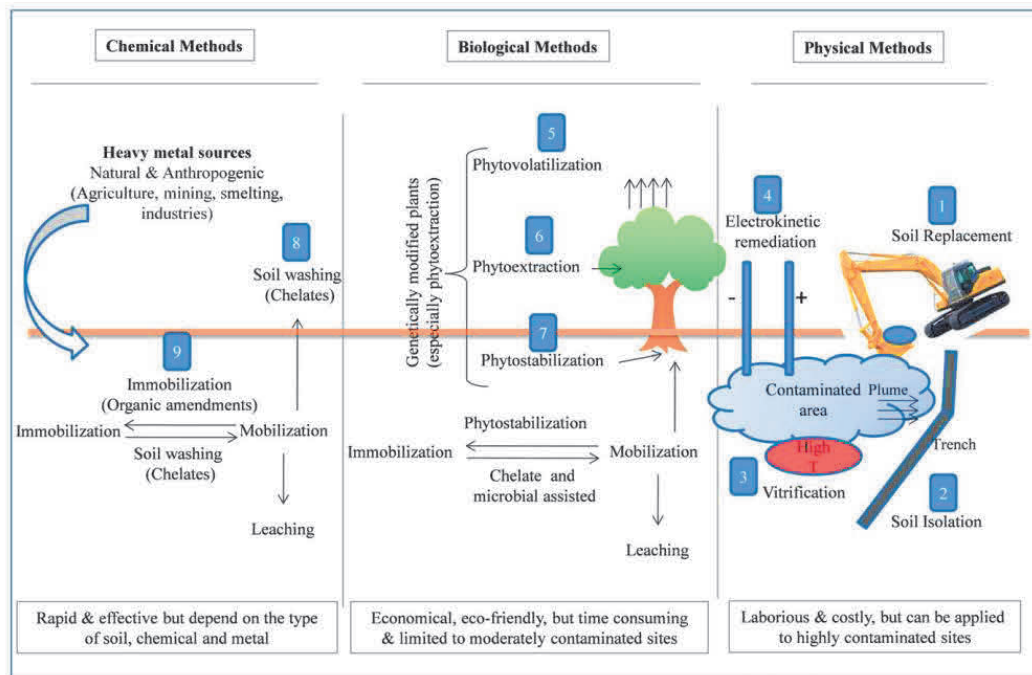


Figure 1.2. Comparison of different heavy metal contaminated soil remediation methods. Soil remediation methods can be broadly divided into three categories: physical, chemical, and biological [36].

1.33 Biological remediation

Biological remediation, a soil purification method, revolves around specific animals, plants, and microorganisms that either absorb or degrade pollutants in the soil (see Figure 1.3). It is primarily categorized into two types: phytoremediation and microbial remediation. Phytoremediation employs hyperaccumulating plants to absorb heavy metals from the soil, accumulating pollutants within the plant through its biological mechanisms. Subsequently, these plants are harvested to concentrate and reduce pollutants in the soil. On the other hand, microorganisms establish chemical bonds or electrostatic interactions with heavy metals via their surface-charged functional groups, facilitating the adsorption of heavy metal ions. Furthermore, certain microorganisms can absorb heavy metals into their cells, while others can secrete specific organic substances to form insoluble precipitates with heavy metals, thereby reducing their migration in the soil [41]. Microbial remediation is relatively gentle during the restoration process, aiding

in maintaining the stability of the soil ecosystem and providing a sustainable option for soil remediation. Therefore, the comprehensive application of phytoremediation and microbial remediation technologies can more effectively and comprehensively address various types of soil pollution [42,43].

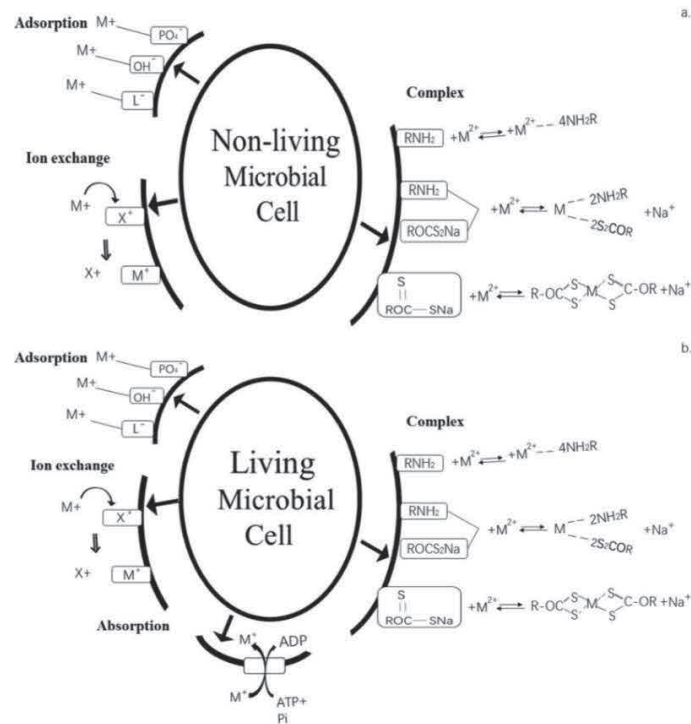


Figure 1.3 Diagram of the adsorption mechanism of microorganisms [44].

1.4 Soil Heavy Metal Pollution Remediation Materials

1.4.1 Carbon-based materials

Carbon-based materials, such as activated carbon, carbon nanotubes, and graphene, exhibit significant potential for broad application in addressing heavy metal pollution, owing to their outstanding adsorption performance. Activated carbon, known for its porous structure, surface area, and functional groups, efficiently adsorbs various heavy metal ions in water bodies. Carbon nanotubes, with their one-dimensional structure and high conductivity, demonstrate highly selective properties in electrochemical sensors and wastewater treatment [45]. When functionalized, graphene can efficiently adsorb specific heavy metals based on its two-dimensional structure, conductivity, and large surface area

[46]. Guo et al. successfully adsorbed Cd (II) and Cu (II) using a magnetic graphene oxide adsorbent [47]. Zhao et al. effectively extracted Pb^{2+} using a TiO_2 and CNT hybrid adsorbent, demonstrating efficient metal adsorption with capacities of 137 mg/g and 78.74 mg/g, respectively [48]. The successful application of these materials in environmental remediation, water treatment, and resource recovery offers sustainable solutions to global heavy metal pollution. Future research should prioritize the engineering optimization and environmental adaptability of these materials to facilitate their widespread use in practical applications.

1.42 Mineral materials

Natural minerals like zeolite and clay have proven to be excellent adsorbents for heavy metals, thanks to their abundant surface functional groups, large specific surface area, and porous structure. Zeolite, a crystalline aluminosilicate, possesses notable ion exchange properties, a high surface area, and hydrophilicity, making it well-suited for extracting heavy metals from wastewater [49]. Rad et al. synthesized NaX nano zeolite through microwave heating and prepared polyvinyl acetate/NaX nanocomposite fibers to explore their potential for Cd^{2+} adsorption. They discovered that the maximum adsorption capacity was 838.7 mg/g at the optimum pH of 5.0, achieving an 80% removal rate [50]. Additionally, Jiang et al. investigated the adsorption efficiency of kaolin clay on Pb^{2+} , Cd^{2+} , Ni^{2+} and Cu^{2+} in wastewater, demonstrating rapid metal absorption with the maximum adsorption achieved within 30 minutes. They successfully reduced the Pb^{2+} concentration in real wastewater from 160.00 mg/L to 8.00 mg/L [51]. These natural adsorbents not only have diverse sources but also exhibit good renderability, offering support for sustainable resource utilization and environmental protection.

1.43 Metal oxide materials

Metal materials play a crucial role in environmental management and water treatment, particularly those with unique surface properties like iron oxide, copper oxide, and zinc oxide, widely utilized for the removal of heavy metal ions from water sources [52]. LI et al. achieved a remarkable removal rate of 98.5% for cadmium ions using

calcined iron oxide nanoparticles. The study identified -OH, -COOH, and FeOH sites in the synthesized iron oxide nanoparticles as the primary adsorption sites for cadmium ions [53]. On the other hand, Sharma et al. successfully synthesized mesoporous ZnO and TiO₂@ZnO materials using nano casting techniques, enhancing the adsorption capacity for Cd²⁺ ions from 643 to 786 mg/g. This notable improvement was attributed to the effective increase in the surface area of ZnO by TiO₂[54]. The functional groups and active sites on the surface of these metal materials can form robust coordination bonds with heavy metals, enabling efficient adsorption. They can be conveniently and effectively applied in wastewater treatment and environmental remediation, offering practical and viable solutions for addressing heavy metal pollution.

1.44 Resin materials

Ion exchange resins play a crucial role in water treatment and wastewater management, enhancing their adsorption capacity for heavy metals through surface functionalization. These resins find widespread applications in wastewater treatment, drinking water purification, and mining wastewater treatment. Researchers, Roy P K et al. have successfully synthesized chelating resins using polystyrene-divinylbenzene as raw materials. The adsorption capacities for Cu²⁺, Ni²⁺, Fe²⁺ and Pb²⁺ were measured at 0.55 mmol/g, 0.63 mmol/g, 0.52 mmol/g, and 0.11 mmol/g, respectively, with removal rates of 98.5%, 96.3%, 97.5%, and 98.65% [55]. On the other hand, Singh A K et al. achieved successful adsorption of Zn²⁺, Cd²⁺, Pb²⁺ and Ni²⁺ using resins containing oxygen and sulfur functional groups, with recovery rates exceeding 97% and the ability to be reused [56]. Future research will focus on modifying and optimizing biomass materials to enhance their adsorption performance and provide practical solutions to global heavy metal pollution.

1.5 Adsorption Model

1.51 Langmuir isothermal adsorption

The Langmuir isothermal equilibrium adsorption equation (see Figure 1.4) is used to describe the process of hydrogel adsorbing heavy metal ions at a specific temperature. It is typically expressed as follows:

$$q_e = \frac{q_{max}K_L C_e}{1 + K_L C_e}$$

The parameter q_e represents the adsorption capacity of the unit mass of hydrogel (mg/g). q_{max} denotes the maximum adsorption capacity according to the Langmuir isotherm, indicating the highest adsorption capacity per unit mass of hydrogel when all adsorption sites are fully occupied (mg/g). K_L is the Langmuir constant, reflecting the binding ability of adsorption. C_e is the concentration of heavy metal ions in the solution at equilibrium (mmol/L). The Langmuir isotherm equilibrium adsorption equation assumes that the adsorption process occurs on single-layered molecules at adsorption sites and that adsorption is reversible. This equation is derived under ideal conditions, assume all adsorption sites have equal affinity, and there is no interaction between adsorbates. The Langmuir isotherm equilibrium adsorption equation is commonly employed to fit data and obtain the Langmuir equilibrium constant, as well as the maximum adsorption capacity [57].

1.52 Freundlich isothermal adsorption

The Freundlich isotherm equation posits that adsorption takes place on the uneven surface of the adsorbent, and the extent of adsorption correlates with the concentration of the pollutant. With an escalating pollutant concentration, the adsorption capacity of the adsorbent tends to increase indefinitely. In this model, each adsorption site features distinct binding energies and affinities, displaying the characteristics of multilayer adsorption. The Freundlich isotherm equation is expressed as follows:

$$q_e = K_F C_e^{1/n}$$

In the equation, K_F and n are constants associated with the adsorption capacity and adsorption strength, respectively. Generally, a $1/n$ value between 0.1 and 0.5 signifies a favorable adsorption process. A larger $1/n$ value indicates poorer adsorption performance, whereas a smaller value suggests better adsorption performance. For more information, please consult reference [58].

1.53 The first-order adsorption Kinetics

First-order adsorption kinetics is typically used to describe the change in adsorption amount over time during the adsorption process. The adsorption expression is as follows:

$$q_t = q_e(1 - e^{-k_1 t})$$

In this context, q_t signifies the adsorption capacity at time t , q_e denotes the maximum adsorption capacity at equilibrium, and k_1 represents the first-order adsorption kinetic constant. The first-order kinetic model posits that the rate of adsorption is proportional to the number of available adsorption sites on the adsorption surface. This model facilitates comprehension of the kinetic behavior during the adsorption process and enables a more precise prediction of the adsorption process by fitting k_1 and q_e through experimental data. For additional details, please refer to reference [59].

1.54 The second-order adsorption kinetic

Secondary adsorption kinetics is a model that describes the change in adsorption amount over time during the adsorption process. Its kinetic equation can be expressed as follows:

$$q_t = \frac{K_2 q_e^2 t}{1 + K_2 q_e t}$$

In this context, q_e represents the adsorption capacity at adsorption equilibrium, q_t signifies the maximum adsorption capacity at time t , and k_2 is the second-order adsorption kinetic constant. In comparison to the first-order kinetic model, the second-order adsorption kinetic model is more intricate as it comprehensively considers the saturation of adsorption sites and molecular interactions during the adsorption process.

The first-order kinetic model typically overlooks the possibility of multilayer adsorption or interactions between adsorption sites in the actual adsorption system. For more details, please refer to references [60, 61].

1.55 Adsorption thermodynamics

The VantHoff equation describes the relationship between the thermodynamic equilibrium of adsorption. This equation is expressed as:

$$\ln \frac{1}{C_e} = \ln k_d - \frac{\Delta H^\theta}{RT}$$

In this equation, C_e represents the concentration of the solution at equilibrium, ΔH^θ denotes the standard enthalpy change, T represents the temperature, and k_d is the constant of the van Hoff equation. By plotting $\ln(1/C_e)$ against T and fitting the equation, the enthalpy change ΔH^θ can be calculated. The change in Gibbs free energy ΔG^θ under standard conditions can be represented by the following formula:

$$\Delta G^\theta = -RT \ln K_d$$

In the equation, ΔG^θ represents the Gibbs free energy change under standard conditions, R is the gas constant 8.314 J/(mol·k), T represents temperature, and K_d represents the thermodynamic equilibrium constant for adsorption. This equation elucidates the thermodynamic characteristics of the adsorption process, with the negative sign indicating that the adsorption process is spontaneous under standard conditions. The relationship between the Gibbs free energy change ΔG^θ , enthalpy change ΔH^θ , and entropy change ΔS^θ is expressed as follows:

$$\Delta G^\theta = \Delta H^\theta - T\Delta S^\theta$$

The equation for calculating ΔS^θ can be derived using the formula. This relationship delineates the connection between the change in Gibbs free energy, enthalpy, and entropy under standard temperature and pressure conditions. This equation holds significant importance in comprehending and optimizing the thermodynamic properties of diverse chemical and physical systems [62].

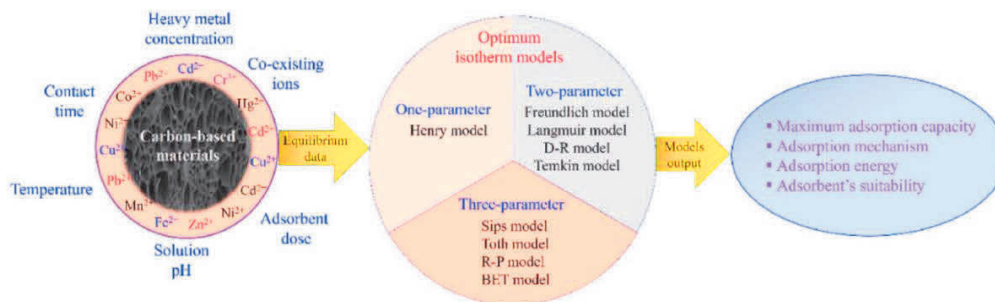


Figure 1.4 Different types of adsorption isotherm models [63].

1.6 Types of Hydrogels

1.6.1 Natural polymer hydrogels

Natural polymer hydrogels find widespread applications in industries such as agriculture, food, healthcare, and environmental purification, thanks to their exceptional adsorption properties. They are particularly favored for wastewater treatment, environmental purification, and addressing heavy metal pollution. These hydrogels predominantly consist of natural polymers or biopolymers, including chitosan-based hydrogels, starch-based hydrogels, cellulose-based hydrogels, and sodium alginate hydrogels. Chitosan-based hydrogels, with chitosan as the primary component, are modified to form a highly porous structure, imparting excellent adsorption capabilities [64]. Conversely, starch-based hydrogels are processed to enhance their adsorption properties, making them suitable for removing heavy metals in various environments [65]. Additionally, Soon Hong Yuk et al. reported a biodegradable superabsorbent polymer that can be decomposed by microorganisms in natural soil. However, once sodium alginate hydrogels degrade, acrylic acid cannot be completely biodegraded [66]. Furthermore, Li et al. synthesized carboxymethyl cellulose/polyethyleneimine hydrogels using a simple one-step method, exhibiting highly efficient adsorption capacity for Cr under slightly acidic conditions [67].

1.62 Synthetic polymer hydrogels

Synthetic polymer hydrogels, as artificially synthesized materials, exhibit outstanding adsorption properties in the treatment of heavy metal pollution. Comprising polymers or inorganic materials such as polyacrylic acid and polyacrylamide, these hydrogels contain common hydrophilic functional groups like -COOH that contribute to their affinity for water molecules. Non-ionic hydrophilic functional groups present in the resin, such as -OH, -C-O-C-, and -NH₂, enable them to maintain excellent adsorption performance even in high salt environments [68]. In a study by Kasgoz et al., amine-functionalized, and sulfonated polyacrylamide hydrogels were examined, revealing that amine-functionalization enhanced selectivity for Cu (II) adsorption rate of 68.5%, while sulfonation exhibited good selectivity for Pb (II) adsorption rate of 78.2% [69]. Furthermore, Chibowski et al. discussed the adsorption mechanisms of PAMs on the surfaces of montmorillonite and kaolinite for Cr (VI) or Pb (II), emphasizing the crucial influence of the internal structure and interlayer spacing of layered aluminosilicates on the adsorption capacity. Montmorillonite demonstrated a higher adsorption ability [70].

1.7 Synthesis Methods of Hydrogels

1.71 Physical synthesis method

Physical crosslinking is a gelation method achieved through non-covalent interactions between molecules, including hydrogen bonding, van der Waals forces, and physical entanglement mechanisms (see the Figure1.5). These interactions facilitate the formation of crosslinks between polymer chains, constructing a spatial network structure that imparts unique properties to the material. Hydrogen bonding, a potent force, occurs through attractive interactions between hydrogen atoms and electronegative oxygen, nitrogen, or fluorine atoms. Van der Waals forces, conversely, are attractive forces resulting from the momentary polarization between molecules, while physical entanglement involves the intertwining of polymer chains, enhancing the material's mechanical stability. The advantage of physical crosslinking lies in its relatively mild preparation process, without the need for introducing chemical crosslinking agents [71]. In a study by Yang et al., a hydrophobic hydrogel was successfully synthesized with

hydrophobic methacrylic acid and hydrophilic N-hydroxyethyl acrylamide as monomers using a solution crosslinking method. Although this hydrogel exhibited excellent performance with a fracture stress of 700 kPa, its gel strength was relatively low. This research outcome provides valuable insights for optimizing the performance of physically crosslinked hydrogels [72].

1.72 Chemical synthesis method

Chemical crosslinking involves introducing crosslinking agents or facilitating chemical reactions to form covalent bonds, resulting in a more stable gel structure, and showcasing superior performance compared to physical crosslinking. Copolymerization crosslinking, a common method, enables gel formation through crosslinking agents in the presence of one or more monomers, providing high tunability to the material [73, 74]. Water-soluble polymer crosslinking is a significant research direction, particularly utilizing water-soluble polymers like polyacrylamide and polyvinyl alcohol to create hydrogels under radiation, widely applied in the biomedical field. Graft copolymerization introduces new side chains onto polymer chains via initiators or photoirradiation, modifying the material's surface properties and performance, with broad applications. In a study by Walaiporn et al. a polyacrylamide/poly pyrrole hydrogel was prepared using N, N'-methylenebisacrylamide as a crosslinking agent through free radical polymerization. The study investigated the effect of polypyrene content on the loading and sustained release properties of salicylic acid. By adjusting monomers, crosslinking agents, and initiators, hydrogels with diverse properties can be prepared to meet the requirements of various fields [75].

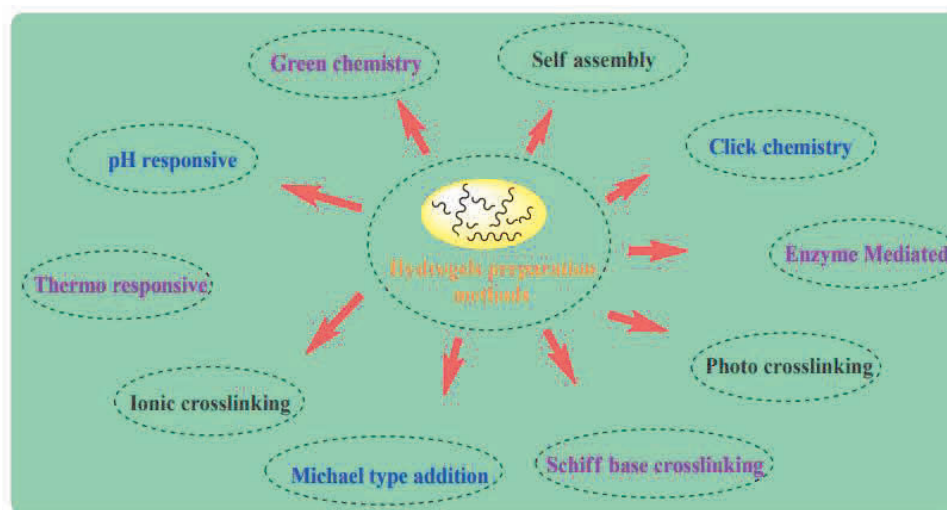


Figure 1.5. Different methods for synthesizing hydrogels [76].

1.8 Hydrogel Functional Groups

1.8.1 Nitrogen-containing functional groups

Nitrogen-containing functional groups are structural units in organic compounds that incorporate nitrogen atoms, including amino groups, amide groups, and quaternary ammonium groups [77]. Amino groups are fundamental components of biomolecules, commonly found in amino acids and basic compounds, participating in biological processes through the formation of amino acid chains and protein structures. Amide groups, composed of an acyl group and an amino group, play a crucial role in proteins and peptides, influencing their structure and function. The stability of amide bonds is an important structural element in protein main chains, directly affecting the folding and stability of biomacromolecules. Quaternary ammonium groups, with a positive charge, exhibit outstanding performance in heavy metal adsorption, as they can interact with negatively charged heavy metal ions, enabling efficient adsorption and fixation. This offers broad application prospects in wastewater treatment, environmental protection, and resource recovery. By designing and synthesizing adsorbents with nitrogen-containing functional groups, it is possible to efficiently remove heavy metal pollutants from water, address environmental issues, and effectively recover valuable metals. Nitrogen-containing functional groups play a significant role in environmental protection and

sustainable development. Lu et al. developed cellulose nanofiber aerogel adsorbent, functionalized with quaternary ammonium, and chemically cross-linked, has demonstrated high efficiency in removing hexavalent chromium from water, with easy separation and reusability [78]. Arshad et al. synthesized calcium alginate beads, embedded with graphene oxide and functionalized/reduced with polyethyleneimine, have successfully enhanced the adsorption capacity for heavy metal ions, showing outstanding removal effects [79]. Tadanori et al. synthesized 2,20-dipyridylamine-functionalized graphene oxide (GO-DPA) using a simple and low-cost method, for the simultaneous adsorption of lead, cadmium, nickel, and copper ions in aqueous solutions, exhibiting high adsorption capacity under optimal conditions [80].

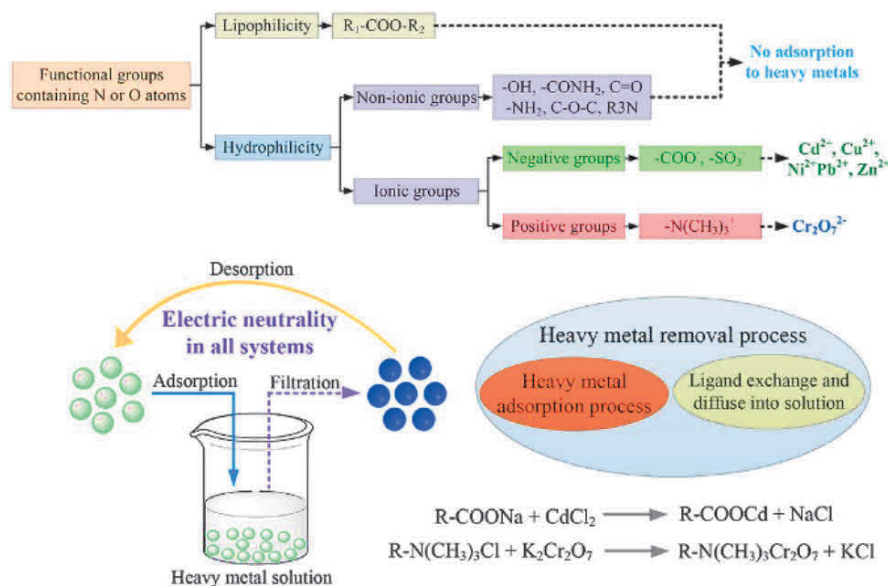


Figure 1.6 Adsorption mechanism of heavy metals by functional groups containing N or O atoms [81].

1.82 Oxygen-containing functional groups

Oxygen-containing functional groups refer to specific structures or groups in a molecule that contain oxygen atoms, with hydroxyl groups and carboxyl groups being the two most common types (see the Figure 1.6). Hydroxyl groups consist of an oxygen atom bonded to a hydrogen atom, typically represented as $-OH$, while carboxyl groups consist

of a structure where a carbon atom is bonded to an oxygen atom and a hydroxyl group (-OH), usually represented as -COOH. These functional groups are widely present in organic molecules, particularly in compounds such as carboxylic acids. Hydroxyl groups play an important role in heavy metal adsorption due to their hydrophilic nature. Their hydrophilicity allows them to form strong hydrogen bonds or coordination bonds with heavy metal ions in water, enabling efficient adsorption of heavy metals. Carboxyl groups, on the other hand, are another common hydrophilic functional group that exhibits strong polarity. Carboxyl groups can form stable complexes with heavy metal ions through electrostatic interactions and coordination bonds. The carboxyl functional group is widely applied in the design of functional materials and adsorbents, particularly in the fields of water treatment and environmental remediation [82]. Huang et al. successfully synthesized potassium polyacrylate (KMAA) hydrogel, demonstrating excellent performance in removing sodium ions from water and supplying potassium ions, providing a valuable solution for addressing high sodium ion concentrations and promoting potassium fertilizer supply [83]. Wang et al. research shows that the oxygen functional groups generated by the aging of microplastics play a key role in improving the adsorption performance of heavy metals, especially the adsorption of uranium (U). Experiments and theoretical calculations reveal the mechanism of uranium adsorption by PS microplastics due to aging and oxygen functional groups (C=O, -OH, phenolic hydroxyl, and -COOH). The results showed that aged PS microplastics showed significant advantages in uranium adsorption. This in-depth study has important implications for assessing the risks of coexisting radionuclides and microplastics in the environment [84]. Gabriela et al. research explored the effect of carbon surface oxidation on the adsorption of Cu (II) ions and found that moderate oxidation treatment can significantly increase the adsorption capacity. This provides a feasible way to prepare efficient Cu (II) adsorbents [85].

1.83 Sulfur-containing functional groups

Sulfur-containing functional groups involve the incorporation of sulfur into organic compounds, with the thiol group as a crucial structural unit consisting of sulfur and hydrogen atoms. In organic chemistry, thiols play a pivotal role and exhibit diverse chemical properties. Due to the presence of sulfur atoms, thiol groups have a strong affinity for metals and can efficiently adsorb heavy metal ions through coordination bonding or chemical adsorption. Additionally, sulfonic acid groups, derivatives of thiol groups, contain bonds formed by sulfur and oxygen in their molecular structure. Due to their strong electron-attracting and oxidative properties, sulfonic acid groups find wide applications in pharmaceutical synthesis, materials science, and organic electronics. They also possess unique characteristics for adsorbing heavy metals [86, 87]. For instance, Wang et al. demonstrated the potential application of microwave-assisted preparation of sulfur-functionalized fiber adsorbents in efficiently removing Hg^{2+} and Cd^{2+} from water, offering prospects for their use in water treatment [88]. Furthermore, Amr El-Hag Ali et al. synthesized CMCA-MPS copolymer hydrogels through γ -radiation-induced copolymerization and cross-linking, exhibiting excellent metal ion recovery performance and chemical stability [89]. These technologies provide powerful tools for environmental protection and sustainable development.

1.84 Phosphorus-containing functional groups

Phosphorus-containing functional groups, such as phosphate and phosphoramidate, play a vital role in functionalizing hydrogel surfaces, providing crucial support for biomedical and heavy metal adsorption research. In the biomedical field, phosphate-based functional groups are extensively used to construct biocompatible materials, enhancing material stability and controllability. These functional groups enable precise control of drug delivery systems through specific interactions with biomolecules, offering innovative solutions for biomedical applications. Moreover, due to their electrophilic and chelating properties, phosphate functional groups strongly interact with heavy metal ions, achieving efficient adsorption. Research conducted by the Estonian Agricultural Research Institute revealed a significant decrease in lead, cadmium, and mercury concentrations in

plants with the application of organic and phosphate fertilizers, while the application of lime fertilizer on acidic soil led to a reduction in heavy metal concentrations [90]. Additionally, surface modification of biochar with phosphoric acid (H_3PO_4) increased surface area and the abundance of oxygen functional groups, significantly enhancing the adsorption capacity for Cu (II) and Cd (II), providing an effective approach for efficient heavy metal adsorption. Similarly [91]. Chen et al. successfully prepared phosphoric acid-functionalized graphene hydrogel electrodes, demonstrating superior performance in uranium adsorption [92]. These studies indicate the wide-ranging potential applications of phosphate functional groups in various fields, offering valuable insights for materials science and environmental research.

1.85 Other functional groups

Silicon functional groups typically consist of silicon atoms, forming molecular structures by introducing silicon elements. These groups are pivotal in materials science and chemistry, imparting unique functionality and chemical reactivity to materials. Like silicon functional groups, hydrazine groups are crucial functional groups widely used, containing amine and oxime groups with diverse chemical properties. Both silicon functional groups and hydrazine groups play vital roles in adsorbing heavy metals. Silicon functional groups, owing to the high affinity and chemical inertness of silicon, are critical in designing heavy metal adsorbents [93]. On the other hand, hydrazine groups also demonstrate excellent performance in heavy metal adsorption. For instance, Wu et al. illustrated that Na-Sic HAP adsorbents, prepared by ultrasonic coprecipitation, exhibited outstanding performance in adsorbing Pb^{2+} and Cd^{2+} , achieving 698.68 mg/g and 129.60 mg/g, respectively [94]. Moreover, PVA hydrogels cross-linked with glutaraldehyde, modified with acrylonitrile grafting initiated by ammonium persulfate (CPVA-PAN) and hydroxylamine hydrochloride (CPVA-AO-PAN), demonstrated an adsorption capacity of 40.7 mg/g for Cu^{2+} [95]. The flexibility and diversity of these functional groups offer abundant possibilities for designing efficient and sustainable heavy metal adsorbent materials, presenting potential sustainable solutions for environmental management and resource recovery. These research findings offer valuable insights for designing environmentally friendly and efficient adsorbent materials.

1.9 The Adsorption Mechanism of Superabsorbent Hydrogels

Superabsorbent hydrogels, a type of polymer material, often feature various functional groups like quaternary ammonium, carboxyl, hydroxyl, phosphate, or silicate groups. These functional components confer unique physical and chemical properties to superabsorbent hydrogels, making them valuable tools for soil remediation and heavy metal adsorption [96, 97]. The positive charge attributes of quaternary ammonium groups empower superabsorbent hydrogels to demonstrate exceptional adsorption capacity for heavy metal anions. This occurs through electrostatic attraction (see the Figure 1.7), bolstering affinity and mitigating pollution risks. Carboxyl and hydroxyl groups elevate the hydrophilicity and adsorption capacity of superabsorbent hydrogels, enabling them to physically absorb water molecules and engage with soil particles. Simultaneously, they release beneficial cations for plant uptake, achieving dual regulation of the soil. Phosphate and silicate groups form stable complexes with heavy metals through ion exchange and chelation reactions, effectively reducing the activity of heavy metals in the soil and minimizing threats to the ecological environment and groundwater. In the realm of soil remediation, superabsorbent hydrogels can act as carriers for remediation agents, such as chelating agents and reducing agents, facilitating the remediation of heavy metals in the soil. In summary, with their diverse functional groups and thoughtful structural design, superabsorbent hydrogels showcase outstanding adsorption and remediation performance, offering innovative and viable solutions for managing heavy metal-contaminated soil. Through the rational design of superabsorbent hydrogels, efficient adsorption, and remediation of heavy metals in the soil can be achieved, providing robust support for environmental protection and sustainable development. While ensuring the effectiveness of superabsorbent hydrogel remediation, it is essential to fully assess its potential impact on the soil ecosystem, including comprehensive evaluations of soil microorganisms, plant growth, and soil texture, to ensure that the remediation process does not cause adverse ecological reactions. This comprehensive assessment and management approach is crucial for achieving sustainable soil remediation solutions.

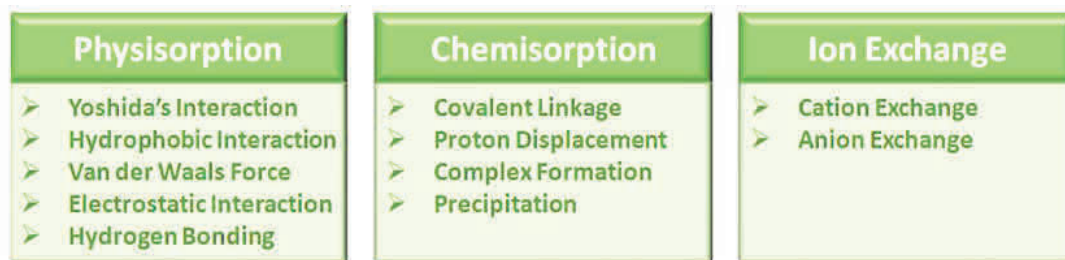


Figure1.7 The mechanism process based on the interaction between adsorbate and adsorbent [52].

References

1. Che, Z., W. Ahmed, J. Weng, L. Wenjie, M. Mahmood, J. M. Alatalo, O. Wenjie, M. M. Nizamani, W. Lu, F. X. Xian, Y. Jie, W. Yunting, W. Li, and S. Mehmood. "Distribution, Pollution, and Human Health Risks of Persistent and Potentially Toxic Elements in the Sediments around Hainan Island, China." *Mar Pollut Bull* 174 (2022): 113278.
2. "Mee, C., 2018. Soil Environmental Quality Risk Control Standard for Soil Contamination of Agricultural Land."
3. Wang, P., H. Chen, P. M. Kopittke, and F. J. Zhao. "Cadmium Contamination in Agricultural Soils of China and the Impact on Food Safety." *Environ Pollut* 249 (2019): 1038-48.
4. Liu, W. H., J. Z. Zhao, Z. Y. Ouyang, L. Soderlund, and G. H. Liu. "Impacts of Sewage Irrigation on Heavy Metal Distribution and Contamination in Beijing, China." *Environ Int* 31, no. 6 (2005): 805-12.
5. Li, J., Y. Lu, W. Yin, H. Gan, C. Zhang, X. Deng, and J. Lian. "Distribution of Heavy Metals in Agricultural Soils near a Petrochemical Complex in Guangzhou, China." *Environ Monit Assess* 153, no. 1-4 (2009): 365-75.
6. Huang, S. S., Q. L. Liao, M. Hua, X. M. Wu, K. S. Bi, C. Y. Yan, B. Chen, and X. Y. Zhang. "Survey of Heavy Metal Pollution and Assessment of Agricultural Soil in Yangzhong District, Jiangsu Province, China." *Chemosphere* 67, no. 11 (2007): 2148-55.

7. Zhao, Yan-Feng, Xue-Zheng Shi, Biao Huang, Dong-Sheng Yu, Hong-Jie Wang, Wei-Xia Sun, I. ÖBoern, and K. BlombÄCk. "Spatial Distribution of Heavy Metals in Agricultural Soils of an Industry-Based Peri-Urban Area in Wuxi, China." *Pedosphere* 17, no. 1 (2007): 44-51.
8. Li, Y., X. Gou, G. Wang, Q. Zhang, Q. Su, and G. Xiao. "Heavy Metal Contamination and Source in Arid Agricultural Soil in Central Gansu Province, China." *J Environ Sci (China)* 20, no. 5 (2008): 607-12.
9. Yang, P., R. Mao, H. Shao, and Y. Gao. "The Spatial Variability of Heavy Metal Distribution in the Suburban Farmland of Taihang Piedmont Plain, China." *C R Biol* 332, no. 6 (2009): 558-66.
10. Liu, W. X., L. F. Shen, J. W. Liu, Y. W. Wang, and S. R. Li. "Uptake of Toxic Heavy Metals by Rice (*Oryza Sativa* L.) Cultivated in the Agricultural Soil near Zhengzhou City, People's Republic of China." *Bull Environ Contam Toxicol* 79, no. 2 (2007): 209-13.
11. Huang, M., S. Zhou, B. Sun, and Q. Zhao. "Heavy Metals in Wheat Grain: Assessment of Potential Health Risk for Inhabitants in Kunshan, China." *Sci Total Environ* 405, no. 1-3 (2008): 54-61.
12. Liang, Y., J. Zhang, X. Xiao, M. Xing, Y. Lu, and L. Wang. "Risk Assessment of Heavy Metals in Overlapped Areas of Farmland and Coal Resources in Xuzhou, China." *Bull Environ Contam Toxicol* 107, no. 6 (2021): 1065-69.
13. Li, R., J. Wang, Y. Zhou, W. Zhang, D. Feng, and X. Su. "Heavy Metal Contamination in Shanghai Agricultural Soil." *Heliyon* 9, no. 12 (2023): e22824.
14. Fu, Kaizhe, Mengyang An, Yanwei Song, Guowei Fu, Weifeng Ruan, Dongming Wu, Xiwen Li, Kun Yuan, Xiaoming Wan, Zeheng Chen, Qipei Li, and Junqiao Long. "Soil Heavy Metals in Tropical Coastal Interface of Eastern Hainan Island in China: Distribution, Sources and Ecological Risks." *Ecological Indicators* 154 (2023).
15. Banerjee, A. D. "Heavy Metal Levels and Solid Phase Speciation in Street Dusts of Delhi, India." *Environ Pollut* 123, no. 1 (2003): 95-105.
16. Keshavarzi, Behnam, Zahra Tazarvi, Mohammad Ali Rajabzadeh, and Ali Najmeddin. "Chemical Speciation, Human Health Risk Assessment and Pollution

- Level of Selected Heavy Metals in Urban Street Dust of Shiraz, Iran." *Atmospheric Environment* 119 (2015): 1-10.
17. Duong, T. T., and B. K. Lee. "Determining Contamination Level of Heavy Metals in Road Dust from Busy Traffic Areas with Different Characteristics." *J Environ Manage* 92, no. 3 (2011): 554-62.
 18. Pagotto, C., N. Remy, M. Legret, and P. Le Cloirec. "Heavy Metal Pollution of Road Dust and Roadside Soil near a Major Rural Highway." *Environ Technol* 22, no. 3 (2001): 307-19.
 19. Ordonez, A., J. Loreda, E. De Miguel, and S. Charlesworth. "Distribution of Heavy Metals in the Street Dusts and Soils of an Industrial City in Northern Spain." *Arch Environ Contam Toxicol* 44, no. 2 (2003): 160-70.
 20. Charlesworth, S., M. Everett, R. McCarthy, A. Ordonez, and E. de Miguel. "A Comparative Study of Heavy Metal Concentration and Distribution in Deposited Street Dusts in a Large and a Small Urban Area: Birmingham and Coventry, West Midlands, Uk." *Environ Int* 29, no. 5 (2003): 563-73.
 21. EDUARDO de MIGUEL, JUAN F. LLAMAS, ENRIQUE CHACON, TORUNN BERG, STEINAR LARSSSEN, ODDVAR ROYSET and MARIT VADSET "Origin and Patterns of Distribution of Trace Elements in Street Dust: Unleaded Petrol and Urban Lead." *Atmospheric Environment* 31, no. 17 (1997): 2733-40.
 22. Zgłobicki, Wojciech, Małgorzata Telecka, Sebastian Skupiński, Aneta Pasierbińska, and Marcin Kozieł. "Assessment of Heavy Metal Contamination Levels of Street Dust in the City of Lublin, E Poland." *Environmental Earth Sciences* 77, no. 23 (2018).
 23. Khairy, Mohammed A., Assem O. Barakat, Alaa R. Mostafa, and Terry L. Wade. "Multielement Determination by Flame Atomic Absorption of Road Dust Samples in Delta Region, Egypt." *Microchemical Journal* 97, no. 2 (2011): 234-42.
 24. Iwegbue, Chukwujindu M. A., Francis O. Arimoro, Godwin E. Nwajei, and Osayonmo I. Eguavoen. "Concentrations and Distribution of Trace Metals in Water and Streambed Sediments of Orogodo River, Southern Nigeria." *Soil and Sediment Contamination: An International Journal* 21, no. 3 (2012): 382-406.

25. P.E. Rasmussen, K.S. Subramanian, B.J. Jessiman. "A Multi-Element Profile of Housedust in Relation to Exterior Dust and Soils in the City of Ottawa, Canada." *The Science of the Total Environment* 267 (2001): 125-40.
26. Ramirez, O., A. M. Sanchez de la Campa, F. Amato, T. Moreno, L. F. Silva, and J. D. de la Rosa. "Physicochemical Characterization and Sources of the Thoracic Fraction of Road Dust in a Latin American Megacity." *Sci Total Environ* 652 (2019): 434-46.
27. Arunakumara, K. K. I. U., Buddhi Charana Walpola, and Min-Ho Yoon. "Current Status of Heavy Metal Contamination in Asia's Rice Lands." *Reviews in Environmental Science and Bio/Technology* 12, no. 4 (2013): 355-77.
28. Takahashi, Goro. "Damage and Heavy Metal Pollution in China's Farmland: Reality and Solutions." *Journal of Contemporary East Asia Studies* 5, no. 1 (2017): 11-25.
29. Huang, Y., L. Wang, W. Wang, T. Li, Z. He, and X. Yang. "Current Status of Agricultural Soil Pollution by Heavy Metals in China: A Meta-Analysis." *Sci Total Environ* 651, no. Pt 2 (2019): 3034-42.
30. Shao, Youyuan, Tao Yan, Kai Wang, Simin Huang, Wuzhi Yuan, and Frank G. F. Qin. "Soil Heavy Metal Lead Pollution and Its Stabilization Remediation Technology." *Energy Reports* 6 (2020): 122-27.
31. Alengebawy, A., S. T. Abdelkhalek, S. R. Qureshi, and M. Q. Wang. "Heavy Metals and Pesticides Toxicity in Agricultural Soil and Plants: Ecological Risks and Human Health Implications." *Toxics* 9, no. 3 (2021).
32. Bouzayani, F., A. Aydi, and T. Abichou. "Soil Contamination by Heavy Metals in Landfills: Measurements from an Unlined Leachate Storage Basin." *Environ Monit Assess* 186, no. 8 (2014): 5033-40.
33. Zhao, L., F. S. Zhang, K. Wang, and J. Zhu. "Chemical Properties of Heavy Metals in Typical Hospital Waste Incinerator Ashes in China." *Waste Manag* 29, no. 3 (2009): 1114-21.
34. Kim, Ah-Young, Ju-Yong Kim, Myoung-Soo Ko, and Kyoung-Woong Kim. "Acid Rain Impact on Phytoavailability of Heavy Metals in Soils." *Geosystem Engineering* 13, no. 4 (2010): 133-38.

35. Azhar, U., H. Ahmad, H. Shafqat, M. Babar, H. M. Shahzad Munir, M. Sagir, M. Arif, A. Hassan, N. Rachmadona, S. Rajendran, M. Mubashir, and K. S. Khoo. "Remediation Techniques for Elimination of Heavy Metal Pollutants from Soil: A Review." *Environ Res* 214, no. Pt 4 (2022): 113918.
36. Khalid, Sana, Muhammad Shahid, Nabeel Khan Niazi, Behzad Murtaza, Irshad Bibi, and Camille Dumat. "A Comparison of Technologies for Remediation of Heavy Metal Contaminated Soils." *Journal of Geochemical Exploration* 182 (2017): 247-68.
37. N. S. Bolan, R. Naidu, M. A. R. Khan, R. W. Tillman, and J. K. Syers. "The Effects of Anion Sorption on Sorption and Leaching of Cadmium." *Aust. J. Soil Res.*, 37 (1999): 445–60.
38. Gu, Jialin, Guoyuan Zou, Shiming Su, Shunjiang Li, Wei Liu, Huiwei Zhao, Liyuan Liu, Liang Jin, Yei Tian, Xinyuan Zhang, Yuning Wang, Tongke Zhao, Lianfeng Du, and Dan Wei. "Effects of Ph on Available Cadmium in Calcareous Soils and Culture Substrates." *Eurasian Soil Science* 55, no. 12 (2022): 1714-19.
39. Greger, M., A. H. Kabir, T. Landberg, P. J. Maity, and S. Lindberg. "Silicate Reduces Cadmium Uptake into Cells of Wheat." *Environ Pollut* 211 (2016): 90-7.
40. Gao, Wenhao, Wentao Zhou, Xianjun Lyu, Xiao Liu, Huili Su, Chuanming Li, and Hui Wang. "Comprehensive Utilization of Steel Slag: A Review." *Powder Technology* 422 (2023).
41. Verma, Samakshi, and Arindam Kuila. "Bioremediation of Heavy Metals by Microbial Process." *Environmental Technology & Innovation* 14 (2019).
42. Meenambigai, P., R. Vijayaraghavan, R. Shyamala Gowri, P. Rajarajeswari, and P. Prabhavathi. "Biodegradation of Heavy Metals – a Review." *International Journal of Current Microbiology and Applied Sciences* 5, no. 4 (2016): 375-83.
43. Ashraf, M. A., I. Hussain, R. Rasheed, M. Iqbal, M. Riaz, and M. S. Arif. "Advances in Microbe-Assisted Reclamation of Heavy Metal Contaminated Soils over the Last Decade: A Review." *J Environ Manage* 198, no. Pt 1 (2017): 132-43.

44. Jin, Yuyao, Yaning Luan, Yangcui Ning, and Lingyan Wang. "Effects and Mechanisms of Microbial Remediation of Heavy Metals in Soil: A Critical Review." *Applied Sciences* 8, no. 8 (2018).
45. Haddon, R. C. "Carbon Nanotubes." *Acc Chem Res* 35, no. 12 (2002): 997.
46. Geim, A. K. "Graphene: Status and Prospects." *Science* 324, no. 5934 (2009): 1530-4.
47. Guo, T., C. Bulin, Z. Ma, B. Li, Y. Zhang, B. Zhang, R. Xing, and X. Ge. "Mechanism of Cd and Cu Adsorption onto Few-Layered Magnetic Graphene Oxide as an Efficient Adsorbent." *ACS Omega* 6, no. 25 (2021): 16535-45.
48. Xiaowei Zhao, Qiong Jia, Naizhong Song, Weihong Zhou, and Yusheng Li. "Adsorption of Pb from an Aqueous Solution by Titanium Dioxide/Carbon Nanotube Nanocomposites: Kinetics, Thermodynamics, and Isotherms." *J. Chem. Eng. Data* 55 (2010): 4428–33.
49. Singh, K., Madhu Agarwal, and Renu. "Heavy Metal Removal from Wastewater Using Various Adsorbents: A Review." *Journal of Water Reuse and Desalination* 7, no. 4 (2017): 387-419.
50. Rad, Leila Roshanfekar, Arash Momeni, Babak Farshi Ghazani, Mohammad Irani, Mehri Mahmoudi, and Bahareh Noghreh. "Removal of Ni²⁺ and Cd²⁺ Ions from Aqueous Solutions Using Electrospun Pva/Zeolite Nanofibrous Adsorbent." *Chemical Engineering Journal* 256 (2014): 119-27.
51. Jiang, Ming-qin, Xiao-ying Jin, Xiao-Qiao Lu, and Zu-liang Chen. "Adsorption of Pb, Cd, Ni and Cu onto Natural Kaolinite Clay." *Desalination* 252, no. 1-3 (2010): 33-39.
52. Gupta, Kanika, Pratiksha Joshi, Rashi Gusain, and Om P. Khatri. "Recent Advances in Adsorptive Removal of Heavy Metal and Metalloid Ions by Metal Oxide-Based Nanomaterials." *Coordination Chemistry Reviews* 445 (2021).
53. Lin, J., B. Su, M. Sun, B. Chen, and Z. Chen. "Biosynthesized Iron Oxide Nanoparticles Used for Optimized Removal of Cadmium with Response Surface Methodology." *Sci Total Environ* 627 (2018): 314-21.

54. Sharma, Manisha, Jasminder Singh, Satyajit Hazra, and Soumen Basu. "Adsorption of Heavy Metal Ions by Mesoporous ZnO and TiO₂@ZnO Monoliths: Adsorption and Kinetic Studies." *Microchemical Journal* 145 (2019): 105-12.
55. Prasun K. Roy, Ashok S. Rawat, Pramod K. Rai . "Synthesis, Characterisation and Evaluation of Polydithiocarbamate Resin Supported on Macroporous Styrene-Divinylbenzene Copolymer for the Removal of Trace and Heavy Metal Ions." *Talanta* 59 (2003): 239-46.
56. P.K. Tewari, Ajai K. Singh "Preconcentration of Lead with Amberlite Xad-2 and Amberlite Xad-7 Based Chelating Resins for Its Determination by Flame Atomic Absorption Spectrometry." *Talanta* 56 (2002): 735-44.
57. Khayyun, Thair Sharif, and Ayad Hameed Mseer. "Comparison of the Experimental Results with the Langmuir and Freundlich Models for Copper Removal on Limestone Adsorbent." *Applied Water Science* 9, no. 8 (2019).
58. Tran, H. N., S. J. You, A. Hosseini-Bandegharai, and H. P. Chao. "Mistakes and Inconsistencies Regarding Adsorption of Contaminants from Aqueous Solutions: A Critical Review." *Water Res* 120 (2017): 88-116.
59. Foo, K. Y., and B. H. Hameed. "Insights into the Modeling of Adsorption Isotherm Systems." *Chemical Engineering Journal* 156, no. 1 (2010): 2-10.
60. Vasanth Kumar, K., and S. Rattanaphani. "Reply to 'Comments on "an Adsorption and Kinetic Study of Lac Dyeing on Silk"' by Yuh-Shan Ho: Discussion on Pseudo Second Order Kinetic Expression." *Dyes and Pigments* 75, no. 1 (2007): 253-54.
61. Qiu, Hui, Lu Lv, Bing-cai Pan, Qing-jian Zhang, Wei-ming Zhang, and Quan-xing Zhang. "Critical Review in Adsorption Kinetic Models." *Journal of Zhejiang University-SCIENCE A* 10, no. 5 (2009): 716-24.
62. Chowdhury, Dr. Papita Saha and Shamik. "Insight into Adsorption Thermodynamics."
63. Chen, X., M. F. Hossain, C. Duan, J. Lu, Y. F. Tsang, M. S. Islam, and Y. Zhou. "Isotherm Models for Adsorption of Heavy Metals from Water - a Review." *Chemosphere* 307, no. Pt 1 (2022): 135545.

64. Ngah, W. S. Wan, and S. Fatinathan. "Adsorption of Cu(II) Ions in Aqueous Solution Using Chitosan Beads, Chitosan–Gla Beads and Chitosan–Alginate Beads." *Chemical Engineering Journal* 143, no. 1-3 (2008): 62-72.
65. Gupta, A. D., K. P. Rawat, V. Bhadauria, and H. Singh. "Recent Trends in the Application of Modified Starch in the Adsorption of Heavy Metals from Water: A Review." *Carbohydr Polym* 269 (2021): 117763.
66. SOON HONG YUK, SUN HANG CHO, BYUNG CHUNL SHIN and HA1 BANG LEE. "A Novel Semi-Interpenetrating Networks System as an Absorbent Material." *Eur. Polym. J* 32 (1996): 101-04.
67. Song, Li, Fuqiang Liu, Changqing Zhu, and Aimin Li. "Facile One-Step Fabrication of Carboxymethyl Cellulose Based Hydrogel for Highly Efficient Removal of Cr(VI) under Mild Acidic Condition." *Chemical Engineering Journal* 369 (2019): 641-51.
68. Wang, Q., S. Zhu, C. Xi, and F. Zhang. "A Review: Adsorption and Removal of Heavy Metals Based on Polyamide-Amines Composites." *Front Chem* 10 (2022): 814643.
69. Kaşgöz, Hasine, Saadet Özgümüş, and Murat Orbay. "Modified Polyacrylamide Hydrogels and Their Application in Removal of Heavy Metal Ions." *Polymer* 44, no. 6 (2003): 1785-93.
70. Wiśniewska, Małgorzata, Gracja Fijałkowska, Katarzyna Szewczuk-Karpisz, Karolina Herda, and Stanisław Chibowski. "Ionic Polyacrylamides as Stability-Modifying Substances of Soil Mineral Suspensions Containing Heavy Metal Impurities." *Processes* 10, no. 8 (2022).
71. Akhtar, M. F., M. Hanif, and N. M. Ranjha. "Methods of Synthesis of Hydrogels ... A Review." *Saudi Pharm J* 24, no. 5 (2016): 554-59.
72. Yang, Fengyu, Baiping Ren, Yongqing Cai, Jianxin Tang, Ding Li, Ting Wang, Zhangqi Feng, Yung Chang, Lijian Xu, and Jie Zheng. "Mechanically Tough and Recoverable Hydrogels Via Dual Physical Crosslinkings." *Journal of Polymer Science Part B: Polymer Physics* 56, no. 19 (2018): 1294-305.

73. Syed K. H. Gulrez, Saphwan Al-Assaf and Glyn O Phillips. "Hydrogels: Methods of Preparation, Characterisation and Applications in Molecular and Environmental Bioengineering."
74. Bashir, S., M. Hina, J. Iqbal, A. H. Rajpar, M. A. Mujtaba, N. A. Alghamdi, S. Wageh, K. Ramesh, and S. Ramesh. "Fundamental Concepts of Hydrogels: Synthesis, Properties, and Their Applications." *Polymers (Basel)* 12, no. 11 (2020).
75. Prissanaroon-Ouajai, Walaiporn, Natthika Koedsombat, and Nuttapol Subbua. "Novel Polyacrylamide/Polypyrrole Hydrogel for Electrically Controlled Release of Salicylic Acid." *Key Engineering Materials* 824 (2019): 176-81.
76. Thakur, S., J. Chaudhary, V. Kumar, and V. K. Thakur. "Progress in Pectin Based Hydrogels for Water Purification: Trends and Challenges." *J Environ Manage* 238 (2019): 210-23.
77. Yang, X., Y. Wan, Y. Zheng, F. He, Z. Yu, J. Huang, H. Wang, Y. S. Ok, Y. Jiang, and B. Gao. "Surface Functional Groups of Carbon-Based Adsorbents and Their Roles in the Removal of Heavy Metals from Aqueous Solutions: A Critical Review." *Chem Eng J* 366 (2019): 608-21.
78. He, X., L. Cheng, Y. Wang, J. Zhao, W. Zhang, and C. Lu. "Aerogels from Quaternary Ammonium-Functionalized Cellulose Nanofibers for Rapid Removal of Cr(VI) from Water." *Carbohydr Polym* 111 (2014): 683-7.
79. Arshad, Fathima, Munirasu Selvaraj, Jerina Zain, Fawzi Banat, and Mohammad Abu Haija. "Polyethylenimine Modified Graphene Oxide Hydrogel Composite as an Efficient Adsorbent for Heavy Metal Ions." *Separation and Purification Technology* 209 (2019): 870-80.
80. Zare-Dorabei, R., S. M. Ferdowsi, A. Barzin, and A. Tadjarodi. "Highly Efficient Simultaneous Ultrasonic-Assisted Adsorption of Pb(II), Cd(II), Ni(II) and Cu (II) Ions from Aqueous Solutions by Graphene Oxide Modified with 2,2'-Dipyridylamine: Central Composite Design Optimization." *Ultrason Sonochem* 32 (2016): 265-76.

81. Zhang, M., S. Hou, Y. Li, Y. Hou, and P. Yang. "Single Evaluation and Selection of Functional Groups Containing N or O Atoms to Heavy Metal Adsorption: Law of Electric Neutrality." *Chemosphere* 287, no. Pt 2 (2022): 132207.
82. Ahmad, S. Z. N., W. N. Wan Salleh, A. F. Ismail, N. Yusof, M. Z. Mohd Yusop, and F. Aziz. "Adsorptive Removal of Heavy Metal Ions Using Graphene-Based Nanomaterials: Toxicity, Roles of Functional Groups and Mechanisms." *Chemosphere* 248 (2020): 126008.
83. Huang, J., T. Gotoh, S. Nakai, and A. Ueda. "A Novel Composite Hydrogel Material for Sodium Removal and Potassium Provision." *Polymers (Basel)* 15, no. 17 (2023).
84. Tang, Zhenping, Feiyu Zhu, Tianyun Jiang, Fuxing Wei, Yuanyuan Gao, Chao Xiang, Yi Duan, Yilong Hua, Shuai Zhou, and Yayi Wang. "Oxygen-Containing Functional Groups Enhance Uranium Adsorption by Aged Polystyrene Microplastics: Experimental and Theoretical Perspectives." *Chemical Engineering Journal* 465 (2023).
85. Hotova, G., V. Slovak, T. Zelenka, R. Marsalek, and A. Parchanska. "The Role of the Oxygen Functional Groups in Adsorption of Copper (II) on Carbon Surface." *Sci Total Environ* 711 (2020): 135436.
86. Velepini, Tarisai, and Kriveshini Pillay. "Sulphur Functionalized Materials for Hg(II) Adsorption: A Review." *Journal of Environmental Chemical Engineering* 7, no. 5 (2019).
87. Darban, Zenab, Syed Shahabuddin, Rama Gaur, Irfan Ahmad, and Nanthini Sridewi. "Hydrogel-Based Adsorbent Material for the Effective Removal of Heavy Metals from Wastewater: A Comprehensive Review." *Gels* 8, no. 5 (2022).
88. Deng, Sheng, Guangshan Zhang, Shuang Liang, and Peng Wang. "Microwave Assisted Preparation of Thio-Functionalized Polyacrylonitrile Fiber for the Selective and Enhanced Adsorption of Mercury and Cadmium from Water." *ACS Sustainable Chemistry & Engineering* 5, no. 7 (2017): 6054-63.
89. El-Hag Ali, Amr. "Removal of Heavy Metals from Model Wastewater by Using Carboxymethyl Cellulose/2-Acrylamido-2-Methyl Propane Sulfonic Acid Hydrogels." *Journal of Applied Polymer Science* 123, no. 2 (2011): 763-69.

90. Mehravaran, A., M. R. Jaafari, S. A. Jalali, A. Khamesipour, M. Tafaghodi, M. Hojatizade, A. Abbasi, and A. Badiie. "Cationic Immune Stimulating Complexes Containing Soluble Leishmania Antigens: Preparation, Characterization and in Vivo Immune Response Evaluation." *Iran J Immunol* 12, no. 4 (2015): 274-87.
91. Peng, H., P. Gao, G. Chu, B. Pan, J. Peng, and B. Xing. "Enhanced Adsorption of Cu and Cd by Phosphoric Acid-Modified Biochars." *Environ Pollut* 229 (2017): 846-53.
92. Liao, Yun, Meng Wang, and Dajun Chen. "Electrosorption of Uranium(Vi) by Highly Porous Phosphate-Functionalized Graphene Hydrogel." *Applied Surface Science* 484 (2019): 83-96.
93. Bois, Laurence, Anne Bonhommé, Annie Ribes, Bernadette Pais, Guy Raffin, and Franck Tessier. "Functionalized Silica for Heavy Metal Ions Adsorption." *Colloids and Surfaces A: Physicochemical and Engineering Aspects* 221, no. 1-3 (2003): 221-30.
94. Zeng, Rongying, Wenqing Tang, Chunxia Ding, Lihua Yang, Daoxin Gong, Zhuo Kang, Zhimin He, and Yuming Wu. "Preparation of Anionic-Cationic Co-Substituted Hydroxyapatite for Heavy Metal Removal: Performance and Mechanisms." *Journal of Solid State Chemistry* 280 (2019).
95. Zeng, Lelin, Qian Liu, Wenyan Xu, Guoxiang Wang, Yixue Xu, and Enxiang Liang. "Graft Copolymerization of Crosslinked Polyvinyl Alcohol with Acrylonitrile and Its Amidoxime Modification as a Heavy Metal Ion Adsorbent." *Journal of Polymers and the Environment* 28, no. 1 (2019): 116-22.
96. Badsha, M. A. H., M. Khan, B. Wu, A. Kumar, and I. M. C. Lo. "Role of Surface Functional Groups of Hydrogels in Metal Adsorption: From Performance to Mechanism." *J Hazard Mater* 408 (2021): 124463.
97. Qasem, Naef A. A., Ramy H. Mohammed, and Dahiru U. Lawal. "Removal of Heavy Metal Ions from Wastewater: A Comprehensive and Critical Review." *npj Clean Water* 4, no. 1 (2021).

Chapter 2 Dual benefits of hydrogel remediation of cadmium-contaminated water or soil and promotion of vegetable growth under cadmium Stress

2.1 Introduction

The current global situation of heavy metal contamination in soil has raised widespread concerns [1-4]. Different regions universally face varying degrees of heavy metal pollution, primarily caused by the release of heavy metal waste during industrial, mining, and agricultural processes. These pollutants enter the soil through processes such as atmospheric deposition and water leakage, causing the accumulation of heavy metals in the soil to exceed safety standards [5-7]. Heavy metal pollution has severe implications for the environment and human health. It not only hampers crop growth and yield, but also permeates the food chain, ultimately negatively impacting human health and giving rise to a range of health issues. Consequently, there is an urgent need to seek efficient methods for addressing heavy metal pollution [8-11].

Currently, addressing soil pollution primarily relies on employing physical and chemical methodologies. Among these, soil displacement stands out as an effective means to significantly reduce the proportion of heavy metal content in contaminated soil [12]. On the other hand, thermal treatment techniques can be utilized to heat the polluted soil to extremely high temperatures, causing the metals to melt into a vitrified form, thereby mitigating their impact on the environment [13]. Additionally, the introduction of animal manure demonstrates efficacy in immobilizing heavy metal components in the soil, thereby diminishing their potential environmental hazards [14]. Meanwhile, the application of chemical agents that react with heavy metals to form precipitated compounds represents another potent remediation approach [15]. Moreover, bacteria exhibit promises by directly interacting with sites of heavy metal contamination through adherence to metal salts, resulting in metal dissolution [16]. However, these treatment

technologies are not without their drawbacks, including relatively high costs and the potential generation of byproducts leading to secondary soil contamination issues.

Hydrogels are a type of polymer material with a three-dimensional network structure, exhibiting excellent adsorption properties, particularly in the removal of heavy metals. They employ surface functional groups such as carboxyl and hydroxyl moieties to engage in ion exchange with excess heavy metal ions in wastewater, securely immobilizing them within the hydrogel matrix [17, 18]. Li et al. research team successfully synthesized a magnetic hydrogel featuring NH_2 functional groups that, through coordination interactions, efficiently adsorb copper [19, 20]. This coordination, facilitated by the formation of chemical bonds, effectively reduces the concentration of heavy metals in both aqueous solutions and soil environments [21]. Moreover, Zhang et al. engineered a dual-network hydrogel composed of alginate and polyvinyl alcohol. Relying on the active sites on the hydrogel surface with charges opposite to those of metal ions, they successfully removed heavy metals such as Pb (II) and Cr (VI) through electrostatic adsorption [22, 23].

Liu et al. developed a composite material comprising FeS nanoparticles encapsulated within a lignin hydrogel matrix. The adsorption mechanism primarily involved the chemical reaction precipitation of cadmium sulfide, lignin complexation, hydrogel swelling, and nanoparticle adsorption [24]. Zhou et al. fabricated a novel composite hydrogel (LR-g-PAA/MMT/urea) that enhances soil fertility and mitigates the toxicity of heavy metals to organisms [25]. Dhiman et al. irrigated spinach with wastewater and incorporated water-absorbing gel–biochar to reduce the uptake of heavy metals by spinach [26]. Additionally, Zhou et al. devised a novel hydrogel that, upon pesticide release, undergoes the breaking of disulfide bonds on the hydrogel, generating thiol groups capable of complexing with heavy metals in the soil, thereby mitigating their toxicity to plants [27].

In this study, we synthesized DMAPAA/DMAPAAQ hydrogels using free radical polymerization and investigated their adsorption capabilities towards cadmium in aqueous environments. Furthermore, their introduction into soil was assessed to evaluate the growth of vegetables under cadmium stress. The aim of this research was to investigate the cadmium adsorption capacity of DMAPAA/DMAPAAQ hydrogels at

varying pH levels, along with relevant thermodynamic and kinetic attributes. To simulate the adsorption process, we employed isotherm models such as Langmuir and Freundlich, while pseudo-first and pseudo-second-order models were utilized to analyze the adsorption kinetics [28]. Additionally, the uptake of cadmium by vegetables in soil with the addition of DMAPAA/DMAPAAQ hydrogels under cadmium stress was evaluated, as well as the content of various elements in vegetable leaves under the influence of both hydrogels and cadmium.

2.2 Experimental Methods

2.21 materials

The monomer DMAPAA/DMAPAAQ was obtained from KJ Chemicals Corporation (Tokyo, Japan), and N, N-dimethyl ethylenediamine (TEMED) was purchased from Nacalai Tesque Co., Ltd. (Kyoto, Japan). N, N'-methylenebisacrylamide (MBAA), ammonium persulfate (APS), and $\text{CdN}_2\text{O}_8 \cdot 4\text{H}_2\text{O}$, $\text{CdCl}_2 \cdot 2.5\text{H}_2\text{O}$ were acquired from Sigma-Aldrich, Inc. (St. Louis, MO, USA). In addition, the $1 \text{ mol} \cdot \text{L}^{-1}$ HCl and NaOH solution was purchased from Sigma-Aldrich Japan (Tokyo, Japan). The soil was purchased from NAFCO (Fukuoka Japan). All the reagents used were of analytical grade and employed as received. The distilled water used in the experiments was produced in the laboratory.

2.22 synthesis of hydrogel

To synthesize the hydrogel, 1.953 g of DMAPAA and 2.584 g of DMAPAAQ monomers were weighed along with 0.193 g of MBAA crosslinker and 0.058 g of TEMED accelerator; this was added to a 20 mL volumetric flask (see Table 4). Distilled water was added to the flask, and the resulting mixture was stirred using a magnetic stirrer. In a separate 5 mL volumetric flask, a solution of 0.114 g of APS initiator was prepared using distilled water. Both the monomer solution and initiator solution were purged with nitrogen for 45 minutes to eliminate any oxygen and prevent the inhibition of free radicals. The initiator solution was then added to the monomer solution and stirred

for 20 s. The resulting mixture was transferred to three plastic tubes using a pipette and immersed in an aqueous solution at 25°C for 24 hours. The resulting gels were removed from the tubes and cut into uniform cylindrical shapes, and then washed with methanol for 24 hours using Soxhlet extractor (Asahi Glass plant Inc., Arao City, Japan) equipment to remove any unreacted components. The gels were subsequently air-dried at room temperature and further dried in a 50°C oven for 24 hours. Finally, the dried gels were ground into a powder using a grinder.

Table 2.1 Synthesis condition of the DMAPAA/DMAPAAQ hydrogel

Materials	Component Type	Molar weight (g/mol)	Concentration (mol/m ³)	Mass(g)
DMAPAA	Monomer	156.22	500	1.953
DMAPAA-Q	Monomer	206.71	500	2.584
MBAA	Linker	154.17	50	0.193
TEMED	Accelerator	116.21	20	0.058
APS	Initiator	228.19	20	0.114

2.3 Swelling Properties of Hydrogels

2.31 Swelling degree of hydrogel in water solutions

A hydrogel weighing 0.02 g (Md) was added to 40 ml of water solution. The mixtures were allowed to equilibrate at room temperature for 24 h to achieve swelling equilibrium. The swollen gels were subsequently filtered through filter paper and their weight recorded as Ms , calculated using the following formula:

$$W_a = \frac{(Ms - Md)}{Md}$$

2.32 Soil water holding rate.

Weighed soil of 10 g was combined with 0.1 g of hydrogel and recorded as m_1 . Subsequently, an appropriate amount of water was added to the beaker at room

temperature, allowing the complete saturation of the mixture. The mass of the resulting mixture and water was measured via filtration using filter paper and recorded as m_2 , calculated using the following formula:

$$W_b = \frac{(m_2 - m_1)}{m_1}$$

2.4 Adsorption Experiment

2.41 Adsorption thermodynamic experiments with different pH values

First, 1000 ppm of cadmium solution was diluted to a concentration of 5, 50, 100, 300, and 500 $\text{mg}\cdot\text{L}^{-1}$. Then, 25 ml of each diluted solution was transferred into 50 ml plastic centrifuge tubes. The pH of the solutions was adjusted to 7.3 by adding 1 $\text{mol}\cdot\text{L}^{-1}$ NaOH solution to a final volume of 40 ml. Furthermore, 20 mg of the adsorbent was introduced into each tube. The tubes were placed in a water bath constant-temperature shaker at 25 °C, with continuous shaking at 150 rpm for 24 h. Following the adsorption period, the samples were filtered through a 0.22 μm membrane filter and analyzed using ICP.

2.42 pH effect experiment

The process began with the dilution of a 1000 ppm cadmium solution to a concentration of 100 $\text{mg}\cdot\text{L}^{-1}$. Then, 25 ml of this diluted solution was carefully transferred into a 50 ml plastic centrifuge tube. To adjust the pH values to 2.0, 3.0, 4.0, 5.0, 6.0, and 7.0, 1 $\text{mol}\cdot\text{L}^{-1}$ of NaOH or HCl solution was added until the final volume reached 40 ml. Subsequently, 20 mg of the adsorbent material was introduced into the mixture. The entire system was placed in a water bath constant-temperature shaker, where continuous adsorption was conducted at 25 °C and 150 rpm for a duration of 24 h. Following adsorption, the samples were filtered through a 0.22 μm membrane filter and analyzed using ICP.

2.43 Adsorption kinetic experiment

The procedure began with the dilution of a 1000 ppm cadmium solution to achieve a concentration of $100 \text{ mg}\cdot\text{L}^{-1}$. Following this, 40 ml of the diluted solution was prepared, and the pH levels were adjusted to 5.7 and 7.3 using $1 \text{ mol}\cdot\text{L}^{-1}$ NaOH solution. Next, 20 mg of the adsorbent material was introduced into the system. The entire setup was placed in a water bath constant-temperature shaker, maintaining a constant temperature of $25 \text{ }^\circ\text{C}$ with a shaking rate of 150 rpm. The adsorption process was conducted for specific time intervals (12, 48, 72, 120, 180, 240, 300, 1200, 1320 and 1440 min). At each predetermined time point, samples were withdrawn from the system and subsequently filtered through a $0.22 \text{ }\mu\text{m}$ membrane filter. The filtered samples were then analyzed using ICP.

2.44 Adsorption thermodynamics at different temperatures

The 1000 ppm original cadmium solutions were diluted to concentrations of 5, 50, 100, 300, and $500 \text{ mg}\cdot\text{L}^{-1}$, respectively. For each concentration, 25 ml of the diluted solution was transferred into a plastic centrifuge tube with a volume of 50 ml. Subsequently, the pH of each solution was adjusted to 5.7 and 7.3 using $1 \text{ mol}\cdot\text{L}^{-1}$ of NaOH solution to reach a final volume of 40 ml. Next, 20 mg of the adsorbent material was added to each solution. The prepared samples were placed in a water bath constant-temperature shaker, maintaining constant temperatures of $25 \text{ }^\circ\text{C}$ and $35 \text{ }^\circ\text{C}$, respectively, with a shaking rate of 150 rpm. The adsorption process was conducted continuously for 24 h. After the adsorption period, the samples were filtered through $0.22 \text{ }\mu\text{m}$ membrane filters to remove any particulate matter. The filtrates were subsequently analyzed using ICP to measure the desired parameters.

2.5 Vegetable Planting Experiment

2.51 Experimental design

A total of 800 g of wet soil was carefully weighed and transferred to a 1/10000a neubauer pot. Subsequently, the DMAPAAA/DMAPAAQ hydrogels were added to the

soil at concentrations of 0%, 2%, and 4% (w/w). CdCl₂ solutions were added to the soil at concentrations of 0, 5, 50 and 500 mg/kg. The mixture was thoroughly mixed to ensure the uniform distribution of the cadmium and gel in the soil. The soil was then allowed to attain a semi-moist state over a few days and subsequently divided into two equal portions. Small holes were made in each of the four directions of the pot, and four seeds of Swiss chard (*Beta vulgaris* L. var. *cicla*) were placed in each hole.

2.52 Dry weight of swiss chard

After two months of cultivation in the greenhouse, eight Swiss chard plants were harvested by cutting the roots with scissors and washing the soil from the roots with water. Harvested plants were placed in envelope bags and dried in a drying oven at 70°C for several days until completely dried. The dry weights of Swiss chard were measured using an electronic balance.

2.53 Plant digestion

Dried plants were crushed using a magnetic grinder (BMS-A20TP, Biomedical Science Corp., Tokyo, Japan) for 15 minutes at 700 rpm/min, after which approximately 50 mg of each sample was weighed and recorded. Subsequently, 2 ml of nitric acid was added to each of the centrifuge tubes, followed by 0.5 ml of hydrogen peroxide, and then subjected to digestion using a heat block incubator (DTU-2BN, Taitec Corp., Saitama, Japan). The digestion process began at 80°C for 30 min, followed by a further increase in temperature to 120°C for 2 hours, and left overnight in a fume hood. After digestion, the resulting solution was filtered through filter paper and made up to 25 ml in a volumetric flask. Finally, the concentration of various elements in the vegetables was determined using ICP.

2.54 Characterization

The concentration of the heavy metal cadmium in the solution was measured using ICP (SPS-3500, Shimadzu Corp., Kyoto, Japan). The daily growth of the vegetable was

monitored and recorded using a high-resolution camera (Xiaomi12 Technology Co., Ltd. China). The elemental concentration of the vegetable was analyzed using ICP. The pH of the soil was measured using a precise pH meter (Hanna Groline Soil PH Tester HI981030). The soil properties were further characterized using EDX (EDX-7000, Shimadzu Corp., Kyoto, Japan) analysis. The structure of the gels was analyzed using IR (FTIR, IRTracer-100, Shimadzu Corp., Kyoto, Japan).

2.6 Result

2.61 Swelling degree of hydrogel

This study investigates the swelling behavior of hydrogels in both aqueous and soil environments. The results indicate that the addition of hydrogels significantly enhances the swelling capacity of both hydrogels and soil, whether placed in water or soil, as shown in Figure 2.1b. In aqueous conditions, the swelling capacity of hydrogels increased 18.6 times, while the incorporation of hydrogels into soil resulted in a 1.7 times enhancement in the soil volumetric water content. This demonstrates the remarkable water retention capabilities of hydrogels. The water-absorbing property of hydrogels is primarily attributed to the three-dimensional network structure formed by their polymer structure, which provides sufficient space for water molecules, leading to an expansion in the volume of the hydrogel. As shown in Figure 2.1a, the elemental analysis of the soil using EDX (EDX-7000 energy dispersive XRF spectrometers) revealed that the elements present were Si, Fe, Ca, Al, K, S, Ti, P, Mn, Zn, Sr, Cu, Rb, and Zr, with respective contents of 33.3%, 25.5%, 15.8%, 7.8%, 7.8%, 3.0%, 2.8%, 1.5%, 0.84%, 0.81%, 0.29%, 0.27%, 0.19%, and 0.18%, some of which are beneficial for plant growth. Furthermore, when hydrogels are added to the soil, soil particles adhere to the surface of the hydrogel. The expansion of the hydrogel provides additional space for water in the soil, making it easier for plants to absorb water and acquire these crucial elements.

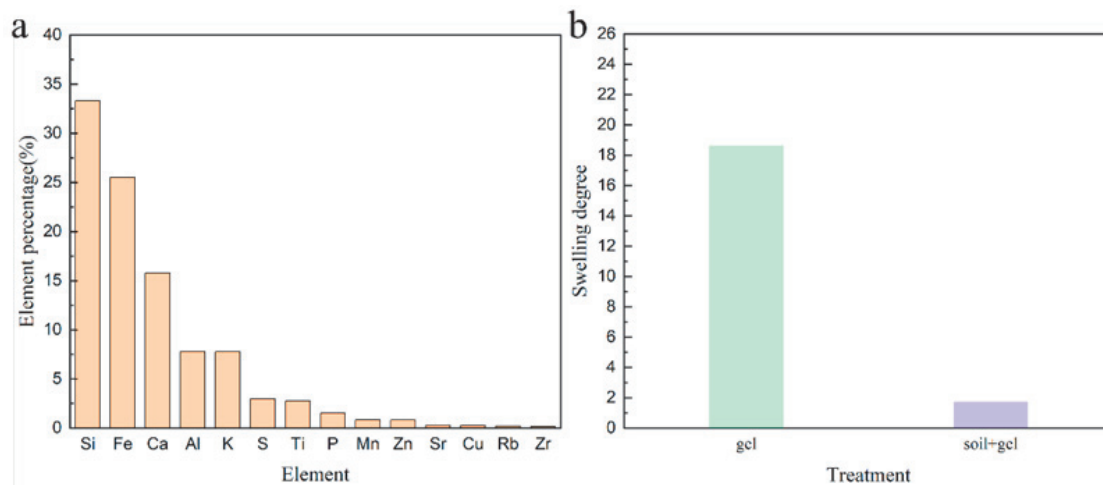


Figure 2.1 (a) Main elements contained in soil, (b) Swelling degree of hydrogel in water and soil.

2.62 Effect of pH on gel adsorption

The aim of this study was to investigate the capture characteristics and effects of DMAPAA/DMAPAAQ hydrogels on cadmium ions under different pH conditions, as shown in Figure 2.2 The experimental results indicate that the capture capacity of the hydrogel for cadmium ions increases with increasing pH at pH 7, that the hydrogel exhibits the maximum capture capacity for cadmium, reaching 50 mg/g, while at pH 2, and that the capture capacity is minimal, at only 5 mg/g. Under acidic conditions, the high concentration of H^+ ions enhance the protonation degree of the hydrogel and increases its surface positive charge, resulting in repulsion, with the positive charge carried by cadmium ions. At this point, Cl^- forms stable complexes with Cd^{2+} , which exists in the solution as $CdCl^+$, $CdCl_2^0$. When the pH is equal to 7, the tertiary amine in the hydrogel undergoes a protonation reaction in the aqueous solution, generating OH^- ions that form cadmium hydroxide precipitates, which are encapsulated within the hydrogel. This is the main mechanism by which the hydrogel effectively adsorbs the heavy metal cadmium.

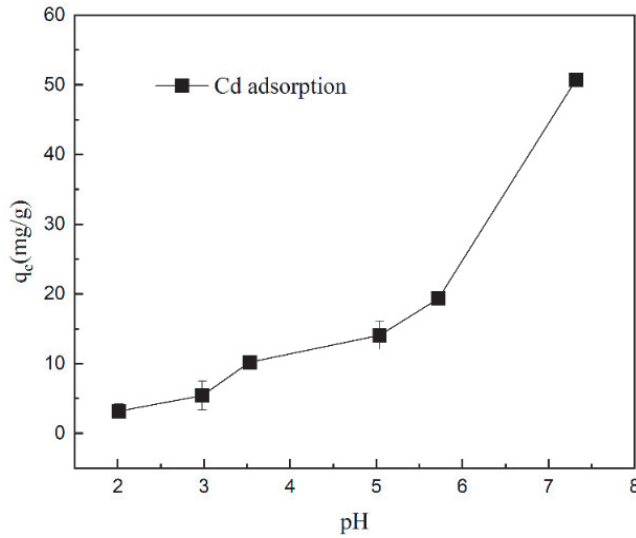


Figure 2.2 Effect of hydrogel adsorption capacity on cadmium ions at different pH values.

2.63 Isothermal adsorption

The experimental results in Figure 2.3 show that, as the concentration of cadmium in the solution increases, the adsorption capture of the DMAPAA/DMAPAAQ hydrogels for cadmium ions also increases. In the Langmuir model, when pH=7.3, the adsorption capacity of the hydrogel is 121 mg/g, significantly higher than that at pH=5.7. This indicates that under acidic conditions, the adsorption of cadmium ions is mainly achieved through the Cl^- and Cd^{2+} from a stable complex. However, the adsorption capacity is limited. In neutral conditions, the amino groups on the hydrogel undergo protonation in water, and OH^- becomes the main adsorption group.

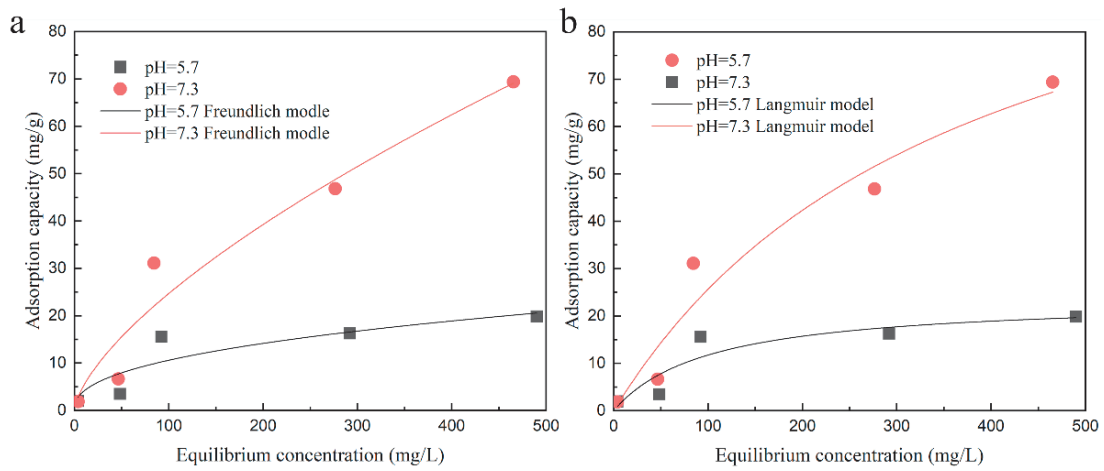


Figure 2.3 Hydrogel isothermal adsorption curve for cadmium ions at pH=5.7, 7.3
 (a) Langmuir simulation fitting curve (b) Freundlich simulation fitting curve.

In the Freundlich model, Table 2.2 shows that the value of parameter n is between 1 and 10, indicating a spontaneous adsorption process. However, the correlation coefficient of the Langmuir model is higher than that of the Freundlich model at different pH values, indicating that the Langmuir model is more suitable for describing the adsorption process of the hydrogel on cadmium ions.

Table 2.2 Parameters of Langmuir and Freundlich isotherm model by DMAPAA/DMAPAAQ gel at pH=5.7 and pH=7.3 cadmium adsorption capacity

Isotherm model	Parameter	Initial pH	
		5.7	7.3
Langmuir	q_{\max} (mg/g)	23.7	121
	K_L (L/mg)	0.0098	0.0027
	R^2	0.8537	0.9526
Freundlich	K_F (mg/g)	1.55	1.13
	n	2.397	1.492
	R^2	0.8164	0.9515

2.64 Adsorption kinetics

By calculating the thermodynamic parameters, including the adsorption enthalpy (ΔH^θ), adsorption free energy (ΔG^θ), and adsorption entropy (ΔS^θ), the adsorption mechanism on the hydrogel was studied. Thermodynamic analysis was conducted on the adsorption experiments to elucidate the influence of different temperatures on the adsorption behavior of cadmium ions, as shown in Figure 2.4. It was found that, when the temperature increased from 298 to 318 K, ΔG^θ was consistently less than 0, indicating that the adsorption of cadmium ions by DMAPAA DMAPAAQ hydrogels is spontaneous and feasible.

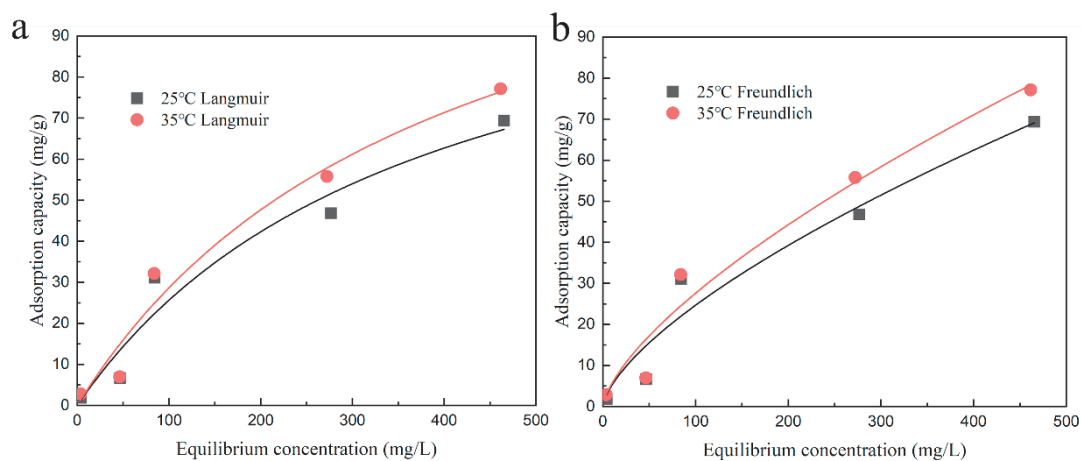


Figure 2.4 adsorption isotherm fit curves of hydrogel at different temperatures (a) Cd²⁺ Adsorption Langmuir model simulated fit curve, (b) Cd²⁺ adsorption Freundlich model simulated fit curve.

For the adsorption process of cadmium, ΔH^θ is positive, and the adsorption capacity of cadmium ions increases with temperature, indicating that the adsorption of cadmium ions by the hydrogel is an endothermic reaction. At the same time, as shown in Table 2.3, ΔS^θ is also positive, indicating an increase in disorder between the surface of the hydrogel and the interface with cadmium ions during the adsorption process. Thermodynamic studies help to understand whether the adsorption behavior of adsorbent materials is an exothermic or endothermic process, thereby expanding the practical applications of adsorbents.

Table 2.3 DMAPAA/DMAPAAQ hydrogel adsorption thermodynamic parameters for Cadmium

T/K	$\Delta G^\theta /(\text{kJ}\cdot\text{mol}^{-1})$	$\Delta H^\theta /(\text{kJ}\cdot\text{mol}^{-1})$	$\Delta S^\theta /(\text{J}\cdot\text{mol}^{-1}\cdot\text{K}^{-1})$
298.15	-3.082	4.677	26.025
308.15	-3.342	4.677	26.025

2.65 Adsorption kinetics

The experimental results in Figure 2.5a show that the entire adsorption process can be divided into two stages. In the initial stage, the adsorption rate is fast. After 200 minutes of adsorption, the DMAPAA/DMAPAAQ hydrogels' capacity for absorbing cadmium has reached 90% of the equilibrium adsorption capacity. As time increases, the cadmium ion adsorption rate gradually decreases and basically reaches an equilibrium state after 24 hours. This is because, in the initial stage, the amine groups on the hydrogel are protonated in water to form many OH⁻ ions, which combine with cadmium ions to form cadmium hydroxide precipitation. Under the condition of pH=5.7,7.3, the coefficients of the pseudo-first-order kinetic model for cadmium ion adsorption are higher than those of the second-order kinetic model. This shows that the hydrogel adsorption process is related to its concentration, and that the adsorption sites mainly come from the amine groups on the hydrogel. The pseudo-first-order kinetic model is more suitable for the process of absorbing cadmium ions via hydrogels. Figure 2.5b shows the adsorption process of the ion internal diffusion model. The first stage is surface adsorption. At this stage, there are many active sites on the hydrogel. Under acidic conditions, adsorption mainly occurs through the chelation of chloride ions and cadmium ions on the hydrogel. Under neutral conditions, it is mainly the OH⁻ ions formed by the protonation of the amine group on the hydrogel that adsorb cadmium. The second stage is the internal diffusion adsorption stage of the hydrogel, which mainly occurs in the gaps of the hydrogel material. The adsorption rate at this stage decreases, and finally the adsorption equilibrium is reached.

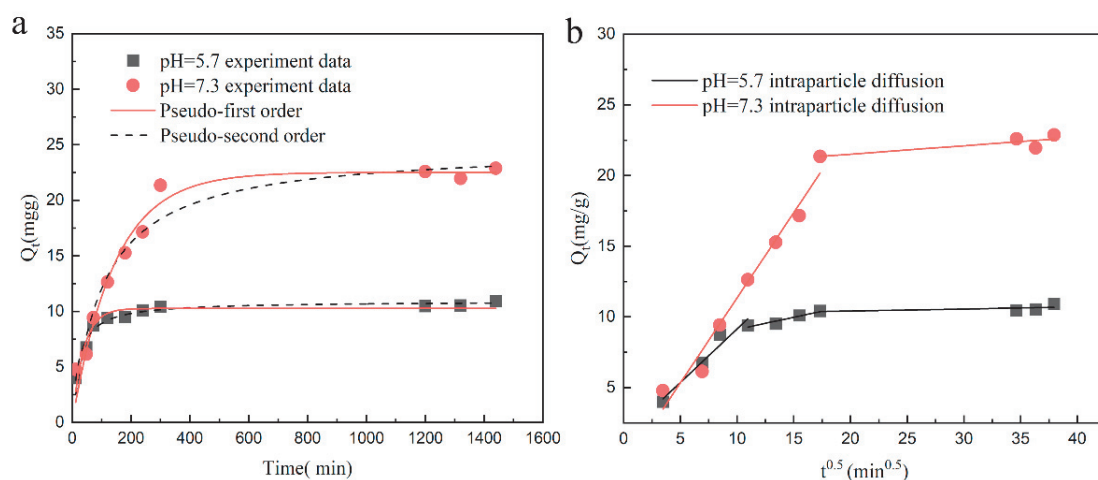


Figure 2.5 Pseudo-first-order and pseudo-second-order dynamic model diagrams of cadmium adsorption by hydrogel; (b) Hydrogel adsorption and diffusion model

Table 2.4 Fit results of Cd^{2+} adsorption kinetics by DMAPAA/DMAPAAQ hydrogel.

Isotherm model	Parameter	Initial pH	
		5.7	7.3
Pseudo-first order	k_1 (min^{-1})	0.007	0.007
	q_e (mg/g)	22.52	32.87
	R^2	0.967	0.979
Pseudo-second order	K_2 (g/mg/min)	3.818	2.539
	q_e (mg/g)	24.76	36.37
	R^2	0.951	0.939

2.66 Characterization of hydrogel structure

In this study, the structural changes in the DMAPAA/DMAPAAQ hydrogels after adsorption were thoroughly analyzed using infrared spectroscopy. Figure 2.6 reveals distinct absorption peaks in the adsorbed hydrogels: 1726 cm^{-1} corresponding to the stretching vibration peak of the amide $\text{C}=\text{O}$, 1514 cm^{-1} corresponding to the stretching vibration peak of $\text{C}-\text{N}$, 1311 cm^{-1} corresponding to the characteristic absorption peak of tertiary amine groups, and 3711 cm^{-1} corresponding to the characteristic peak of $\text{O}-\text{H}$. It

is worth noting that the tertiary amines on the hydrogel undergo protonation in aqueous solution, forming hydroxyl groups that bind with cadmium ions to form cadmium hydroxide precipitates, thereby enabling the hydrogel to encapsulate the cadmium. The hydrogel can be potentially applied in the form of tea bags for the removal of cadmium from soil through adsorption and precipitation, without altering the soil's acidity and alkalinity characteristics.

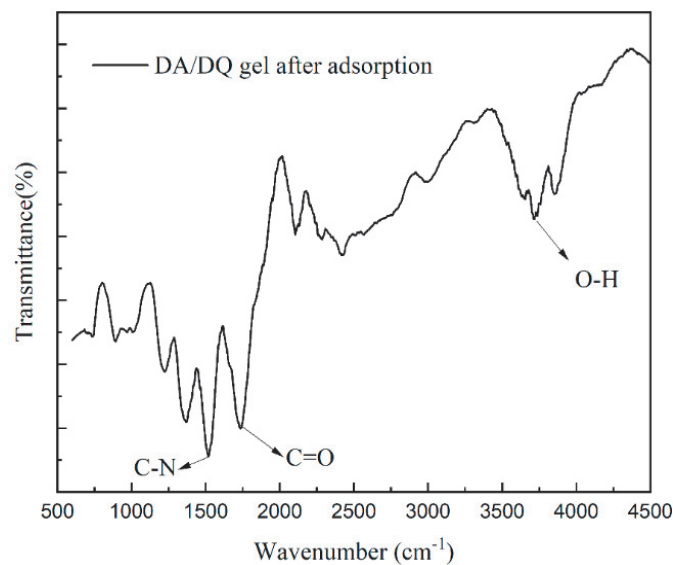


Figure 2.6 FTIR spectrum of hydrogel after adsorption at 600-4500

2.67 Physical picture of vegetable growth

This study recorded the growth status of plants using cameras, as shown in Figure 2.7. The results indicate that the addition of the hydrogel significantly improves the growth conditions of Swiss chard, presenting a larger growth status. This suggests that the application of the hydrogel has a positive promoting effect on plant growth under normal conditions and cadmium stress. This promoting effect has two main aspects: firstly, the hydrogel possesses a three-dimensional network structure. When added to the soil, it can absorb a large amount of water, keeping the soil moist, which is conducive to the reproduction of microorganisms and provides a more favorable growth environment. At the same time, the expansion of the hydrogel in the soil increases the gaps between soil particles, facilitating the respiration of roots, thus enhancing the growth rate of Swiss

chard. Secondly, the DMAPAA/DMAPAAQ composite hydrogels could adsorb cadmium, reducing the biotoxicity of cadmium to vegetables and significantly improving the growth condition of vegetables.

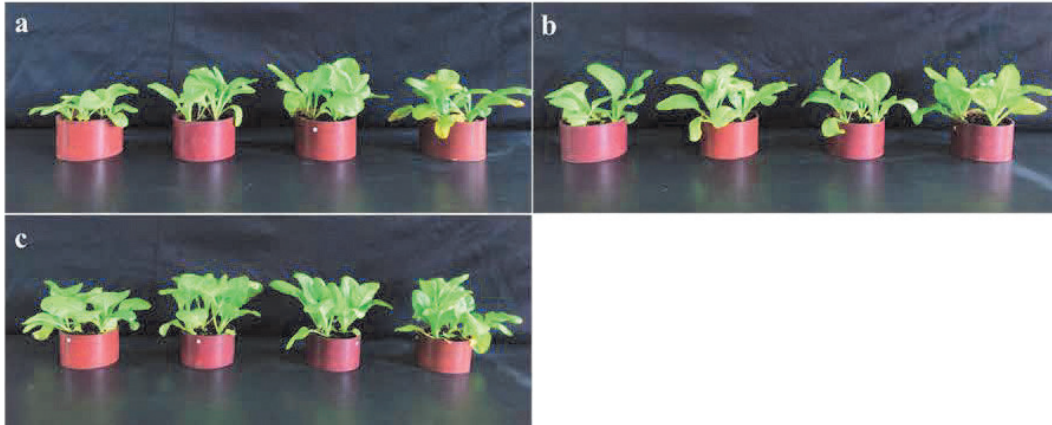


Figure 2.7 Physical image of vegetable growth, (a), (b), and (c); the addition of hydrogel is 0%, 2%, 4%. From left to right, the amount of cadmium added is 500, 50, 5 mg/kg, 0 mg/kg.

2.68 Shoot dry Weight.

The dry weight of Swiss chard shoots was measured using an electronic balance, as shown in Figure 2.8. The results revealed that, with an increase in the amount of hydrogel added, the dry weight of Swiss chard shoots also exhibited an increasing trend. Under low cadmium concentration conditions (less than 50mg/kg), when the hydrogel addition was 4%, the maximum dry weight reached 0.765g, which was 2.5 times higher compared to the situation without hydrogel addition. However, at a cadmium concentration of 500mg/kg, with 4% hydrogel addition, the dry weight increased with the amount of hydrogel used, reaching a maximum value of approximately 0.503g and a minimum value of 0.145g. This indicates that the hydrogel not only possesses a capacity for cadmium adsorption, but also enhances the moisture retention ability of soil, thereby increasing the vegetable's yield. The dry weight of plants mainly comprises organic matter and trace elements. By assessing the dry weight of plants, we can accurately determine the content of elements such as carbon, hydrogen, and oxygen. This further contributes to a comprehensive evaluation of plant growth conditions and soil fertility.

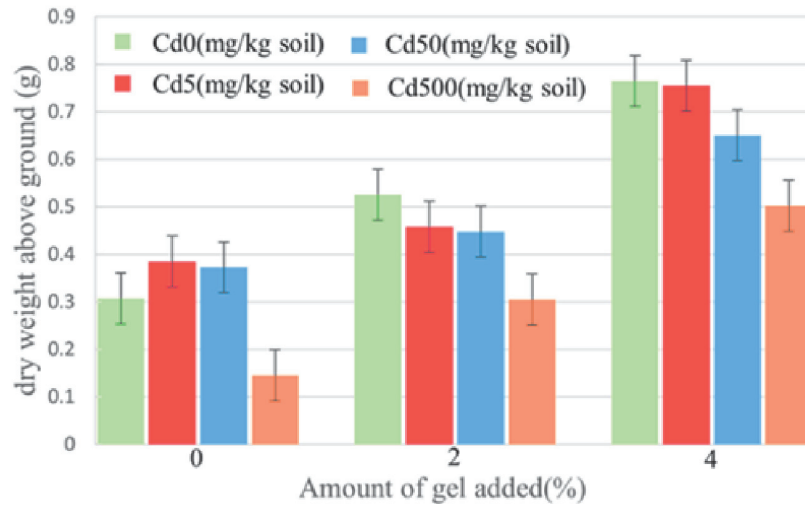


Figure 2.8 Dry weight of Swiss chard shoots.

2.69 Cadmium uptake in swiss chard

The cadmium content in Swiss chard was measured using ICP, as shown in Figure 2.9. As the amount of hydrogel added increased, the absorption of cadmium in Swiss chard gradually decreased. Under low cadmium concentration conditions (less than 50mg/kg), the absorption of cadmium by Swiss chard was undetectable when no hydrogel was added, indicating that the soil had a certain fixation effect on cadmium. When the cadmium concentration increased to 500mg/kg, the absorption of cadmium by Swiss chard increased significantly, but as the amount of hydrogel added increased, the absorption of cadmium by Swiss chard gradually decreased. Specifically, without the addition of the hydrogel, the absorption of cadmium by Swiss chard was 0.075mg/g, while when the hydrogel addition was 4%, the absorption of cadmium by Swiss chard decreased to 0. This indicates that the addition of a hydrogel can effectively inhibit the absorption of heavy metal cadmium by Swiss chard. These results demonstrate that the application of hydrogels has a significant effect on reducing the absorption of cadmium in soil by vegetables and plays a positive role in reducing the phytotoxicity of heavy metal cadmium to plants.

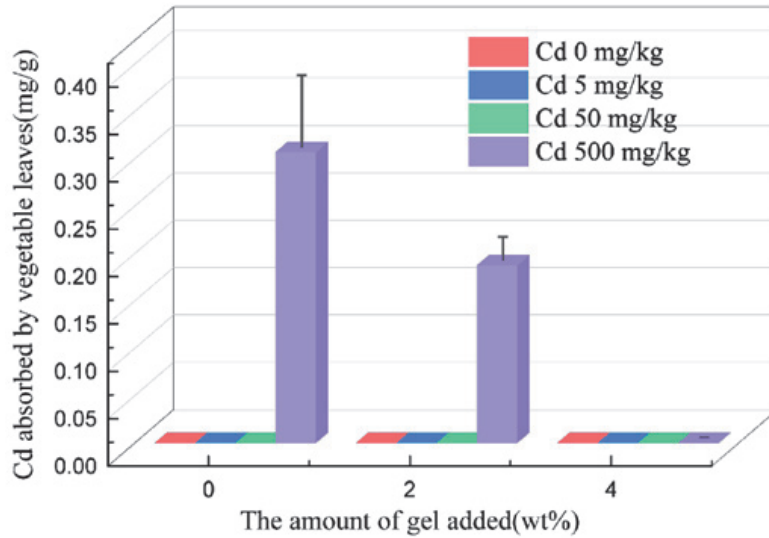
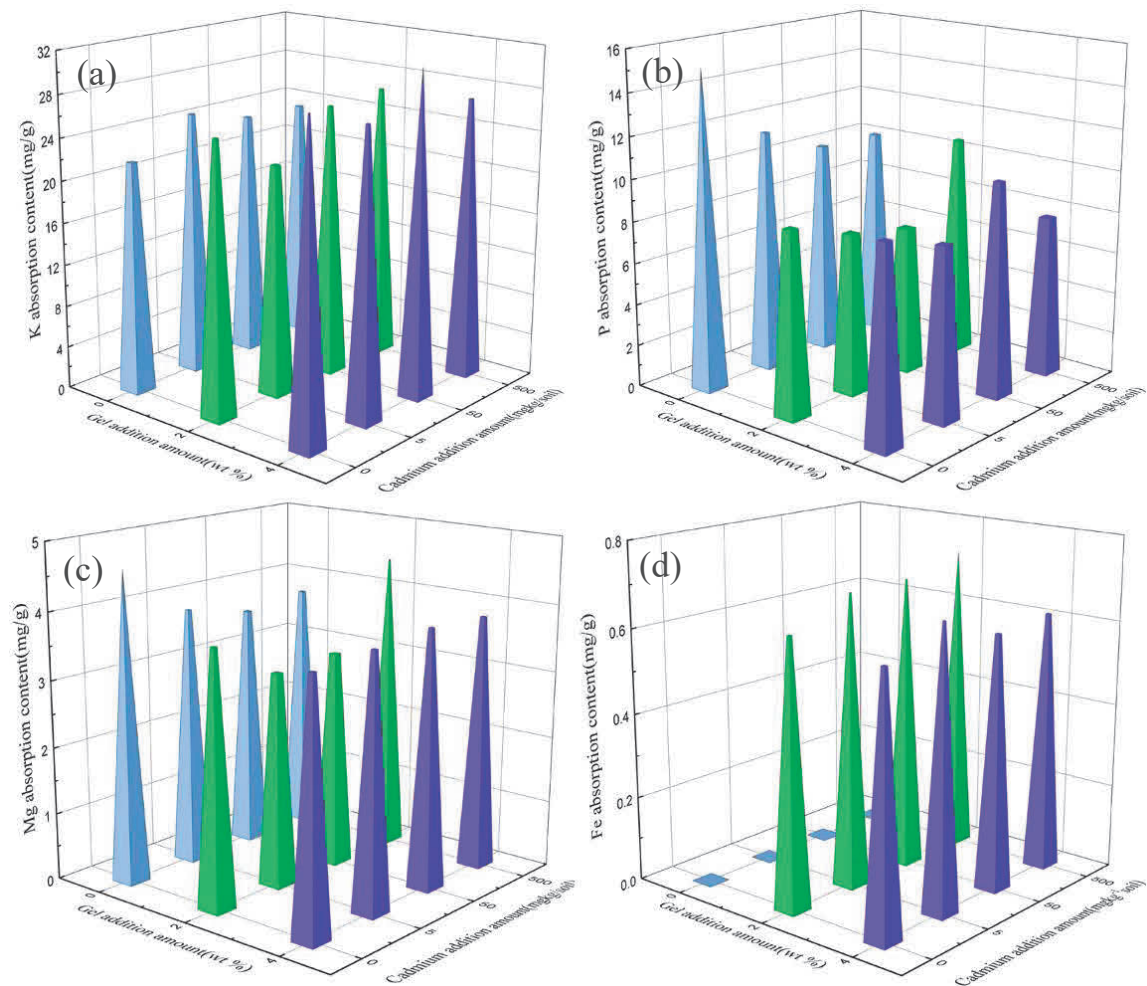


Figure 2.9 Cadmium absorption by Swiss chard shoots.

2.7 Other Elements

In this study, the content of elements in Swiss chard was analyzed utilizing Inductively Coupled Plasma (ICP) measurement techniques. Among them, potassium (K), phosphorus (P), and magnesium (Mg) emerged as pivotal elements in the photosynthetic process, and it is possible that the chemical reactions involved in these elements increased the sugar content in the plant. The main elements in sugar are C, H and O. Plants convert light energy into organic matter and store it in their bodies through photosynthesis. The introduction of hydrogels in the study holds significance regarding the exploration of their impact on plant photosynthesis. The application of hydrogels may enhance the efficiency of plant photosynthesis. This revelation holds substantial implications for future studies relating to the accumulation of organic compounds within plant organisms. In particular, there is broad applicative potential for using hydrogels in the cultivation of plants such as corn near mining areas. Furthermore, the study found that, in soil with a raised iron content, plants exhibited a notable deficiency in iron absorption when the hydrogel was not incorporated, resulting in leaf chlorosis. Contrastingly, with the introduction of the hydrogel, there was a significant increase in the iron content within plant tissues (Figure2.10). This indicates that the addition of hydrogels induces a shift in the utilization pattern of soil-bound iron, potentially by facilitating the adhesion

of metallic ions to the surface of the hydrogel. Concurrently, plants release low-molecular-weight acids from their roots, promoting the reduction of trivalent iron to a more readily absorbable divalent state. Building upon this revelation, the cocultivation of seaweed with a hydrogel and iron supplements emerges as a potential technique, given the substantial iron demands of seaweed. Additionally, elements such as Ca, Cu, and Zn stand out as essential elements, Na is beneficial to some plants at a certain concentration. Monitoring the contents of these elements provides a means to assess the growth status and nutritional condition of plants, thereby providing a scientific basis for the optimization of cultivation environments.



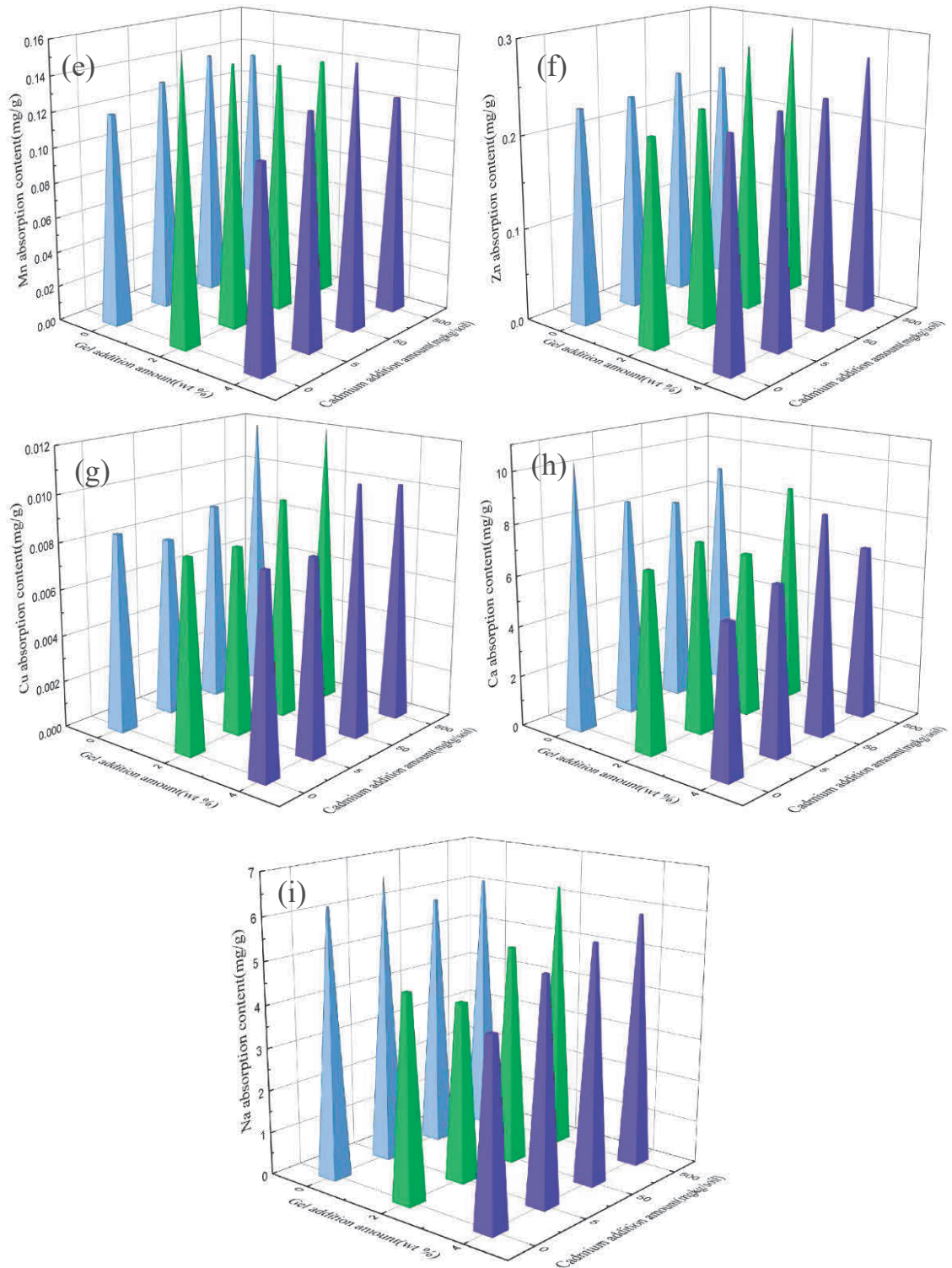


Figure 2.10 Contents of various elements in vegetable leaves: (a) Potassium; (b) Phosphorus; (c) Magnesium; (d) Iron; (e) Manganese; (f) Zinc; (g) Copper; (h) Calcium; (i) Sodium.

2.8 Discussion

The use of hydrogels for the adsorption of heavy metals in water primarily relies on the functional groups on the surface of the hydrogel. Cadmium is a harmful heavy metal substance. Cadmium salts undergo hydrolysis in water, typically resulting in an acidic solution. In acidic solutions, the amine groups on the surface of the hydrogel sequester protons from the solution, increasing the positive charge on the hydrogel surface. Due to the same charges, this leads to hydrogel expansion [29-31]. At this point, the hydrogel primarily complexes and adsorbs cadmium with chloride ions. Under alkaline conditions, the hydrogel volume contracts, exhibiting pH responsiveness. This property finds widespread application in areas such as drug antimicrobial compounds and fertilizer release [32-36]. In neutral solutions, the tertiary amine group of DMAPAA is protonated in water to form OH^- ions. DMAPAAQ will exchange cadmium-containing anion compounds through ion exchange, such as nitrate ions and phosphate ions. These ions are useful nutrients for plants in the soil. Chloride ions are also released. Then chloride ions and OH^- through the ion exchange method let OH^- ions combines with the protonated tertiary amine group of DMAPAA. Finally, OH^- ions adsorb Cd ions to form cadmium hydroxide precipitate, which is wrapped by hydrogel. The adsorption mechanism is shown in Figure 2.11. This method exhibits good responsiveness to different pH conditions in the process of remediating the heavy metal cadmium. Additionally, this strategy holds broad applicative potential in areas such as drug antimicrobial compounds and fertilizer release. Introducing the hydrogel into soil, which is rich in elements like iron and manganese, leads to its expansion due to its water-absorbing properties. This, in turn, enlarges the gaps between soil particles, promoting oxidation reactions. During the oxidation process, the manganese and iron in the soil undergo oxidation reactions, forming manganese oxide ($\text{MnO}_2/\text{Mn}_2\text{O}_3$) and iron oxide ($\text{Fe}(\text{OH})_3/\text{FeOOH}$) [37]. In this process, some heavy metal ions, such as cadmium, precipitate together with the oxides. Furthermore, the silicon and cadmium in the soil also undergo chelation, forming a Si–Cd structure to stabilize the cadmium ions [38]. The application of a hydrogel to the soil mainly enhances the plant yield via two processes: Firstly, plant growth relies on the process of photosynthesis, where chlorophyll absorbs sunlight and converts it into chemical energy through a series of chemical reactions, storing it in the form of biomass.

Introducing a hydrogel into the soil forms a colloidal structure, widening the gaps between soil particles and enhancing the plant's ability to absorb water. Additionally, hydrogels possess certain water-retaining properties, gradually releasing water to provide plants with more moisture and nutrients. Secondly, under neutral conditions, hydrogels exhibit a certain capacity for adsorbing heavy metals. Furthermore, they do not alter the pH value of the soil, effectively preventing soil acidification. Moreover, considering that soil is a highly complex environment with a diverse range of microbial species, the water-retaining property of hydrogels provides favorable conditions for microbial activity. For instance, microorganisms like *Rhizobium pusense* and *Bacillus* spp. can not only dissolve metals but can also participate in the oxidation and reduction processes of metals [39]. In summary, the application of hydrogels to soil plays a crucial role in promoting plant growth and increasing yield. Additionally, it provides favorable conditions for the environmental protection and microbial activity of soil [40].

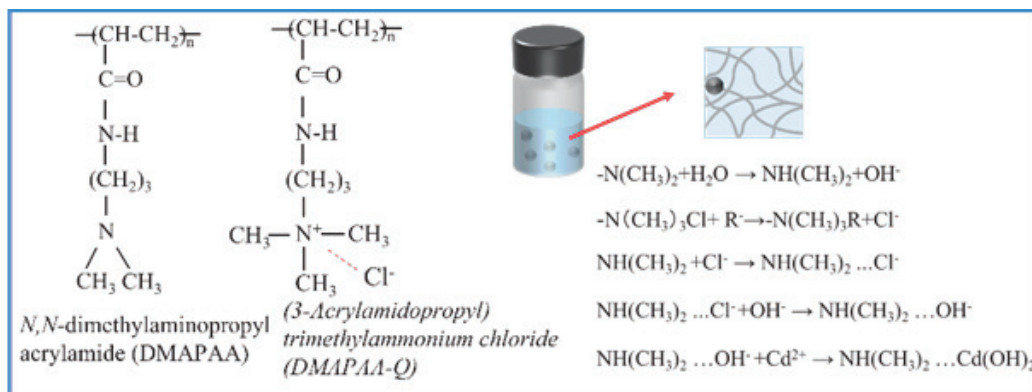


Figure 2.11 Mechanism diagram of hydrogel adsorption of heavy metals.

2.9 Conclusion

In this study, DMAPAA/DMAPAAQ hydrogels were successfully synthesized using the free radical polymerization method, and their adsorption performance was comprehensively evaluated under different pH values and cadmium concentrations. The results show that the hydrogels exhibited an excellent cadmium capture performance under neutral conditions. we used the Langmuir model to fit the data and obtained a

correlation coefficient as high as 0.97, indicating that the Langmuir model is more suitable for describing the process of capture cadmium in hydrogels. Under neutral conditions, cadmium is wrapped to the hydrogel mainly through the precipitation of cadmium hydroxide formed by OH⁻, which is generated via the protonation of the tertiary amine on the hydrogel structure in water. We added the hydrogel to soil and observed the growth of Swiss chard under cadmium stress. Under low-concentration cadmium conditions (less than 50 mg/kg), when the added amount of hydrogel was 4%, the dry weight of Swiss chard reached up to 0.765 g, which is 2.5 times higher than when no hydrogel was added. When the cadmium concentration reached 500 mg/kg and the hydrogel addition amount was 4%, the dry weight of Swiss chard increased with the increase in the amount of hydrogel, reaching a maximum of 0.503g and a minimum of 0.145g. Under high-cadmium concentration conditions (500 mg/kg), when no hydrogel was added, the cadmium absorbed by Swiss chard was 0.075 mg/g. After adding 4% hydrogel, the absorption of cadmium by Swiss chard dropped to an undetectable level. In summary, the results of this study show that in a cadmium-polluted environment, the use of DMAPAA/DMAPAAQ hydrogels can effectively promote the growth of vegetables and enhance the cadmium immobilize capacity of hydrogel in soil. To further enhance the soil adsorption capacity of cadmium, future research could consider the combined application of hydrogels with microorganisms or various wastes, such as steel slag, seaweed, animal manure, and plant ash.

References

1. Diarra, Ivan, and Surendra Prasad. "The Current State of Heavy Metal Pollution in Pacific Island Countries: A Review." *Applied Spectroscopy Reviews* 56, no. 1 (2020): 27-51.
2. Barsova, N., O. Yakimenko, I. Tolpeshta, and G. Motuzova. "Current State and Dynamics of Heavy Metal Soil Pollution in Russian Federation-a Review." *Environ Pollut* 249 (2019): 200-07.

3. Arunakumara, K. K. I. U., Buddhi Charana Walpola, and Min-Ho Yoon. "Current Status of Heavy Metal Contamination in Asia's Rice Lands." *Reviews in Environmental Science and Bio/Technology* 12, no. 4 (2013): 355-77.
4. Wang, L., X. Cui, H. Cheng, F. Chen, J. Wang, X. Zhao, C. Lin, and X. Pu. "A Review of Soil Cadmium Contamination in China Including a Health Risk Assessment." *Environ Sci Pollut Res Int* 22, no. 21 (2015): 16441-52.
5. Qi, M., Y. Wu, S. Zhang, G. Li, and T. An. "Pollution Profiles, Source Identification and Health Risk Assessment of Heavy Metals in Soil near a Non-Ferrous Metal Smelting Plant." *Int J Environ Res Public Health* 20, no. 2 (2023).
6. Ma, H., M. Mi, C. Wang, X. Wu, and Z. Zhen. "The Concentrations, Sources, Ecological, and Human Health Risk Assessment of Heavy Metals in Roadside Soils of Six Cities in Shanxi Province, China." *Environ Toxicol Chem* 42, no. 7 (2023): 1485-500.
7. Zhang, Yunxia, Bo Song, and Ziyang Zhou. "Pollution Assessment and Source Apportionment of Heavy Metals in Soil from Lead – Zinc Mining Areas of South China." *Journal of Environmental Chemical Engineering* 11, no. 2 (2023).
8. Azhar, U., H. Ahmad, H. Shafqat, M. Babar, H. M. Shahzad Munir, M. Sagir, M. Arif, A. Hassan, N. Rachmadona, S. Rajendran, M. Mubashir, and K. S. Khoo. "Remediation Techniques for Elimination of Heavy Metal Pollutants from Soil: A Review." *Environ Res* 214, no. Pt 4 (2022): 113918.
9. Khalid, Sana, Muhammad Shahid, Nabeel Khan Niazi, Behzad Murtaza, Irshad Bibi, and Camille Dumat. "A Comparison of Technologies for Remediation of Heavy Metal Contaminated Soils." *Journal of Geochemical Exploration* 182 (2017): 247-68.
10. Aparicio, Juan Daniel, Enzo Emanuel Raimondo, Juliana María Saez, Stefanie Bernardette Costa-Gutierrez, Analía Álvarez, Claudia Susana Benimeli, and Marta Alejandra Polti. "The Current Approach to Soil Remediation: A Review of Physicochemical and Biological Technologies, and the Potential of Their Strategic Combination." *Journal of Environmental Chemical Engineering* 10, no. 2 (2022).

11. Sharma, S., S. Tiwari, A. Hasan, V. Saxena, and L. M. Pandey. "Recent Advances in Conventional and Contemporary Methods for Remediation of Heavy Metal-Contaminated Soils." *3 Biotech* 8, no. 4 (2018): 216.
12. Yao, Zhitong, Jinhui Li, Henghua Xie, and Conghai Yu. "Review on Remediation Technologies of Soil Contaminated by Heavy Metals." *Procedia Environmental Sciences* 16 (2012): 722-29.
13. Navarro, Andrés, Esteve Cardellach, Inmaculada Cañadas, and José Rodríguez. "Solar Thermal Vitriification of Mining Contaminated Soils." *International Journal of Mineral Processing* 119 (2013): 65-74.
14. Khan, F. I., T. Husain, and R. Hejazi. "An Overview and Analysis of Site Remediation Technologies." *J Environ Manage* 71, no. 2 (2004): 95-122.
15. Lawrence K. Wang, PhD, PE, DEE. "Physicochemical Treatment Processes." *HANDBOOK OF ENVIRONMENTAL ENGINEERING* 3.
16. Rozas, E. E., M. A. Mendes, C. A. Nascimento, D. C. Espinosa, R. Oliveira, G. Oliveira, and M. R. Custodio. "Bioleaching of Electronic Waste Using Bacteria Isolated from the Marine Sponge *Hymeniacidon Heliophila* (Porifera)." *J Hazard Mater* 329 (2017): 120-30.
17. Wawrzekiewicz, Monika, and Zbigniew Hubicki. "Anion Exchange Resins as Effective Sorbents for Removal of Acid, Reactive, and Direct Dyes from Textile Wastewaters." In *Ion Exchange - Studies and Applications*, 2015.
18. Saber-Samandari, Samaneh, Saeed Saber-Samandari, and Mustafa Gazi. "Cellulose-Graft-Polyacrylamide/Hydroxyapatite Composite Hydrogel with Possible Application in Removal of Cu (II) Ions." *Reactive and Functional Polymers* 73, no. 11 (2013): 1523-30.
19. Li, Peiyi, Miaomiao Zhou, Hezhen Liu, Haozhe Lei, Boxing Jian, Ruiyan Liu, Xinping Li, Yun Wang, and Bingyao Zhou. "Preparation of Green Magnetic Hydrogel from Soybean Residue Cellulose for Effective and Rapid Removal of Copper Ions from Wastewater." *Journal of Environmental Chemical Engineering* 10, no. 5 (2022).

20. Darban, Zenab, Syed Shahabuddin, Rama Gaur, Irfan Ahmad, and Nanthini Sridewi. "Hydrogel-Based Adsorbent Material for the Effective Removal of Heavy Metals from Wastewater: A Comprehensive Review." *Gels* 8, no. 5 (2022).
21. Hashem, Ali, Chukwunonso Onyeka Aniagor, Mohamed Abdel-Fattah Afifi, Ashraf Abou-Okeil, and Sayed Hussein Samaha. "Synthesis of Super-Absorbent Poly(an)-G-Starch Composite Hydrogel and Its Modelling for Aqueous Sorption of Cadmium Ions." *Korean Journal of Chemical Engineering* 38, no. 10 (2021): 2157-70.
22. Zhang, Peng, Kui Zou, Li Yuan, Jing Liu, Bingzhi Liu, Tai-Ping Qing, and Bo Feng. "A Biomass Resource Strategy for Alginate-Polyvinyl Alcohol Double Network Hydrogels and Their Adsorption to Heavy Metals." *Separation and Purification Technology* 301 (2022).
23. Hu, Z. H., A. M. Omer, X. K. Ouyang, and D. Yu. "Fabrication of Carboxylated Cellulose Nanocrystal/Sodium Alginate Hydrogel Beads for Adsorption of Pb(II) from Aqueous Solution." *Int J Biol Macromol* 108 (2018): 149-57.
24. Liu, Y., Y. Huang, C. Zhang, W. Li, C. Chen, Z. Zhang, H. Chen, J. Wang, Y. Li, and Y. Zhang. "Nano-Fes Incorporated into Stable Lignin Hydrogel: A Novel Strategy for Cadmium Removal from Soil." *Environ Pollut* 264 (2020): 114739.
25. Zhou, T., M. Zhao, X. Zhao, Y. Guo, and Y. Zhao. "Simultaneous Remediation and Fertility Improvement of Heavy Metals Contaminated Soil by a Novel Composite Hydrogel Synthesized from Food Waste." *Chemosphere* 275 (2021): 129984.
26. Dhiman, Jaskaran, Shiv O. Prasher, Eman ElSayed, Ramanbhai M. Patel, Christopher Nzediegwu, and Ali Mawof. "Effect of Hydrogel Based Soil Amendments on Heavy Metal Uptake by Spinach Grown with Wastewater Irrigation." *Journal of Cleaner Production* 311 (2021).
27. Hou, X., Y. Li, Y. Pan, Y. Jin, and H. Xiao. "Controlled Release of Agrochemicals and Heavy Metal Ion Capture Dual-Functional Redox-Responsive Hydrogel for Soil Remediation." *Chem Commun (Camb)* 54, no. 97 (2018): 13714-17.

28. Tran, H. N., S. J. You, A. Hosseini-Bandegharai, and H. P. Chao. "Mistakes and Inconsistencies Regarding Adsorption of Contaminants from Aqueous Solutions: A Critical Review." *Water Res* 120 (2017): 88-116.
29. Zhou, N., X. Cao, X. Du, H. Wang, M. Wang, S. Liu, K. Nguyen, K. Schmidt-Rohr, Q. Xu, G. Liang, and B. Xu. "Hyper-Crosslinkers Lead to Temperature- and Ph-Responsive Polymeric Nanogels with Unusual Volume Change." *Angew Chem Int Ed Engl* 56, no. 10 (2017): 2623-27.
30. Freire, J. J., A. Ahmadi, and C. McBride. "Molecular Dynamics Simulations of the Protonated G4 Pamam Dendrimer in an Ionic Liquid System." *J Phys Chem B* 117, no. 48 (2013): 15157-64.
31. Geng, Wenda, Juncong Zou, Qiuya Niu, Yan Lin, Haiyang Liu, Yachao Jing, and Chunping Yang. "Recovery of Magnesium from Flue Gas Desulfurization Wastewater Using Thermomorphic Hydrophilicity Amines." *Separation and Purification Technology* 316 (2023).
32. Schmaljohann, D. "Thermo- and Ph-Responsive Polymers in Drug Delivery." *Adv Drug Deliv Rev* 58, no. 15 (2006): 1655-70.
33. Rizwan, M., R. Yahya, A. Hassan, M. Yar, A. D. Azzahari, V. Selvanathan, F. Sonsudin, and C. N. Abouloula. "Ph Sensitive Hydrogels in Drug Delivery: Brief History, Properties, Swelling, and Release Mechanism, Material Selection and Applications." *Polymers (Basel)* 9, no. 4 (2017).
34. Shaghaleh, Hiba, Yousef Alhaj Hamoud, Xu Xu, Shifa Wang, and He Liu. "A Ph-Responsive/Sustained Release Nitrogen Fertilizer Hydrogel Based on Aminated Cellulose Nanofiber/Cationic Copolymer for Application in Irrigated Neutral Soils." *Journal of Cleaner Production* 368 (2022).
35. Azeem, Muhammad Khalid, Atif Islam, Muhammad Rizwan, Atta Rasool, Nafisa Gul, Rafi Ullah Khan, Shahzad Maqsood Khan, and Tahir Rasheed. "Sustainable and Environment Friendlier Carrageenan-Based Ph-Responsive Hydrogels: Swelling Behavior and Controlled Release of Fertilizers." *Colloid and Polymer Science* 301, no. 3 (2023): 209-19.
36. Ravikumar, T., H. Murata, R. R. Koepsel, and A. J. Russell. "Surface-Active Antifungal Polyquaternary Amine." *Biomacromolecules* 7, no. 10 (2006): 2762-9.

37. Turner, A., S. M. Le Roux, and G. E. Millward. "Adsorption of Cadmium to Iron and Manganese Oxides During Estuarine Mixing." *Marine Chemistry* 108, no. 1-2 (2008): 77-84.
38. Khan, I., S. A. Awan, M. Rizwan, S. Ali, M. J. Hassan, M. Brestic, X. Zhang, and L. Huang. "Effects of Silicon on Heavy Metal Uptake at the Soil-Plant Interphase: A Review." *Ecotoxicol Environ Saf* 222 (2021): 112510.
39. Zulfiqar, U., F. U. Haider, M. F. Maqsood, W. Mohy-Ud-Din, M. Shabaan, M. Ahmad, M. Kaleem, M. Ishfaq, Z. Aslam, and B. Shahzad. "Recent Advances in Microbial-Assisted Remediation of Cadmium-Contaminated Soil." *Plants (Basel)* 12, no. 17 (2023).
40. Nassaj-Bokharaei, S., B. Motesharezedeh, H. Etesami, and E. Motamedi. "Effect of Hydrogel Composite Reinforced with Natural Char Nanoparticles on Improvement of Soil Biological Properties and the Growth of Water Deficit-Stressed Tomato Plant." *Ecotoxicol Environ Saf* 223 (2021): 112576.

Chapter 3 Functional hydrogel promotes vegetable growth in cadmium-contaminated soil.

3.1 Introduction

The escalating process of global industrialization has given rise to a concerning surge in the presence of heavy metals in soil [1, 2]. Among these metals, cadmium, a member of the second group of the periodic table, stands out for its pronounced toxicity and classification as one of the most hazardous elements. While the concentration of cadmium in natural soil has a limited impact on human health, anthropogenic activities such as atmospheric pollution, sewage irrigation, and excessive use of chemical fertilizers have led to the accumulation of cadmium in soil, heightening the risk it poses to human health [3, 4]. Recent scientific reports reveal that heavy metal pollution has affected approximately 500,000 sites in Europe and over 60,000 hectares of land in the United States [5-7]. Given that heavy metals enter the food chain through soil and plant uptake, they present a severe threat to human health. Consequently, maintaining unpolluted soil is paramount for safeguarding the overall ecological environment and ensuring human well-being [8].

Addressing cadmium contamination in soil has underscored the growing importance of soil remediation techniques. Various methods, including physical, chemical, and biological approaches, have been employed, utilizing a diverse range of materials such as household discards, nanomaterials, and biomass materials. Among these, living discards like eggshells, shells, oysters, and oyster shells have garnered attention for their calcium content, offering a potential substitute for cadmium in plants [9-11]. Research has demonstrated that the addition of shell powder to cadmium-contaminated soil can elevate soil pH and diminish cadmium accumulation in crops, as exemplified by the synergistic application of biochar and oyster shell [12, 13]. For instance, introducing coconut shell biochar into soil alongside earthworms resulted in the removal of 94.38% of total cadmium from soil samples [14]. These findings highlight the promise of these materials as effective tools for remediating cadmium-contaminated soil.

The detrimental impact of cadmium contamination in soil has spurred the exploration of novel materials for its remediation, with nanoparticles gaining significant attention due to their substantial specific surface area and numerous surface-active sites [15, 16]. For example, Watanabe et al. applied zero-valent iron to Cd-contaminated rice fields, observing a 10-20% decrease in Cd concentrations in seeds and leaves [17]. Similarly, Natasha Manzoor et al. utilized FeO nanoparticles to treat Cd-contaminated soil, resulting in a notable 72.5% reduction in Cd uptake by wheat plants [18]. CuO nanoparticles have also exhibited potential in mitigating Cd toxicity, with low concentrations (5 mg/L) leading to reduced Cd uptake in rice and barley plants [19]. Additionally, the use of zinc sulfate has demonstrated a 19-28% reduction in Cd concentrations in spinach leaves and a substantial 42% reduction in roots [20]. These findings underscore the efficacy of nanoparticles and other materials in remediating Cd-contaminated soil.

Biomass, derived from organic matter through photosynthesis, encompasses a diverse array of materials, including plants, animals, their excreta, garbage, and organic wastewater. The presence of hydroxyl and carboxyl groups in biomass materials renders them excellent adsorbents for heavy metals. For example, sludge, rich in organic materials and soluble ions, can effectively enhance soil pH. Bovine manure biochar, characterized by its porous structure and negatively charged surface, has demonstrated efficacy in removing heavy metals from soil through electrostatic adsorption [21, 22]. Field experiments conducted by Atsushi Sato et al. showed that the addition of animal manure resulted in a 34-38% reduction in cadmium concentration in spinach compared to the use of chemical fertilizers [21]. Furthermore, the addition of humic acid and stainless-steel slag to soil led to a 16.30% reduction in total cadmium concentrations and a 58.04% reduction in available cadmium concentrations, as reported by Lin et al. [23]. Research by Evanise Silva Penido et al. revealed that the addition of wood biochar and biochar derived from sewage sludge to soil increased soil pH, effectively mitigating the impact of cadmium contamination [24]. These studies underscore the potential of various biomass materials in the remediation of cadmium-contaminated soil.

While various materials show promise in mitigating cadmium contamination in soil, certain limitations hinder their widespread application. Some materials are not produced

on a large scale, and their adsorption of cadmium may alter its form in the soil without complete removal. Moreover, these materials often serve a singular function, primarily fixing cadmium without actively promoting plant growth. Additionally, under conditions such as acid rain or elevated carbon dioxide concentrations, the form of cadmium may change, potentially leading to its release into the environment. The emergence of superabsorbent gel as a novel polymer material for soil remediation presents a promising solution. Its hydrophilic three-dimensional mesh structure enables it to absorb and retain water solutions up to hundreds of times its weight. Beyond its capacity to adsorb heavy metals in the soil, this gel improves soil moisture, providing plants with ample water to expedite their growth cycles [25, 26]. Studies have highlighted the potential effectiveness of this material in mitigating cadmium contamination in soil. For instance, Liu et al. developed a ferrous sulfide (FeS) nanoparticle lignin hydrogel composite with a Cd adsorption capacity of 833.3 g/kg. Wei et al. applied FeS@LH to Cd-contaminated rice fields, resulting in the removal of 36.6% of Cd in soil and 34.5% of cadmium in water spinach after 30 days of treatment [27, 28]. Zhou et al. also introduced a novel soil remediation agent, a composite hydrogel (LR-g-PAA/MMT/urea), demonstrating significant reduction rates of Cu, Pb, and Zn in the residual state [29].

In this study, we successfully synthesized two types of hydrogels, namely DMAPAA/DMAPAAQ and DMAA, using a free radical polymerization method. The main objective of this research was to explore the effects of incorporating these hydrogels into soil and comprehensively evaluate the growth of vegetables under cadmium stress or without cadmium. Specifically, we focused on investigating the impact of adding DMAPAA/DMAPAAQ ionic hydrogel on vegetable growth under cadmium stress, as well as the effects of DMAA non-ionic hydrogel and DMAPAA/DMAPAAQ ionic hydrogel on vegetable growth without cadmium. We conducted a comprehensive assessment of the influence of these two hydrogels on plant growth by measuring the dry weight of the vegetables. Additionally, we evaluated the amount of cadmium absorbed by the vegetables when DMAPAA/DMAPAAQ was added to the soil under cadmium stress. Finally, we conducted an in-depth study on the content of elements in plants under the combined influence of hydrogels and cadmium. This comprehensive research aims to provide a deeper understanding of the application of hydrogels in vegetable cultivation

and to provide scientific evidence for regulating plant growth under cadmium stress in soil.

3.2 Materials and Methods

3.21 materials

The monomer DMAPAA/DMAPAAQ was obtained from KJ Chemicals Corporation (Tokyo, Japan), while N, N-dimethyl ethylenediamine (TEMED), HNO₃, and H₂O₂ were procured from Nacalai Tesque Co., Ltd. (Kyoto, Japan). DMAA is purchased at Tokyo chemical industry Co., LTD. (Tokyo, Japan), N, N'-methylenebisacrylamide (MBAA), ammonium persulfate (APS), and CdN₂O₈·H₂O, CdCl₂·2.5·H₂O were obtained from Sigma-Aldrich, Inc. (St. Louis, MO, USA). Additionally, 1 mol/L HCl solutions were purchased from Sigma-Aldrich Japan (Tokyo, Japan). The soil used in the study was acquired from NAFCO (Fukuoka, Japan). All reagents utilized were of analytical grade and used as received. Distilled water for the experiments was produced in the laboratory.

3.22 Synthesis of DMAPAA/DMAPAAQ hydrogel

To synthesize the hydrogel, 1.953 g of DMAPAA and 2.584 g of DMAPAAQ monomers were accurately weighed, along with 0.193 g of MBAA crosslinker and 0.058 g of TEMED accelerator. These components were combined in a 20 mL volumetric flask (refer to Table 3.1). Distilled water was then added to the flask, and the resulting mixture was stirred using a magnetic stirrer. In a separate 5 mL volumetric flask, a solution containing 0.114 g of APS initiator was prepared using distilled water. Both the monomer solution and the initiator solution underwent a 45-minute purge with nitrogen to eliminate any oxygen and prevent the inhibition of free radicals. Subsequently, the initiator solution was added to the monomer solution and stirred for 20 seconds. The resulting mixture was transferred to three plastic tubes using a pipette and immersed in an aqueous solution at 25°C for 24 hours. Afterward, the formed gels were removed from the tubes, cut into uniform cylindrical shapes, and washed with methanol for 24 hours using a Soxhlet extractor (Asahi Glass plant Inc., Arao City, Japan) to eliminate any unreacted

components. The gels were then air-dried at room temperature and further dried in a 50°C oven for 24 hours. Finally, the dried gels were ground into a powder using a grinder.

3.23 Synthesis of DMAA hydrogel

In the hydrogel synthesis process, 2.478 g of DMAA monomers were precisely measured and combined with 0.193 g of MBAA crosslinker and 0.058 g of TEMED accelerator in a 20 mL volumetric flask (refer to Table 3.2). Distilled water was added to the flask, and the resulting mixture was stirred using a magnetic stirrer. Concurrently, a solution containing 0.057 g of APS initiator was prepared in a separate 5 mL volumetric flask using distilled water. To eliminate any oxygen and prevent the inhibition of free radicals, both the monomer solution and initiator solution underwent a 45-minute nitrogen purge. Subsequently, the initiator solution was added to the monomer solution and stirred for 20 seconds. The resulting mixture was transferred to three plastic tubes using a pipette and immersed in an aqueous solution at 25°C for 24 hours. After the immersion period, the formed gels were extracted from the tubes, shaped into uniform cylindrical forms, and subjected to a 24-hour methanol wash using a Soxhlet extractor (Asahi Glass plant Inc., Arao City, Japan) to remove any unreacted components. Following this, the gels were air-dried at room temperature and further dried in a 50°C oven for 24 hours. Finally, the dried gels were finely ground into a powder using a grinder.

Table 3.1 Synthesis condition of the DMAPAA/DMAPAAQ hydrogel.

Materials	Component Type	Molar weight (g/mol)	concentration (mol/m ³)	mass(g)
DMAPAA	monomer	156.22	500	1.953
DMAPAA-Q	monomer	206.71	500	2.584
MBAA	linker	154.17	50	0.193
TEMED	accelerator	116.21	20	0.058
APS	Initiator	228.19	20	0.114

Table 3.2 Synthesis condition of the DMAA hydrogel.

Materials	Component Type	Molar weight (g/mol)	concentration (mol/m ³)	mass(g)
DMAA	monomer	99.13	1000	2.478
MBAA	linker	154.17	50	0.193
TEMED	accelerator	116.21	20	0.058
APS	Initiator	228.19	20	0.114

3.24. Experimental design

A total of 800 g of moist soil was accurately measured and transferred to a Neubauer pot with a precision of 1/10000a. Subsequently, varying concentrations (0%, 2%, and 4% w/w) of DMAPAA/DMAPAAQ and DMAA hydrogels were introduced into the soil. Additionally, CdCl₂ solutions at concentrations of 0, 2, and 500 mg/kg were incorporated into the soil which only containing DMAPAA/DMAPAAQ hydrogel. Another experimental group, the DMAPAA/DMAPAAQ and DMAA group, did not include cadmium. Thorough mixing was conducted to ensure the even distribution of cadmium and the hydrogel within the soil matrix. The soil was then allowed to reach a semi-moist state over a span of several days, following which it was divided into two equal portions. To facilitate plant growth, small holes were made in each of the four directions of the pot. Subsequently, four seeds of Swiss chard (*Beta vulgaris* L. var. *cicla*) were carefully placed in each hole.

3.25 Dry weight of vegetables

Following a two-month cultivation period in the greenhouse, the roots of eight Swiss chard plants were harvested by cutting them with scissors. The soil adhering to the roots was washed away with water. Subsequently, the harvested plants were carefully arranged in envelope bags and subjected to drying in an oven set at 70°C for several days until complete dryness was achieved. The electronic balance was then employed to measure the dry weights of the Swiss chard.

3.26 Plant digestion

The dried plant samples underwent crushing for 15 minutes at 700 rpm/min using a magnetic grinder (BMS-A20TP, Biomedical Science Corp., Tokyo, Japan). Subsequently, approximately 50 mg of each crushed sample was carefully weighed and recorded. Following this, 2 ml of nitric acid and 0.5 ml of hydrogen peroxide were added to each centrifuge tube, and the mixture underwent digestion using a heat block incubator (DTU-2BN, Taitec Corp., Saitama, Japan). The digestion process initiated at 80 °C for 30 minutes, followed by a gradual increase in temperature to 120 °C for 2 hours, and was left overnight in a fume hood. After digestion, the resulting solution was filtered through filter paper and adjusted to a volume of 25 ml in a volumetric flask. Finally, the concentration of various elements in the vegetables was determined using ICP.

3.27 Experiment on cadmium precipitation from soil

First, by preparing two separate 40-milliliter solutions utilizing 1 mol/L hydrochloric acid (HCl) and adjust their pH values to 2 and 7, respectively. Then, incorporate 4 grams of soil into each solution, achieving a solid-to-liquid ratio of 1:10. Stir the mixture on a shaker at 25 °C for 18 hours to ensure comprehensive and uniform mixing. Following this, filter the mixture through a 0.22-micrometer syringe filter to obtain a clear solution. Lastly, utilize inductively coupled plasma (ICP) mass spectrometry to measure the concentration of cadmium in the solution.

3.28 Characterization

The concentration of the heavy metal cadmium in the solution was determined through ICP (SPS-3500, Shimadzu Corp., Kyoto, Japan). The daily growth of the vegetables was monitored and recorded using a high-resolution camera (Xiaomi12 Technology Co., Ltd., China). Additionally, the elemental concentration of the vegetables was analyzed using ICP. The pH of the soil was measured with precision using a pH meter (Hanna Groline Soil pH Tester HI981030). Further characterization of the soil

properties was conducted through EDX analysis (EDX-7000, Shimadzu Corp., Kyoto, Japan).

3.3 Result and Discussion

3.31 Detection of elements in soils

For elemental composition analysis of the soil, we employed EDX (EDX-7000 energy dispersive XRF spectrometers) detection method, and the detection results are illustrated in Figure 3.1. Silicon and iron emerged as the predominant elements in the soil samples, collectively constituting over 50% of the total composition. It is noteworthy that the presence of manganese and iron can exert an influence on the availability of cadmium in the soil. This influence is facilitated through the oxidation process of these elements, resulting in the formation of manganese oxide ($\text{MnO}_2/\text{Mn}_2\text{O}_3$) and iron oxide ($\text{Fe}(\text{OH})_3/\text{FeOOH}$). In this process, heavy metal ions of cadmium coprecipitate with manganese oxide and iron oxide, impeding their release from the soil and consequently diminishing the toxicity of cadmium to plants. Moreover, silicon reacts with cadmium, leading to the formation of cadmium silicate precipitates. This reaction effectively diminishes the content of highly active exchangeable cadmium in the soil, thereby mitigating its biological toxicity. This series of processes contributes to the optimization of the soil environment, ultimately enhancing the health of the plant growth environment.

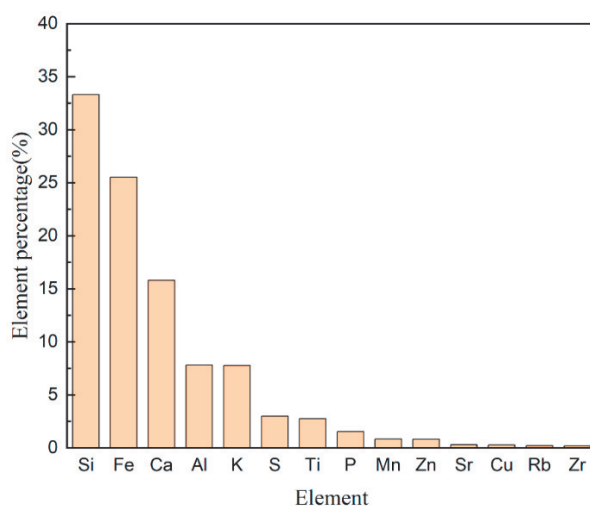


Figure 3.1 Elements in Soil.

3.32 Soil pH

The pH value of the soil, depicted in Figure 3.2 and measured using a pH meter, exhibited a slight increase with the addition of hydrogel, indicating that the introduction of the polymer contributes to an improvement in soil pH. The hydrogel, being a three-dimensional network polymer, possesses the capability to absorb water exceeding its own weight, thereby aiding in the maintenance of soil moisture. As the cadmium concentration in the soil increased, a slight decrease in pH was observed, signifying that cadmium induced hydrogen ion exchange within the soil. This exchange led to the release of hydrogen ions, resulting in a subtle decrease in soil pH. However, overall, the variation in soil pH remained minimal, consistently maintaining a balanced state at pH 7.

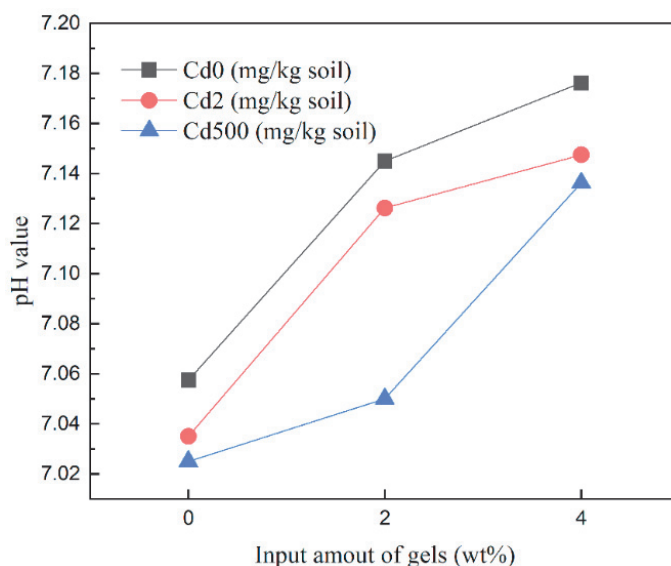


Figure 3.2 pH value of soil.

3.33 Cadmium precipitation experiments in soils.

In an experiment examining cadmium desorption in soils with varying cadmium concentrations, the pH of the solution was adjusted across different conditions, as illustrated in Figure 3.3. In a solution with a pH of 2 and cadmium concentrations in the soil at 0 or 2 mg/kg, the cadmium concentration in the filtrate remained at 0 mg/L. However, when the cadmium concentration in the soil was elevated to 500 mg/kg, the cadmium concentration in the filtrate gradually decreased with an increase in the amount

of gel added. In the control group without gel addition, the Cd concentration in the solution was 0.015 mg/L, whereas after adding 4% gel, the Cd concentration in the filtrate reached 0 mg/L. In a solution with a pH of 7, the desorption values of Cd in the soil were consistently 0. This suggests that at low cadmium concentrations, Si, Fe, and Mn in the soil can form insoluble compounds with cadmium. However, at high cadmium concentrations, the negative charge on the soil surface and certain metal colloids cannot absorb sufficient cadmium. The addition of gel proves effective in absorbing excess cadmium. DMAPAA water gel protonates its surface in water, generating hydroxyl groups that react with cadmium to form insoluble cadmium hydroxide precipitates, ultimately encapsulated by the gel.

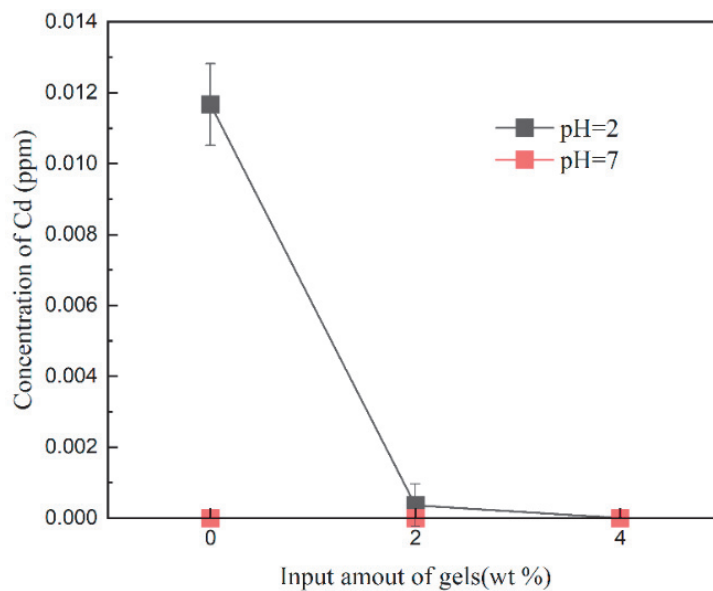


Figure 3.3 Cadmium precipitation values of soil in different pH solutions.

3.34 Growth state of vegetable under cadmium stress

The growth status of vegetables under cadmium stress was recorded using a camera after the addition of DMAPAA/DMAPAAQ hydrogel to the soil (Figure 3.4). The results revealed a positive correlation between the growth condition of vegetables and the quantity of hydrogel added, suggesting a beneficial impact on vegetable growth under cadmium stress. The hydrogel serves two pivotal roles: firstly, its three-dimensional network structure absorbs a substantial amount of water, enhancing root respiration and

promoting photosynthesis, thereby accelerating vegetable growth. Secondly, the DMAPAA/DMAPAAQ composite hydrogel can adsorb cadmium, stabilizing more cadmium in the soil and significantly reducing the biotoxicity of cadmium to vegetables, ultimately improving their growth condition.

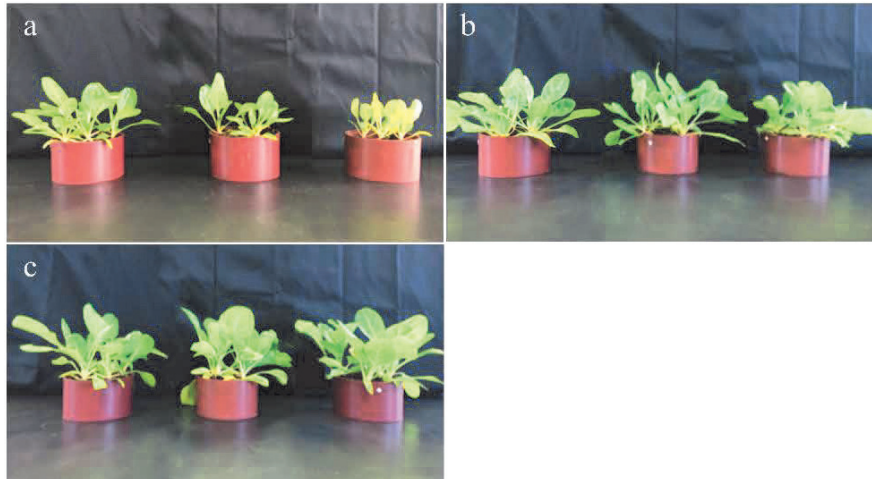


Figure 3.4 Physical image of vegetable growth, (a), (b), and (c) the addition of hydrogel is 0%. 2%. 4%. From left to right, the amount of cadmium added is 0,2mg/kg,500mg/kg.

3.35 vegetables growth status under two types of hydrogels

We conducted experiments with two distinct control groups utilizing different types of hydrogels, namely DMAA and DMAPAA/DMAPAAQ hydrogels, with a focus on understanding their impact on plant growth under cadmium-free conditions (Figure 3.5). DMAA represents a non-ionic polymer, while DMAPAA/DMAPAAQ falls into the category of ionic polymers. Despite some structural similarities, both containing amide groups and exhibiting the ability to absorb a substantial amount of water for soil moisture retention, these hydrogels differ in their functionalities. The experimental results clearly demonstrate that an increasing amount of DMAPAA/DMAPAAQ hydrogel leads to more vigorous vegetable growth, indicating a positive impact on plant development. Specifically, DMAPAA undergoes protonation in water, resulting in a positively charged surface capable of electrostatically adsorbing certain cations in the soil, such as K and Ca—soluble ions known to promote plant growth. Conversely, DMAPAAQ hydrogel engages in the exchange of NO_3^- and PO_4^{3-} ions in the soil through ion exchange,

subsequently releasing them gradually for plant absorption, further promoting plant growth. In contrast, the DMAA hydrogel, utilized as the control group, despite its water absorption properties, did not exhibit any notable promotion of plant growth based on the experimental results. These findings offer valuable insights for selecting suitable hydrogels to enhance plant growth under cadmium-free conditions.



Figure 3.5 Physical image of vegetable growth, (a) from left to right the DMAPAA/DMAPAAQ hydrogel addition amount is 4%,2%,0%. (b) from left to right the DMAA hydrogel addition amount is 4%,2%,0%.

3.36 Cadmium element in vegetable

Based on the ICP determination results depicted in Figure 3.6, we conducted a meticulous examination of the cadmium content in vegetables. Notably, with an increasing amount of gel added, there is a gradual decrease in the absorption of cadmium by vegetables. In the absence of gel addition, the cadmium absorption by vegetables is measured at 0.07 mg/g, which is three times higher than the amount absorbed when 4% gel is added. However, with the addition of 4% gel, the accumulation of cadmium in vegetables diminishes to only 0.03 mg/g. This observation underscores that the incorporation of DMAPAA/DMAPAAQ hydrogel effectively reduces the absorption of cadmium by vegetables. Hence, the DMAPAA/DMAPAAQ hydrogel not only

demonstrates efficacy in promoting plant growth but also exhibits significant potential in mitigating the absorption of harmful metal elements in soil. These findings provide valuable empirical support for the utilization of hydrogels in agricultural production, contributing to the enhancement of soil environmental quality.

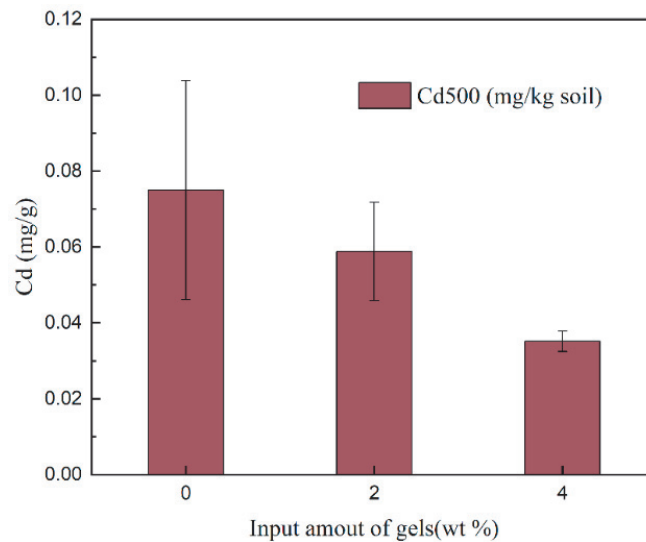
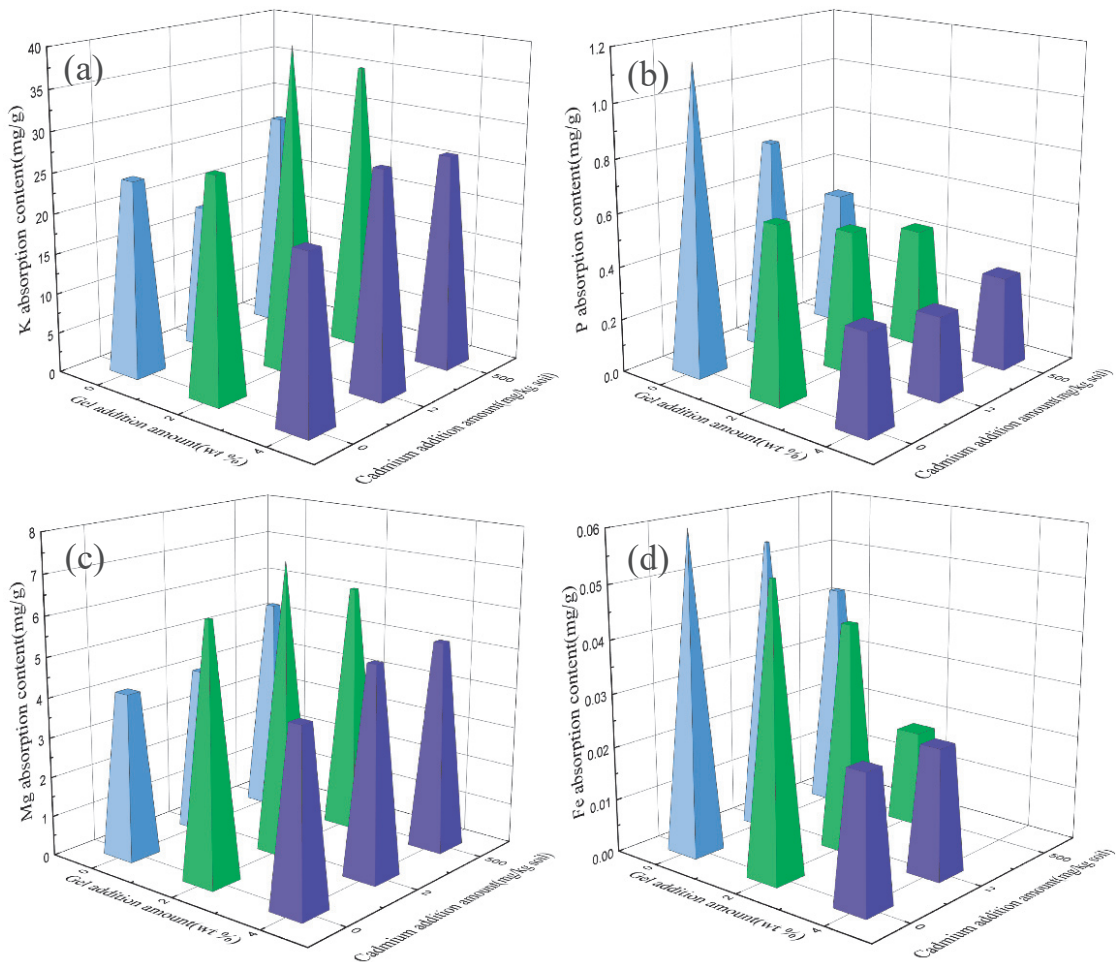


Figure 3.6 The amount of Cd absorbed by vegetables.

3.37 vegetable uptake of elements

We employed ICP analysis to assess the concentrations of essential elements, including Na, Mg, K, Ca, P, Fe, Mn, Cu, and Zn, in vegetables (Figure 3.7). These elements are pivotal for the normal growth and development of vegetables, serving as integral components of enzymes, vitamins, and hormones. Notably, iron contributes directly to chlorophyll synthesis, and manganese plays a crucial role in protein and organic acid metabolism. Additionally, these elements serve as critical parameters for evaluating soil fertility. A substantial portion of the nutrient elements in plants originates from the soil, with soil organic matter primarily deriving from deceased organic materials of animals and plants. Over time, microorganisms break down these large organic molecules into smaller molecules or even inorganic substances, which are subsequently absorbed by plants. Consequently, the measurement of essential element concentrations in vegetables allows us to assess not only whether hydrogels facilitate nutrient transport to promote plant growth but also indirectly evaluate soil fertility. Observations from the

Figure 7 indicates relatively high concentrations of K, P, Mg, and Na in vegetables, suggesting corresponding elevated levels in the soil. Additionally, the addition of hydrogels aids in the absorption of these elements by plants, particularly benefiting the normal growth of plants, as elements like K, P, and Mg are essential for most plant species. However, sodium, while harmful to most plants, exhibits a promoting effect on some C4 plants at low concentrations. Interestingly, despite the soil containing high iron content, the iron concentration in plants is not significant. This observation suggests that iron primarily exists in the soil in a non-ionic form rather than an ionic form. Notably, the addition of hydrogels does not enhance the absorption of iron from the soil by plants, indicating that hydrogels may exert selective effects on the absorption of different forms of elements in the soil. These detailed observations provide valuable insights for a deeper understanding of the mechanisms through which hydrogels influence nutrient absorption in the soil and plant growth.



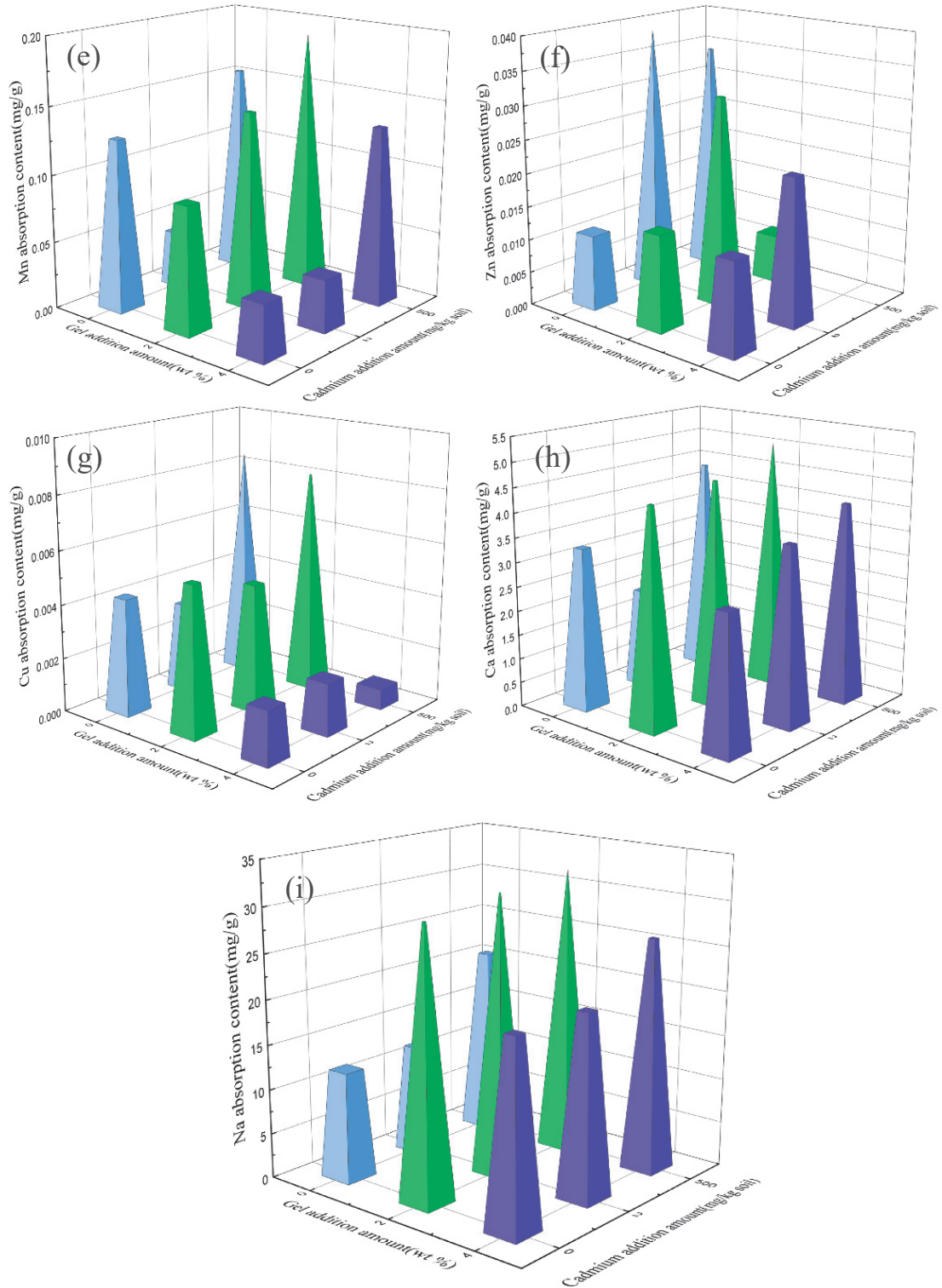


Figure 3.7 Contents of various trace elements in vegetable leaves: (a) Potassium; (b) Phosphorus; (c) Magnesium; (d) Iron; (e) Manganese; (f) Zinc; (g) Copper; (h) Calcium; (i) Sodium.

3.38. Dry weight of vegetable

Utilizing an electronic balance to measure the dry weight of the aboveground parts of vegetables (Figure 3.8), we observed a progressive increase in dry weight corresponding to the escalating content of DMAPAA/DMAPAAQ gel. Specifically, with the addition of water gel at a concentration of 4%, the maximum dry weight of the vegetables reached 1.46g, surpassing the value observed in the absence of gel. This unequivocally demonstrates that the incorporation of gel significantly enhances vegetable yield, creating favorable conditions for plant growth and development. In stark contrast, the addition of DMAA gel revealed a distinct decreasing trend in vegetable dry weight as the gel content increased. This trend suggests that DMAA, functioning as a non-ionic gel, does not promote plant growth and appears to exert a negative impact on vegetable dry weight. This sharp disparity underscores the superior efficacy of DMAPAA/DMAPAAQ gel in promoting plant growth and increasing yield. These observational results provide crucial experimental support for a more comprehensive understanding of the diverse effects of different types of gel on plant growth.

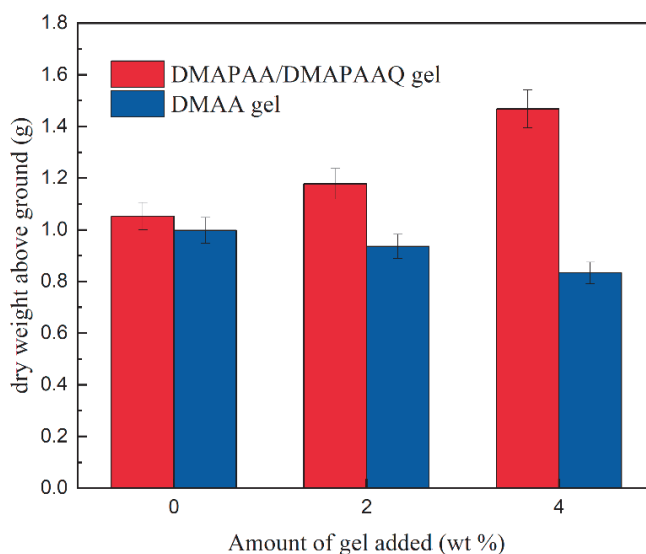


Figure 3.8 Dry weight of Swiss chard shoots.

3.39. Hydrogel repair cadmium soil mechanism

In the soil, manganese and iron undergo oxidation, giving rise to manganese oxide ($\text{MnO}_2/\text{Mn}_2\text{O}_3$) and iron oxide ($\text{Fe}(\text{OH})_3/\text{FeOOH}$). This process facilitates the

coprecipitation of specific heavy metal ions, including cadmium. Notably, iron, silicon, and cadmium in the soil possess chelating properties, allowing them to form Fe-Cd and Si-Cd structures, effectively immobilizing cadmium. DMAPAA/DMAPAAQ hydrogels, as ion-type polymers, play a pivotal role in these processes. Conversely, DMAA hydrogel, functioning as a non-ionic polymer, operates differently. DMAPAA undergoes protonation in water, generating hydroxyl groups on its surface that enable the adsorption of metal cations. Subsequently, it forms hydroxide precipitates with heavy metals, encapsulating them within the hydrogel and providing an effective mechanism for cadmium immobilization. Additionally, DMAPAA can adsorb potassium and calcium in their ionic forms, forming soluble compounds that facilitate plant uptake. On the other hand, DMAPAAQ, as a cationic polymer, engages in the exchange of anions in the soil, such as NO_3^- and PO_4^{3-} , through ion exchange (see Figure 3.9). Given that these anions are typically not adsorbed by the soil and are prone to leaching away with rainfall, DMAPAAQ adsorbs them and gradually releases them for plant uptake, promoting plant growth. Simultaneously, the release of chloride ions by DMAPAAQ has a promoting effect on certain plants, such as corn. The mechanisms of action elucidated for these hydrogels highlight their versatility in regulating heavy metal ions and providing essential nutrient elements in the soil. This versatility positions them as a potential environmentally friendly solution for enhancing soil quality and promoting plant growth.

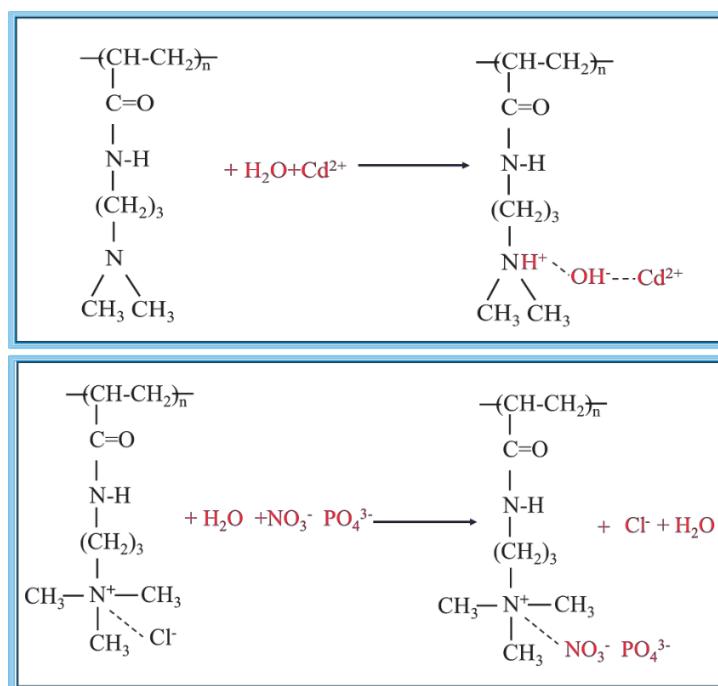


Figure 3.9 The removal mechanism of heavy metal cadmium by DMAPAA/DMAPAAQ composite hydrogel.

3.4 Conclusions

We investigated involving two distinct hydrogel types: DMAA non-ionic hydrogel and DMAPAA/DMAPAAQ ionic hydrogel. Within cadmium-contaminated soil, our focus was on assessing the influence of these hydrogels on vegetable growth. We observed a progressive enhancement in the soil immobilization capability of cadmium, particularly in high-iron soil, with the addition of DMAPAA/DMAPAAQ hydrogel. In a hydrochloric acid solution with a soil pH of 2, the cadmium leaching value in the soil reached zero at a 4% hydrogel addition, indicating an optimal effect on soil immobilization for cadmium. Simultaneously, plant cadmium absorption decreased to a minimal value of 0.03 mg/g. In comparison, the ionic hydrogel demonstrated significant advantages in vegetable cultivation. Its capacity to absorb nutrients in the soil, such as nitrate ions and phosphate ions, which are not easily adsorbed by the soil, the ionic hydrogel can slowly release these nutrients through ion exchange, thereby fostering vegetable growth. Conversely, the incorporation of the non-ionic hydrogel DMAA led to

a reduction in vegetable dry weight. Overall, our research findings underscore the potential of applying ionic hydrogels in soil, not only for promoting plant growth but also for effectively immobilizing the heavy metal cadmium. Future studies may explore natural ionic polymers that are safe and non-toxic, capable of absorbing heavy metals while providing essential nutrients for plant growth.

Reference

1. Wang, P., H. Chen, P. M. Kopittke, and F. J. Zhao. "Cadmium Contamination in Agricultural Soils of China and the Impact on Food Safety." *Environ Pollut* 249 (2019): 1038-48.
2. Guo, K., W. Xiang, W. Zhou, Y. Zhao, Y. Cheng, and M. He. "In Situ Plant Bionic Remediation of Cadmium-Contaminated Soil Caused by a High Geological Background in Kaihua, Zhejiang Province, China." *Chemosphere* 269 (2021): 128693.
3. Che, Z., W. Ahmed, J. Weng, L. Wenjie, M. Mahmood, J. M. Alatalo, O. Wenjie, M. M. Nizamani, W. Lu, F. X. Xian, Y. Jie, W. Yunting, W. Li, and S. Mehmood. "Distribution, Pollution, and Human Health Risks of Persistent and Potentially Toxic Elements in the Sediments around Hainan Island, China." *Mar Pollut Bull* 174 (2022): 113278.
4. Li, T., Q. Chang, X. Yuan, J. Li, G. A. Ayoko, R. L. Frost, H. Chen, X. Zhang, Y. Song, and W. Song. "Cadmium Transfer from Contaminated Soils to the Human Body through Rice Consumption in Southern Jiangsu Province, China." *Environ Sci Process Impacts* 19, no. 6 (2017): 843-50.
5. Takahashi, Goro. "Damage and Heavy Metal Pollution in China's Farmland: Reality and Solutions." *Journal of Contemporary East Asia Studies* 5, no. 1 (2017): 11-25.
6. Li, H., W. Xu, M. Dai, Z. Wang, X. Dong, and T. Fang. "Assessing Heavy Metal Pollution in Paddy Soil from Coal Mining Area, Anhui, China." *Environ Monit Assess* 191, no. 8 (2019): 518.

7. Surriya, Orooj, Sayeda Sarah Saleem, Kinza Waqar, and Alvina Gul Kazi. "Phytoremediation of Soils." In *Soil Remediation and Plants*, 1-36, 2015.
8. Wang, L., X. Cui, H. Cheng, F. Chen, J. Wang, X. Zhao, C. Lin, and X. Pu. "A Review of Soil Cadmium Contamination in China Including a Health Risk Assessment." *Environ Sci Pollut Res Int* 22, no. 21 (2015): 16441-52.
9. Ok, Y. S., S. S. Lee, W. T. Jeon, S. E. Oh, A. R. Usman, and D. H. Moon. "Application of Eggshell Waste for the Immobilization of Cadmium and Lead in a Contaminated Soil." *Environ Geochem Health* 33 Suppl 1 (2011): 31-9.
10. Hong, Chang Oh, Sang Yoon Kim, Jessie Gutierrez, Vance N. Owens, and Pil Joo Kim. "Comparison of Oyster Shell and Calcium Hydroxide as Liming Materials for Immobilizing Cadmium in Upland Soil." *Biology and Fertility of Soils* 46, no. 5 (2010): 491-98.
11. Bi, D., G. Yuan, J. Wei, L. Xiao, and L. Feng. "Conversion of Oyster Shell Waste to Amendment for Immobilising Cadmium and Arsenic in Agricultural Soil." *Bull Environ Contam Toxicol* 105, no. 2 (2020): 277-82.
12. Zhao, Haodong, Liyu Du, Tingting An, Yan Wu, and Yuhao Zhao. "Evaluation of Shell Powder Remediation Effect in Cadmium-Contaminated Soil: A Score Approach Based on Entropy Indexes." *CLEAN – Soil, Air, Water* 50, no. 5 (2022).
13. Wu, Bin, Jia Li, Mingping Sheng, He Peng, Dinghua Peng, and Heng Xu. "The Application of Biochar and Oyster Shell Reduced Cadmium Uptake by Crops and Modified Soil Fertility and Enzyme Activities in Contaminated Soil." *Soil* 8, no. 1 (2022): 409-19.
14. Noronha, F. R., S. K. Manikandan, and V. Nair. "Role of Coconut Shell Biochar and Earthworm (*Eudrilus Euginea*) in Bioremediation and Palak Spinach (*Spinacia Oleracea* L.) Growth in Cadmium-Contaminated Soil." *J Environ Manage* 302, no. Pt A (2022): 114057.
15. Lin, J., F. He, B. Su, M. Sun, G. Owens, and Z. Chen. "The Stabilizing Mechanism of Cadmium in Contaminated Soil Using Green Synthesized Iron Oxide Nanoparticles under Long-Term Incubation." *J Hazard Mater* 379 (2019): 120832.

16. Zha, Yan, Bo Zhao, and Tianxin Niu. "Bamboo Biochar and Zinc Oxide Nanoparticles Improved the Growth of Maize (*Zea Mays* L.) and Decreased Cadmium Uptake in Cd-Contaminated Soil." *Agriculture* 12, no. 9 (2022).
17. Watanabe, Toshihiro, Yasutoshi Murata, Takashi Nakamura, Yuki Sakai, and Mitsuru Osaki. "Effect of Zero-Valent Iron Application on Cadmium Uptake in Rice Plants Grown in Cadmium-Contaminated Soils." *Journal of Plant Nutrition* 32, no. 7 (2009): 1164-72.
18. Manzoor, N., T. Ahmed, M. Noman, M. Shahid, M. M. Nazir, L. Ali, T. S. Alnusaire, B. Li, R. Schulin, and G. Wang. "Iron Oxide Nanoparticles Ameliorated the Cadmium and Salinity Stresses in Wheat Plants, Facilitating Photosynthetic Pigments and Restricting Cadmium Uptake." *Sci Total Environ* 769 (2021): 145221.
19. Fu, Liangbo, Tingting Su, Dongming Wei, Dezhi Wu, Guoping Zhang, and Qiufang Shen. "Copper Oxide Nanoparticles Alleviate Cadmium Toxicity in Cereal Crops." *Environmental Science: Nano* 9, no. 9 (2022): 3502-13.
20. Gray, Colin William, and Bridget Elizabeth Wise. "Can the Application of Zinc Decrease Cadmium Concentrations in Spinach in a Zinc Sufficient Soil?" *New Zealand Journal of Crop and Horticultural Science* 48, no. 2 (2020): 117-29.
21. Sato, A., H. Takeda, W. Oyanagi, E. Nishihara, and M. Murakami. "Reduction of Cadmium Uptake in Spinach (*Spinacia Oleracea* L.) by Soil Amendment with Animal Waste Compost." *J Hazard Mater* 181, no. 1-3 (2010): 298-304.
22. Pinto, Filipa R., Miguel P. Mourato, Joana R. Sales, David Fangueiro, and Luísa Louro Martins. "Effect of Cattle Slurry on the Growth of Spinach Plants in Cd-Contaminated Soil." *Communications in Soil Science and Plant Analysis* 51, no. 10 (2020): 1370-81.
23. Zhuo, L., H. Li, F. Cheng, Y. Shi, Q. Zhang, and W. Shi. "Co-Remediation of Cadmium-Polluted Soil Using Stainless Steel Slag and Ammonium Humate." *Environ Sci Pollut Res Int* 19, no. 7 (2011): 2842-8.
24. Penido, E. S., G. C. Martins, T. B. M. Mendes, L. C. A. Melo, I. do Rosario Guimaraes, and L. R. G. Guilherme. "Combining Biochar and Sewage Sludge for Immobilization of Heavy Metals in Mining Soils." *Ecotoxicol Environ Saf* 172 (2019): 326-33.

25. Ghobashy, Mohamed Mohamady, H. Abd El-Wahab, Mohamed A. Ismail, A. M. Naser, Farag Abdelhai, Basem Kh El-Damhougy, Norhan Nady, Abeer S. Meganid, and Sheikha A. Alkhursani. "Characterization of Starch-Based Three Components of Gamma-Ray Cross-Linked Hydrogels to Be Used as a Soil Conditioner." *Materials Science and Engineering: B* 260 (2020).
26. Sarkar, Kangkana, and Kamalika Sen. "Polyvinyl Alcohol Based Hydrogels for Urea Release and Fe(III) Uptake from Soil Medium." *Journal of Environmental Chemical Engineering* 6, no. 1 (2018): 736-44.
27. Liu, Y., Y. Huang, C. Zhang, W. Li, C. Chen, Z. Zhang, H. Chen, J. Wang, Y. Li, and Y. Zhang. "Nano-Fe₃O₄ Incorporated into Stable Lignin Hydrogel: A Novel Strategy for Cadmium Removal from Soil." *Environ Pollut* 264 (2020): 114739.
28. Zhou, T., M. Zhao, X. Zhao, Y. Guo, and Y. Zhao. "Simultaneous Remediation and Fertility Improvement of Heavy Metals Contaminated Soil by a Novel Composite Hydrogel Synthesized from Food Waste." *Chemosphere* 275 (2021): 129984.
29. Wei, Xiujiao, Huayi Chen, Diao Lin, Huijuan Xu, Jinjin Wang, Jiabin Zhang, Zheng Hu, Jianbin Deng, JianPeng Gao, Hanhao Li, Yongtao Li, Yonglin Liu, and Yulong Zhang. "A Field Study of Nano-Fe₃O₄ Loaded Lignin Hydrogel Application for Cd Reduction, Nutrient Enhancement, and Microbiological Shift in a Polluted Paddy Soil." *Chemical Engineering Journal* 451 (2023).

Chapter 4 A novel composite hydrogel material for sodium removal and potassium provision

4.1 Introduction

Sodium ions, an essential nutrient for human health, can lead to various health problems such as hypertension and cardiovascular diseases when excessively consumed. The World Health Organization (WHO) has recommended a daily sodium intake not exceeding 2 grams per day [1-3]. Nevertheless, natural water sources like rivers, lakes, and groundwater can contain elevated concentrations of sodium ions due to the weathering of rocks and leaching from soils. This excessive sodium content can lead to soil salinization, posing a serious threat to crop growth. Consequently, it is imperative to develop efficient methods for removing sodium ions from aqueous solutions and mitigating soil salinization. [4, 5]

Currently, existing methods for sodium removal from water solutions, such as ion exchange resin, reverse osmosis, distillation, electrodialysis, and vacuum evaporation, have limitations [6]. Some require high energy consumption, leading to environmental damage, while others are inefficient and less effective [7-9]. To overcome these challenges, hydrogels are promising due to their unique properties as high-molecular-weight materials with a three-dimensional network structure. Hydrogels have porous architecture and large surface area, making them efficient in adsorbing harmful substances in water and soil. Additionally, hydrogels can rapidly absorb significant amounts of water. Moreover, hydrogels are environmentally friendly, posing minimal pollution risk when applied in ecosystems [10, 11].

Hydrogels, both natural and synthetic, offer promising solutions for sodium ion removal and soil salinization challenges. Recent advances in hydrogel research include superabsorbent hydrogels, salt-tolerant polymers, and innovative composites with improved soil water retention [12, 13]. KMAA hydrogel adsorbent demonstrates exceptional water adsorption characteristics. It effectively captures trace sodium ions while concurrently releasing abundant potassium ions, thus serving as a valuable source

of potassium fertilizer for plants with potassium requirements in the soil. Nonetheless, it is important to acknowledge that certain limitations exist within the methanol cleansing stage of the hydrogel preparation process. This becomes particularly relevant in the context of large-scale hydrogel synthesis, where a staged approach to cleansing might be warranted. Hydrogels also show positive effects on plant growth under drought and salt stress. Guo et al. work showcased successful synthesis of a cellulose-based superabsorbent hydrogel. This hydrogel exhibited extraordinary water uptake capacities of 604% in distilled water and 119% in saltwater. Notably, the hydrogel demonstrated a remarkable ammonia nitrogen adsorption capacity of 30 mg/g, effectively mitigating nutrient leaching in soil [14]. Zhang et al. contributions led to the development of a salt-tolerant superabsorbent polymer (ST-SAP) that exhibited exceptional swelling ability (69.04 g/g) under high salinity conditions [15]. Xiong et al. pioneering work involved the synthesis of a novel superabsorbent polymer composite, wherein the addition of calcium alginate significantly enhanced soil water retention and facilitated controlled water release. Consequently, this composite exhibited increased water uptake rates of 25.8% and 10% in distilled water and saltwater, respectively. The study highlights the immense potential of this approach in mitigating soil water evaporation and its application in saline-alkali soils in agriculture [16]. Tian et al. research resulted in an exceptional superabsorbent polymer composite with outstanding water uptake abilities in various solutions, promising for water management and agriculture [17]. Shi et al. investigation employed two hydrophilic polymers, Stockosorb and Luquasorb, to enhance the growth of one-year-old poplar cuttings under drought and salt stress conditions. Remarkably, the addition of 0.5% Stockosorb or Luquasorb significantly alleviated growth inhibition induced by drought and salt stress [18]. Islam et al. study revealed that the combined application of salicylic acid (SA) and trehalose (Tre) had a more pronounced positive impact on mustard plants under sodium chloride (NaCl) stress compared to individual treatments [19]. Fathy et al. pioneering work involved the synthesis of a stable composite cation exchange adsorbent through suspension polymerization, which exhibited an impressive 4.22 meq g^{-1} exchange capacity for Na^+ ions. This research holds significant potential for further advancements in water purification and soil salinity management [20].

In this study, we synthesized KMAA hydrogel using free radical polymerization and explored its sustainable application strategies for sodium removal from water resources, sodium elimination in saline-alkali soils, and enhancement of potassium content as expressed in Figure 4.1. The primary aim was to investigate the sodium adsorption capacity and potassium exchange capacity of KMAA hydrogel under varying pH conditions, along with relevant thermodynamic and adsorption kinetic properties. To simulate the adsorption process, we employed isotherm models such as Langmuir and Freundlich, while pseudo-first and pseudo-second-order models were utilized to analyze the adsorption kinetics. Additionally, we assessed the impact of KMAA application in soil on sodium and potassium ion leaching, providing valuable insights for agricultural practices. Through these investigations, we aim to establish a theoretical foundation for effective sodium removal and potassium enrichment, offering feasible solutions for environmental restoration and agricultural production.

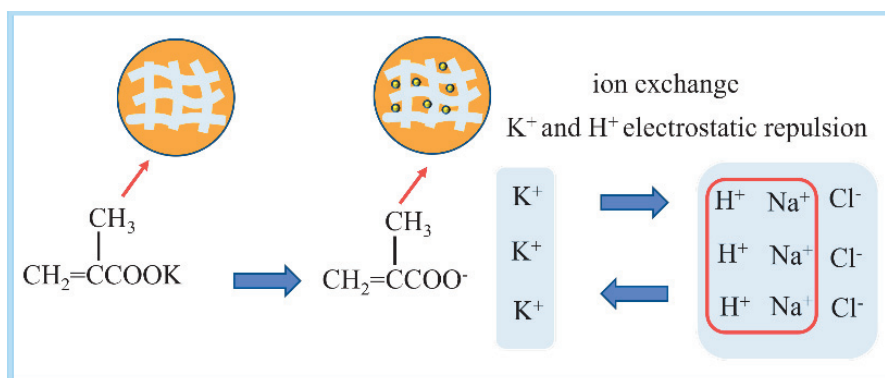


Figure 4.1 Schematic diagram of the mechanism of KMAA hydrogel to adsorb sodium and provide potassium in water and soil.

4.2 Experimental Methods

4.2.1 materials

The monomer KMAA was obtained from KJ Chemicals (Tokyo, Japan). N, N'-dimethyl ethylenediamine (TEMED) was purchased from Nacalai Tesque Co., Ltd. (Kyoto, Japan). N, N'-methylenebisacrylamide (MBAA), ammonium persulfate (APS), and sodium chloride were acquired from Sigma-Aldrich, Inc. (St. Louis, Missouri, USA).

Hydrochloric acid (HCl) was purchased from Sigma-Aldrich Japan (Tokyo). The soil is purchased from NAFCO supermarket, the main elements are Si, Fe, Ca, Al, Mn. The element contents detected by EDS are 49.1%, 18.8%, 10.2%, 9.6%, and 0.5%, respectively. All reagents used were of analytical grade and employed as received. distilled water used in the experiments was produced in the laboratory.

4.22 Synthesis of hydrogel

A mass of 3.105 g of the monomer KMAA, 0.193 g of the cross-linking agent MBAA, and 0.058 g of the accelerator TEMED were weighed using an electronic balance and transferred into a 20 ml volumetric flask. Distilled water was added to the volumetric flask, and the mixture was stirred using a magnetic stirrer. Simultaneously, a mass of 0.057 g of the initiator APS was weighed and dissolved in 5 ml of distilled water to form an initiator solution. Both the monomer solution and the initiator solution were purged with nitrogen gas for 45 minutes to eliminate oxygen and prevent inhibition of free radicals. Subsequently, the initiator solution was poured into the monomer solution while stirring for 25 seconds. The resulting mixture was transferred into three plastic tubes using a pipette. The monomer solution and the initiator solution were then immersed in a water solution at 25°C for 24 hours. The resulting gels were removed from the tubes and cut into uniform cylindrical shapes, and then washed with methanol for 24 hours using a Soxhlet extractor (Asahi Glass plant Inc., Arao City, Japan) equipment to remove any unreacted components. The gel was then air-dried at room temperature and further dried in an oven at 50°C for 24 hours. Finally, the gel was pulverized into powder using a grinder. The synthesis condition of the gel is summarized in Table 4.1.

Table 4.1 Synthesis condition of the KMAA hydrogel

Materials	Component Type	Molar weight (g/mol)	concentration (mol/m ³)	mass(g)
KMAA	monomer	124.18	1000	3.105
MBAA	linker	154.17	50	0.193
TEMED	accelerator	116.21	20	0.058
APS	Initiator	228.19	10	0.057

4.3 Swelling Properties of Hydrogels

4.31 Swelling degree of hydrogel in sodium chloride solution

A hydrogel weighing 0.02 g (Md) was added to 40 ml of sodium chloride solutions with concentrated of 10, 50, 100, 300, and 500 mg/L. The mixture was allowed to equilibrate at room temperature for 24 hours to achieve swelling equilibrium. The swollen gel was subsequently filtered through filter paper and its weight recorded as Ms . Calculated by the following formula:[21]

$$W_a = \frac{(M_s - M_d)}{M_d} * \%$$

4.32 Soil water holding rate.

Weighed 10 g of dry soil and combined with 0.1 g of hydrogel, recorded as m_1 . Subsequently, an appropriate amount of water was added to the beaker at room temperature, allowing complete saturation of the mixture. The mass of the resulting mixture and water was measured by filtration using filter paper, recorded as m_2 . Calculated by the following formula:

$$W_b = \frac{(m_2 - m_1)}{m_1} * \%$$

4.4. Adsorption Experiment

4.41 Adsorption thermodynamic experiments with different pH values

The solutions were prepared by diluting the 1000ppm NaCl solution to concentrations of 10, 50, 100, 300, and 500 mg/L. Subsequently, 25 mL of each diluted solution was transferred to a plastic centrifuge tube with a capacity of 50 mL. The pH of the solutions was adjusted to 4.0 and 7.0 by adding 1 mol/L HCl solution to a final volume of 40 mL. Additionally, 20 mg of the adsorbent was added to each tube. The tubes were then placed in a water bath constant temperature shaker at 25°C with continuous shaking at 150 rpm for 24 hours. After the adsorption period, the samples were filtered through a 0.22 μm membrane filter and analyzed using ICP.

4.42 pH effect experiment

The 1000ppm sodium chloride (NaCl) solution was diluted to a concentration of 100 mg/L. Subsequently, 25 mL of the diluted solution was transferred into a plastic centrifuge tube with a total volume of 50 mL. To adjust the pH values to 2.0, 3.0, 4.0, 5.0, 6.0, and 7.0, 1 mol/L HCl solution was added until the final volume reached 40 mL. Next, 20 mg of the adsorbent material was added to the mixture. The entire system was placed in a water bath constant temperature shaker, where continuous adsorption was conducted at 25°C and 150 rpm for a duration of 24 hours. Following adsorption, the samples were filtered through a 0.22 µm membrane filter and analyzed using ICP.

4.43 Adsorption kinetic experiment

The 1000ppm NaCl solution was diluted to a concentration of 100 mg/L. Subsequently, 40 mL of the diluted solution was adjusted to pH 4.0 and 7.0 using a 1 mol/L HCl solution. Next, 20 mg of the adsorbent material was introduced into the system. The entire setup was placed in a water bath constant temperature shaker, maintaining a constant temperature of 25°C with a shaking rate of 150 rpm. The adsorption process was conducted for specific time intervals (1, 10, 60, 180, 240, 300, 1200, 1380, 1440 minutes). At each predetermined time point, samples were withdrawn from the system and subsequently filtered through a 0.22 µm membrane filter. The filtered samples were then analysis using (ICP) to measured.

4.44 Adsorption thermodynamics at different temperatures

The 1000ppm NaCl solutions were prepared by diluting the original solution to concentrations of 10, 50, 100, 300, and 500 mg/L. For each concentration, 25 mL of the diluted solution was transferred into a plastic centrifuge tube with a volume of 50 mL. Subsequently, the pH of each solution was adjusted to 4.0 and 7.0 using a 1 mol/L hydrochloric acid (HCl) solution reached the final volume to 40 mL. Next, 20 mg of the adsorbent material was added to each solution. The prepared samples were placed in water bath constant temperature shaker, maintaining a constant temperature of 25°C and 35°C, respectively, with a shaking rate of 150 rpm. The adsorption process was

conducted continuously for 24 hours. After the adsorption period, the samples were filtered through 0.22 μm membrane filters to remove any particulate matter. The filtrates were subsequently analysis using ICP to measure the desired parameters.

4.45 Adsorbent dosage experiment

The 1000ppm NaCl solution was diluted to a concentration of 100 mg/L. Subsequently, 25 mL of the diluted solution was transferred into a plastic centrifuge tube with a volume of 50 mL. The pH of each solution was adjusted to 4.0 and 7.0 by adding 1 mol/L HCl solution until the final volume reached 40 mL. Next, different amounts of the adsorbent 3, 5, 10, 15, and 20 mg were added to the samples. The prepared samples were subjected to continuous adsorption for 24 hours in a water bath constant temperature shaker at 25°C with a sharking rate of 150 rpm. After the adsorption period, the samples were filtered through a 0.22 μm membrane filter to remove any particulate matter. The filtrates were then analyzed using ICP.

4.5 Soil Experiment

4.51 Preparation of soil containing NaCl

Three separate beakers, labeled as A1, A2, and A3, were used for the soil sample analysis. A total of 10 g of soil was weighed and placed into each respective beaker. Beaker A1 served as the blank control, while beaker A2 received the addition of 5 mL of a 1000 ppm NaCl solution. Similarly, beaker A3 also received 5 mL of a 1000 ppm NaCl solution, along with added of 0.2 g of KMAA hydrogel. To ensure proper mixing, an appropriate amount of water was added to each beaker, and thorough stirring was conducted. Subsequently, the beakers were transferred to an oven for drying.

4.52 pH value affects the precipitation of sodium and potassium ions in soil.

Two aqueous solutions with pH values of 4 and 7 were prepared by measuring out 40 mL of each solution. Subsequently, 4 grams of soil samples (A1, A2, and A3) were individually added to separate beakers, followed by the addition of 40 mL of the

respective pH solution. The solid-to-liquid ratio was maintained at 1:10. The soil-solution mixture was shaken for 24 hours in a water bath constant temperature at 25°C with a shaking rate of 150 rpm. Afterward, the mixtures were filtered through a 0.22 µm membrane filter and analyzed using ICP.

4.53 Amount of hydrogel affects precipitation of sodium and potassium ions in soil

Two aqueous solutions were prepared by combining 40 mL of pH 4 and pH 7 solutions. Subsequently, 4 grams of soil samples containing 2% and 4% hydrogels were individually added to separate containers. The mixtures were then placed in a water bath constant temperature shaker at 25°C with continuous shaking at 150 rpm for 24 hours. Following this, the mixtures were filtered using a 0.22 µm membrane filter and subsequently analyzed ICP.

4.6 Result and Discussion

4.61 Swelling degree of hydrogel

This study investigates the water retention capacity of a hydrogel prepared for soil application. Upon incorporation of the hydrogel into the soil, a remarkable enhancement in water-holding capability was observed, as depicted in Figure 4.2(a). The soil's water retention capacities were measured to be 187% without hydrogel and 452% with hydrogel. However, after 6 days in the presence of the hydrogel, the soil's water-holding capacity diminished to zero. The superior water retention ability of the soil can be attributed to the hydrogel's three-dimensional network structure and surface hydrophilic groups, which facilitated the diffusion of water molecules into the hydrogel's internal matrix. Furthermore, the hydrophilic groups within the polymeric network of the hydrogel underwent ionization with the internal solution, leading to the generation of osmotic pressure and continuous diffusion of water molecules into the interconnected network of the hydrogel until reaching the equilibrium swelling state. Consequently, the introduction of the hydrogel significantly strengthened the soil's water retention capacity. From Figure 4.2(b), it can be observed that the swelling capacity of the hydrogel in

sodium chloride solution decreased with increasing sodium chloride concentration. At 500 ppm sodium chloride concentration, the hydrogel exhibited the lowest swelling capacity, measuring 135%. This decline in swelling can be attributed to the formation of osmotic pressure both inside and outside the hydrogel, thereby suppressing the inward diffusion of water. At high concentrations of sodium chloride, the hydrogel's structure could even be compromised, resulting in a reduction of its water absorption performance. In summary, this study reveals the potential of hydrogels in improving soil water retention, thereby providing valuable insights for future applications in agriculture and water management [22].

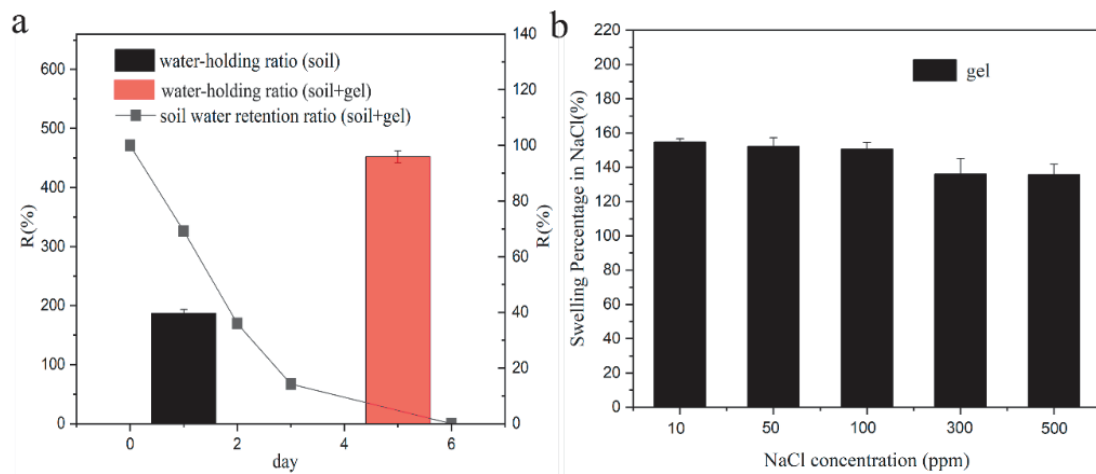


Figure 4.2 (a) water retention capability of hydrogel in soil, (b) swelling behavior of hydrogel in NaCl solution.

4.62 pH affects the adsorption of the gel.

This study investigates the performance of KMAA hydrogel in the removal of Na^+ and the exchange of K^+ under different pH conditions, as depicted in Figure 4.3a. The removal efficiency of Na^+ decreases with increasing sodium chloride concentration when the same KMAA hydrogel is added. At a 10ppm sodium chloride concentration, the highest removal efficiency for Na^+ reaches 62%. Conversely, the exchange rate of K^+ increases with higher concentrations of sodium chloride, with the maximum exchange rate of 48% observed at 500 ppm sodium chloride concentration. Figure 4.3b illustrates the adsorption of Na^+ and the exchange of K^+ by KMAA hydrogel under various pH conditions in a 100ppm sodium chloride solution. The adsorption of sodium ions by

KMAA hydrogel increases with higher pH values. However, at pH 2 and 3, the hydrogel exhibits no adsorption of Na^+ . This phenomenon can be attributed to the competition between the highly concentrated hydrogen ions (H^+) in the strong acid condition and the carboxylic acid groups on the hydrogel, leading to a further increase in the protonation degree of carboxylic acid. Consequently, the quantity of negatively charged carboxylate ions on the hydrogel surface is fundamentally reduced, resulting in diminished binding capacity with sodium ions in the solution. Therefore, under strong acidic conditions, the KMAA hydrogel exhibits minimal capacity to adsorb Na^+ . On the other hand, the exchange capacity of K^+ by KMAA hydrogel decreases with increasing pH of the solution. At pH=2, the hydrogel displays the highest K^+ exchange capacity, reaching 249mg/g. As the solution's acidity increases, the concentration of hydrogen ions also rises. These hydrogen ions (H^+) form associations with carboxyl groups (COO^-) and create a repulsive force with potassium ions, enhancing the exchange capacity of K^+ on the hydrogel surface.

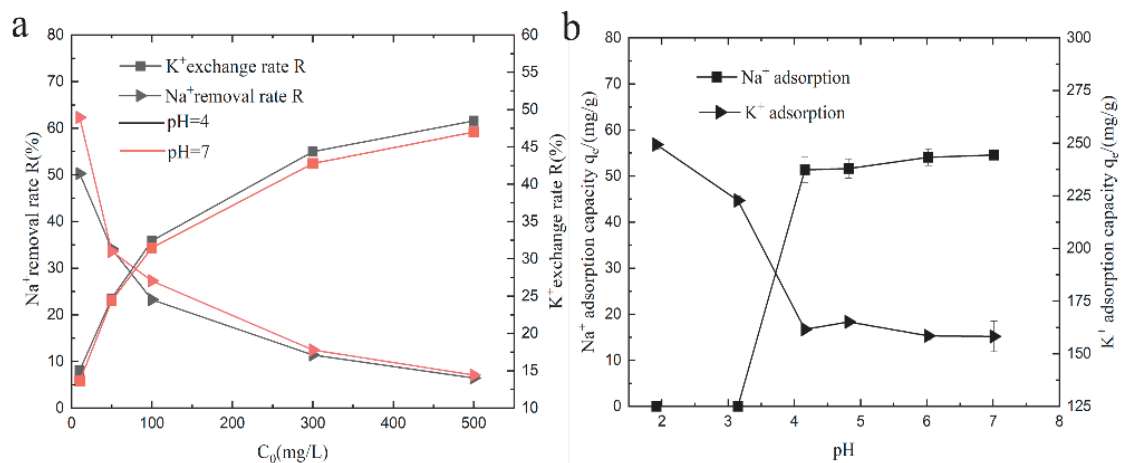


Figure 4.3 (a) Na^+ removal efficiency and K^+ exchange rate of hydrogel under various initial NaCl concentrations. (b) effect of different pH values on Na^+ adsorption and K^+ exchange capacity of hydrogel.

4.63 Isothermal adsorption

The adsorption of sodium ions and the exchange of potassium ions by KMAA hydrogel at pH=4 and pH 7 were investigated, and the isotherms are depicted in Figure

4.4. To analyze the adsorption behavior, two isothermal adsorption models of Langmuir and Freundlich are used for fitting.

$$q_e = \frac{q_{max}K_L C_e}{1 + K_L C_e}$$

$$q_e = K_F C_e^{1/n}$$

In the equations, q_e represents the adsorption capacity at equilibrium (mg/g), q_{max} is the maximum adsorption capacity calculated from the Langmuir model (mg/g), K_L is the Langmuir constant (L/mg), and $1/n$ and K_F are the constants of the Freundlich model (mg/g). With increasing sodium chloride concentration, the adsorption of sodium ions and the exchange of potassium ions by KMAA hydrogel both increases. The Langmuir model assumes that the adsorption of the adsorbent to the target is only a single-layer adsorption, and the interaction force between the adsorbed molecules can be ignored. The Freundlich model assumes that the adsorption of the adsorbent to the target is heterogeneous multilayer adsorption. According to the Langmuir model calculation, the maximum adsorption capacity of KMAA hydrogel for sodium ions at pH=7 reaches 80.5 mg/g, while the actual maximum adsorption capacity is 70.7 mg/g. From the Freundlich model calculation, the maximum exchange capacity of potassium ions at pH=4 reaches 254.6 mg/g, and the actual maximum exchange capacity is 243.7 mg/g. The KMAA hydrogel exhibits a three-dimensional network structure with high selective adsorption properties. The value of parameter n in the Freundlich model ranges from 1 to 10, indicating a spontaneous adsorption process.

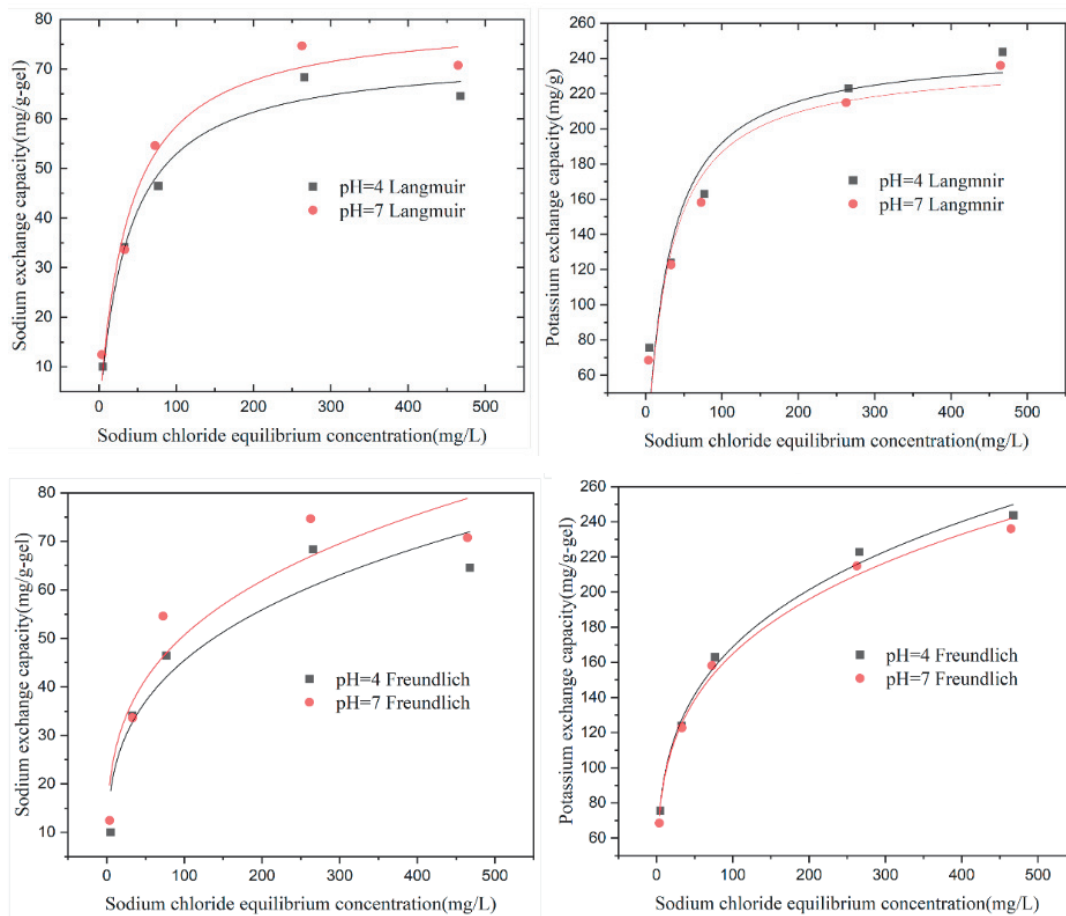


Figure 4.4 isothermal adsorption of Na^+ adsorption and K^+ exchange by hydrogel at pH=4 and 7 (a) Langmuir model simulated fit curve, (b) Freundlich model simulated fit curve.

Table 4.2 shows that the correlation coefficients of the Langmuir model are higher than those of the Freundlich model at different pH values. At pH=4 and 7, the correlation coefficients of the Langmuir model are 0.98 and 0.97, respectively, indicating that the Langmuir model is more suitable for describing the adsorption process of sodium ions. Table 4.3 reveals that the correlation coefficients of the Freundlich model are higher than those of the Langmuir model. At pH=4 and 7, the correlation coefficients of the Freundlich model are 0.9934 and 0.9936, respectively, suggesting that the Freundlich model is more appropriate for describing the exchange of potassium ions.

Table 4.2 Parameters of Langmuir and Freundlich isotherm model by KMAA gel at pH=4 and pH=7 sodium ion adsorption capacity

Isotherm model	Parameter	Initial pH	
		4	7
Langmuir	q_{\max} (mg/g)	72.9	80.5
	K_L (L/mg)	0.0264	0.0265
	R^2	0.98	0.97
Freundlich	K_F (mg/g)	11.54	13.47
	n	3.448	3.571
	R^2	0.909	0.905

Table 4.3 Parameters of Langmuir and Freundlich isotherm model by KMAA gel at pH=4 and pH=7 potassium ion exchange capacity

Isotherm model	Parameter	Initial pH	
		4	7
Langmuir	q_{\max} (mg/g)	254.6	238.4
	K_L (L/mg)	0.0358	0.0361
	R^2	0.8964	0.8931
Freundlich	K_F (mg/g)	52.37	52.26
	n	3.937	4.016
	R^2	0.9934	0.9936

4.64 Adsorption thermodynamic

To investigate the thermodynamic properties of the adsorption of sodium ions and the exchange of potassium ions by KMAA hydrogel at pH 4= and 7, the calculations of Gibbs free energy ΔG , enthalpy change ΔH , and entropy change ΔS were performed. The formulas for these calculations are as follows:[23]

$$K_D = \frac{q_e}{C_e}$$

$$\Delta G^\theta = -RT \ln K_D$$

$$\Delta G^\theta = \Delta H^\theta - T\Delta S^\theta$$

In the equations, K_D represents the distribution coefficient, R is the ideal gas constant ($8.314 \text{ J mol}^{-1} \text{ K}^{-1}$), T is the thermodynamic temperature (K), ΔG^θ represents the Gibbs free energy (kJ/mol), ΔH^θ represents the enthalpy change (kJ/mol), and ΔS^θ represents the entropy change ($\text{J mol}^{-1} \text{ K}^{-1}$). By calculating the thermodynamic parameters, including the adsorption enthalpy ΔH^θ , adsorption free energy ΔG^θ , and adsorption entropy ΔS^θ , the adsorption mechanism on the hydrogel was studied. Thermodynamic analysis was performed to elucidate the effect of different temperatures on the adsorption of sodium ions and the exchange of potassium ions on KMAA hydrogel, as shown in Figure 4.5. Tables 4.4 and 4.5 show the KMAA hydrogel adsorption thermodynamic parameters for sodium and for potassium, respectively. It was found that when the temperature increased from 298 K to 318 K, ΔG^θ remained negative, indicating that the adsorption of sodium ions and the exchange of potassium ions on KMAA hydrogel are spontaneous and feasible processes. For the adsorption of sodium ions, ΔH^θ was positive, and the adsorption capacity of sodium ions increased with temperature, indicating an endothermic reaction. Additionally, ΔS^θ was positive, indicating an increase in disorder at the interface between the hydrogel surface and sodium ions during the adsorption process. Regarding the exchange of potassium ions on the hydrogel, as the temperature increased from 298 K to 318 K, ΔH^θ was negative, suggesting that the exchange process is exothermic. Simultaneously, ΔS^θ was also negative, indicating a decrease in randomness at the solid/liquid interface during the exchange process. Thermodynamic investigations provide insights into whether the adsorption process is endothermic or exothermic, thereby expanding the practical application of adsorbents. Overall, the thermodynamic study enables a better understanding of the adsorption behavior of the hydrogel, including whether it is exothermic or endothermic, and contributes to the broader application of adsorbents.

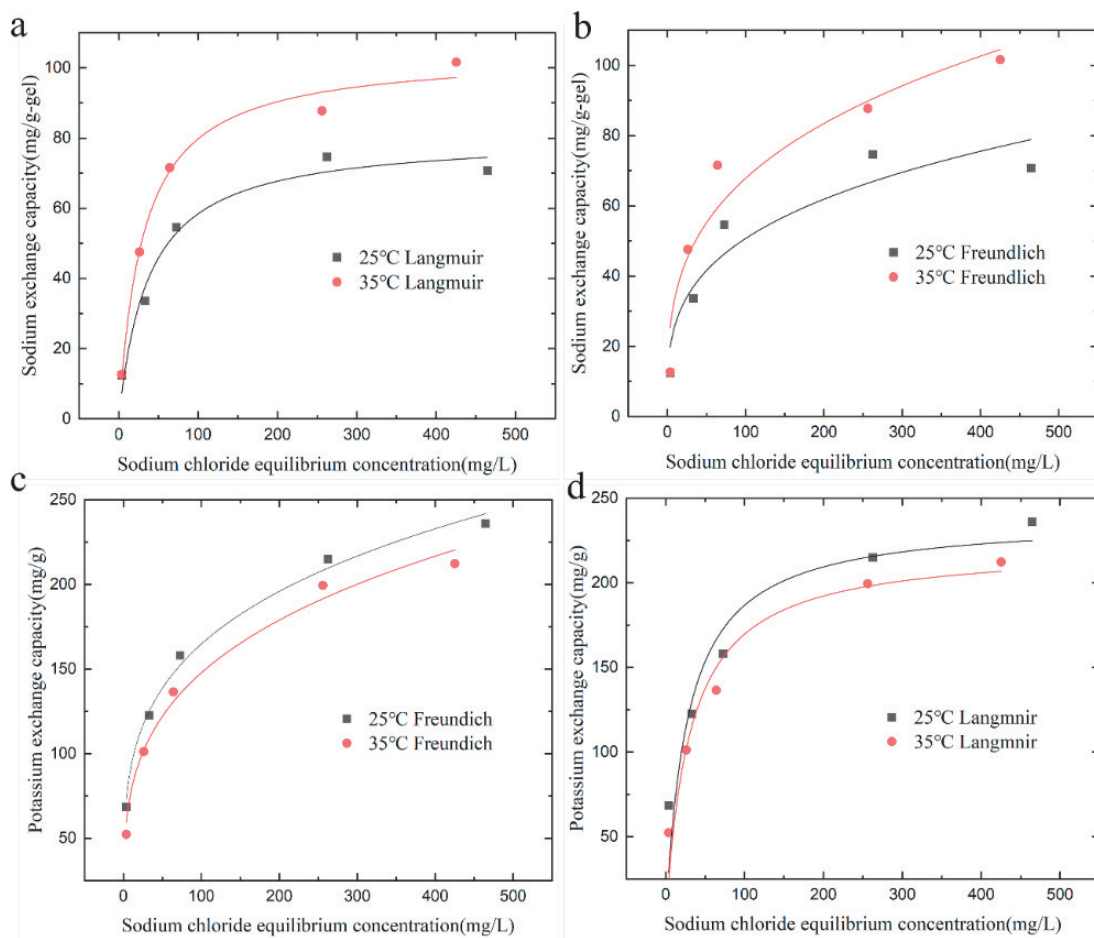


Figure 4.5 adsorption isotherm fit curves of KMAA hydrogel at different temperatures (a) Na⁺ Adsorption Langmuir model simulated fit curve, (b) Na⁺ adsorption Freundlich model simulated fit curve, (c) K⁺ exchange Langmuir model simulated fit curve, (d) K⁺ exchange Freundlich model simulated fit curve.

Table 4.4 KMAA hydrogel adsorption thermodynamic parameters for sodium

T/K	$\Delta G^\theta / (\text{kJ} \cdot \text{mol}^{-1})$	$\Delta H^\theta / (\text{kJ} \cdot \text{mol}^{-1})$	$\Delta S^\theta / (\text{J} \cdot \text{mol}^{-1} \cdot \text{K}^{-1})$
298.15	-2.965	2.762	19.21
308.15	-3.157	2.762	19.21

Table 4.5 KMAA hydrogel exchange thermodynamic parameters for potassium.

T/K	$\Delta G^\theta / (\text{kJ}\cdot\text{mol}^{-1})$	$\Delta H^\theta / (\text{kJ}\cdot\text{mol}^{-1})$	$\Delta S^\theta / (\text{J}\cdot\text{mol}^{-1}\cdot\text{K}^{-1})$
298.15	-1.406	-1.589	-44.21
308.15	-0.964	-1.589	-44.21

4.65 Adsorption kinetics

The study of adsorption kinetics can reflect the rate and mechanism of the adsorption target of the adsorbent material. The exchange kinetics of KMAA hydrogel for the adsorption of sodium and potassium is shown in figure 4.6. Two kinds of isotherm adsorption models, pseudo-first-order kinetic model and pseudo-second-order kinetic model, were used for fitting [24].

$$q_t = q_e(1 - e^{-k_1 t})$$

$$q_t = \frac{(K_2 q_e^2 t)}{1 + K_2 q_e t}$$

In the equations, q_t represents the adsorption capacity at time t (mg/g), q_e represents the adsorption capacity at equilibrium (mg/g), k_1 is the rate constant of the pseudo-first-order kinetics (min^{-1}), k_2 is the rate constant of the pseudo-second-order kinetics ($\text{g}\cdot\text{mg}^{-1}\cdot\text{min}^{-1}$). The entire adsorption process can be divided into two stages. In the initial stage, the adsorption rate is rapid, and the adsorption capacity of sodium ions and the exchange of potassium ions by KMAA hydrogel reaches approximately 90% of the equilibrium adsorption capacity after 10 minutes. As time progresses, the rate of sodium ion adsorption and potassium ion exchange gradually decreases, and equilibrium is nearly reached after 24 hours. This may be attributed to the dissociation of -COOK groups on the hydrogel surface, leading to the formation of many COO^- and K^+ ions in the solution during the initial stage. The COO^- sites bind extensively with sodium ions. With the increase of time, many Na ions bind to COO^- sites, resulting in an equilibrium in the osmotic pressure of the solution and the hydrogel. Lead to the adsorption of sodium ions, and the exchange of potassium ions decreased, and finally reached the adsorption equilibrium.

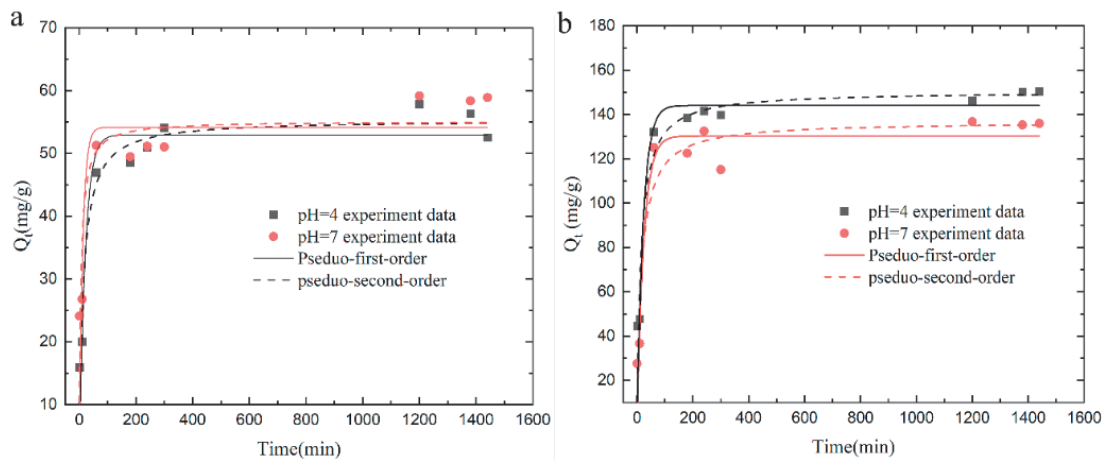


Figure 4.6 (a) dynamic modeling of pseudo-first order and pseudo-second-order Na^+ Adsorption by KMAA hydrogel at Initial $NaCl$ concentration of 100 mg/L; (b) dynamic modeling of pseudo-first-order and pseudo-second-order K^+ exchange by KMAA hydrogel at initial $NaCl$ concentration of 100 mg/L

From table 4.6, it can be observed that, at pH=4 and 7, the coefficients of the pseudo-second-order kinetic model for sodium ion adsorption are consistently higher than those of the pseudo-first-order kinetic model, indicating the presence of chemical adsorption during sodium adsorption. Thus, the pseudo-second-order kinetic model is more suitable for describing the adsorption process of sodium ions. From Table 4.7, it is evident that, at pH=4 and 7, the coefficients of the pseudo-second-order kinetic model for potassium ion exchange are lower than those of the pseudo-first-order kinetic model. This suggests that the exchange process of potassium ions is mainly governed by electrostatic repulsion, indicating that the pseudo-first-order kinetic model is more appropriate for describing the exchange process of potassium ions.

Table 4.6 Fit results of Na⁺ adsorption kinetics by KMAA hydrogel.

Isotherm model	Parameter	Initial pH	
		4	7
Pseudo-first order	k ₁ (min ⁻¹)	0.049	0.084
	q _e (mg/g)	52.94	54.13
	R ²	0.872	0.631
Pseudo-second order	K ₂ (g/mg/min)	0.00133	0.0312
	q _e (mg/g)	55.34	57.31
	R ²	0.90191	0.714

Table 4.7 Fit results of K⁺ adsorption kinetics by KMAA hydrogel.

Isotherm model	Parameter	Initial pH	
		4	7
Pseudo-first order	k ₁ (min ⁻¹)	0.00044	0.04131
	q _e (mg/g)	136.82	130.28
	R ²	0.92195	0.935
Pseudo-second order	k ₂ (g/mg/min)	0.000467	0.04468
	q _e (mg/g)	150.41	144.08
	R ²	0.89644	0.89122

4.66 The effect of hydrogel dosage

In practical applications of adsorption materials, the quantity of added material is a critical parameter. As depicted in Figure 4.7, the initial sodium chloride concentration was 100 mg/L, and the amount of KMAA hydrogel added varied from 3 mg to 20 mg. The results reveal that with an increase in the amount of KMAA hydrogel, the removal efficiency of Na⁺ rose from 13% to 32%, while the exchange capacity for K⁺ decreased from 37% to 26%. Notably, at an addition of 3 mg of hydrogel, the adsorption capacity for Na⁺ and K⁺ exchange reached their lowest values of 20 mg/g and 25 mg/g, respectively. Conversely, at a higher addition of 20 mg, the KMAA hydrogel exhibited its

maximum adsorption capacity for Na^+ 60 mg/g and K^+ exchange 130 mg/g. These findings underscore a significant enhancement in adsorption and exchange performance with the increasing quantity of KMAA hydrogel. These results hold paramount importance for guiding the practical application of adsorption materials.

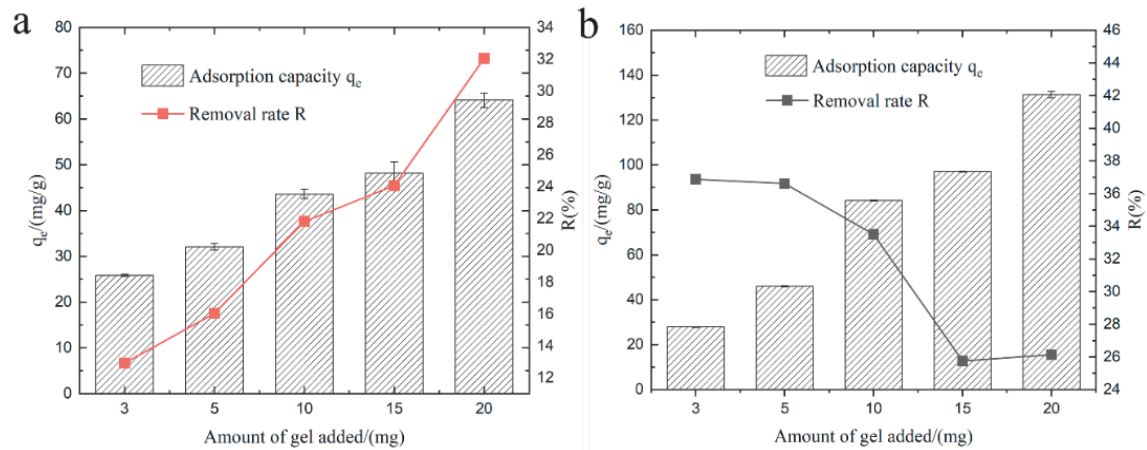


Figure 4.7 (a) Effect of different dosages of KMAA Hydrogel on Na^+ adsorption capacity and sodium removal efficiency. (b) effect of different dosages of KMAA hydrogel on K^+ exchange capacity and potassium exchange rate

4.7 Hydrogel Applied Soil Experiments.

4.7.1 Soil precipitation liquid experiment

The addition of KMAA hydrogel experiments in sodium-containing soils was studied, as shown in Figure 4.8. The concentration of sodium in the soil filtrate decreased with the addition of the hydrogel. In the control group without hydrogel and the group with added sodium, the concentration of sodium in the soil filtrate was 120 ppm and 116 ppm at pH=4 and pH 7, respectively. When 2% hydrogel was added, the concentration of sodium in the soil filtrate decreased to 88 ppm and 85 ppm, representing a reduction of 26%. Conversely, the concentration of potassium in the filtrate increased with the addition of the hydrogel. In the control group without hydrogel and the group with added sodium, the concentration of potassium in the soil filtrate was 184 ppm and 180 ppm at pH=4 and pH 7, respectively. When 2% hydrogel was added to the soil, the concentration of potassium in the filtrate increased to 317 ppm and 309 ppm, showing a 72% increase.

These results indicate that the addition of KMAA hydrogel effectively reduces the concentration of sodium in the soil filtrate while increasing the concentration of potassium. This suggests that the hydrogel acts as a selective adsorbent, selectively adsorbing sodium ions and promoting the release of potassium ions into the filtrate. This finding has significant implications for soil remediation and nutrient management in agricultural practices.

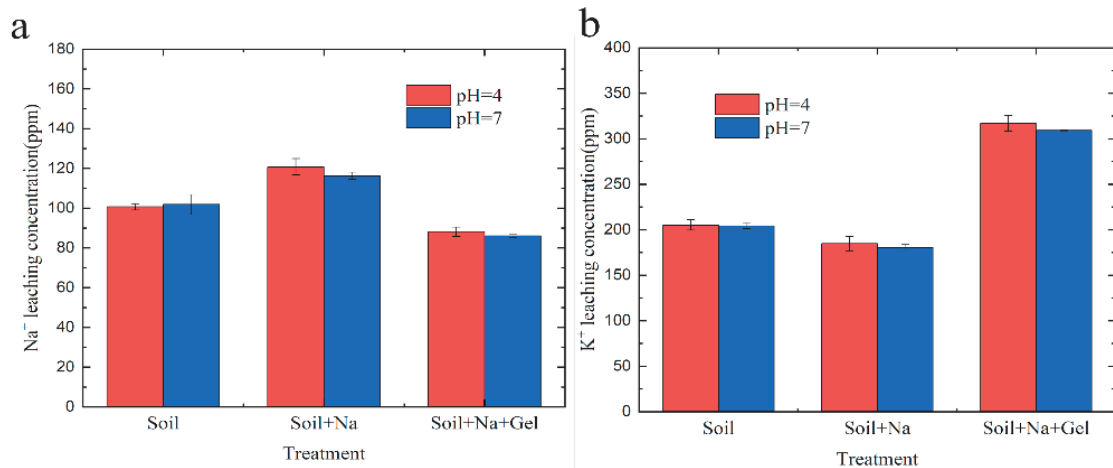


Figure 4.8 (a) Na⁺ leaching in soil solution at different pH levels. (b) K⁺ leaching in soil solution at different pH levels.

4.72. Effect of different gel amounts on precipitate.

The experiment of adding different amounts of gel to the soil and recording the concentration of sodium and potassium in the filtrate was studied. From Figure 4.9, it can be observed that, with an increase in the amount of hydrogel, the concentration of sodium in the soil filtrate did not decrease at pH=4 and pH 7. This suggests that sodium may have been replaced by other ions present in the soil. However, at pH=4 and pH 7, the concentration of potassium in the soil filtrate increased with the addition of the hydrogel. Sodium is known to be a harmful element for plant growth, while potassium is an essential nutrient for plant growth. By examining the sodium and potassium content in the filtrate, it is possible to determine the appropriate amount of hydrogel to add. This approach can help mitigate the harmful effects of sodium on plants while providing an adequate supply of potassium for plant growth.

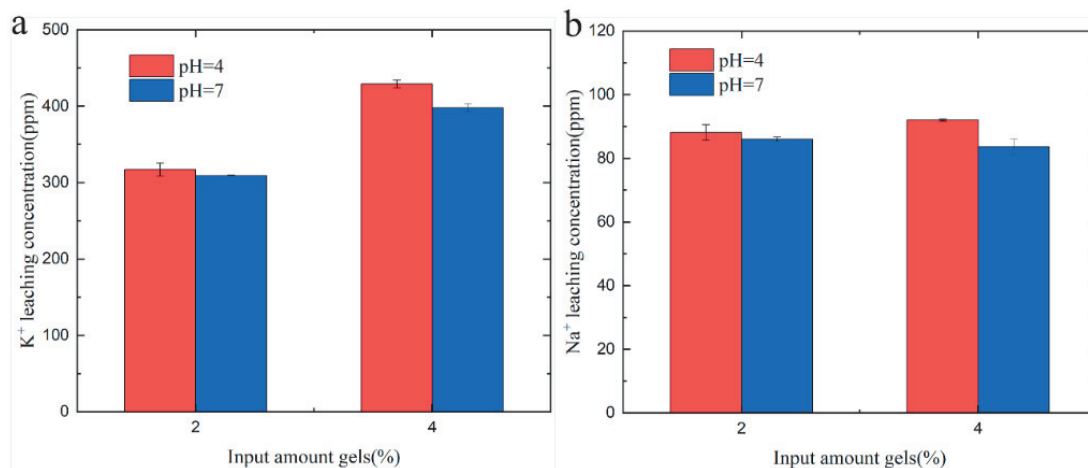


Figure 4.9 (a) K⁺ leaching in soil solution with varying gel amounts. (b) Na⁺ leaching in soil solution with varying gel amounts.

4.8 Structural Characteristics of Hydrogel

The chemical structure of KMAA was detected by Fourier transform infrared spectroscopy (FTIR). Figure 4.10 shows the infrared images of KMAA hydrogel before and after adsorption in 100ppm sodium chloride solution. The pristine KMAA hydrogel exhibited distinct absorption peaks: the C-C bond displayed a peak at 1128 cm⁻¹, the C=C double bond featured at 1517 cm⁻¹, the C=O moiety of the carboxyl group manifested at 1720 cm⁻¹, and the O-H band of the carboxyl group was evident at 3579 cm⁻¹. After adding the KMAA hydrogel to a 100-ppm sodium chloride solution for adsorption, the ensuing alterations were observed: the C-C single bond peak shifted to 1186 cm⁻¹, the C=C double bond peak shifted to 1537 cm⁻¹. The C=O peak of the carboxyl group exhibited a marginal redshift to 1639 cm⁻¹, the C-H peak of the methyl group emerged at 2927 cm⁻¹. The O-H peak of the carboxyl group exhibited a redshift to 3269 cm⁻¹[25]. These changes collectively suggest the adsorption of sodium ions from the solution by the hydrogel, coupled with the concomitant release of potassium species. These structural transformations can be attributed to the adsorptive interaction of the hydrogel in the sodium chloride solution, leading to an augmented intermolecular irregularity. Consequently, an enhanced hydrogen bonding effect between the solution and the hydrogel is invoked, thereby inducing the redshift phenomena observed in the O-H and C=O bands.

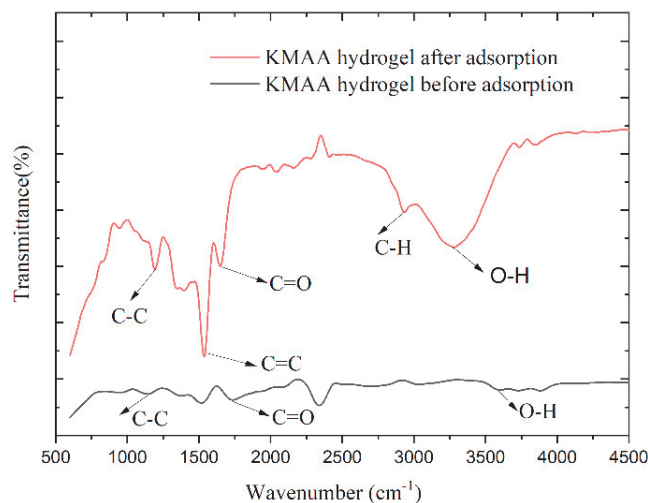


Figure 4.10 FTIR spectrum of gels before and after adsorption at 600-4500

4.9 Mechanism of KMAA Hydrogel Adsorbing Sodium and Exchanging Potassium

Potassium methacrylate polymer is a kind of high water-absorbing polymer, which will dissociate into carboxylate ions and potassium ions in solution, and the pH value will affect the dissociation degree of hydrogel. Potassium ions and sodium ions belong to the same group of elements, and their atomic radii are very similar. In the solution, through the form of cation exchange, sodium ions are adsorbed by the hydrogel, and potassium ions will be replaced into the aqueous solution. In addition, the stronger the acidity, the more H^+ value in the solution, which is more conducive to the release of potassium ions into the solution, but at the same time the amount of sodium adsorption is reduced [26]. The novelty of the experiment is an in-depth study of the experimental evaluation of the Na ion adsorption and potassium ion release of the KMAA hydrogel in acidic and neutral solutions, providing tangible evidence to bolster their potential utility in soil applications. Looking forward, KMAA hydrogels exhibit promise as a plausible potassium fertilizer for soil application, addressing the crucial need for essential potassium nutrients in plants. This application holds promise for various crops, encompassing maize cultivation, among others. Moreover, these hydrogels display the capability to mitigate mildly saline-alkaline soils to a certain extent, making them suitable for cultivating crops like rice. These

insights open fresh avenues and possibilities for innovating soil amendments within the realm of agricultural practices.

4.10 Conclusions

In this study, we successfully synthesized potassium polyacrylic acid (KMAA) hydrogel using free radical polymerization and investigated its pH-sensitive properties. The results demonstrated that the hydrogel exhibited remarkable efficiency in sodium ion adsorption under neutral conditions (pH=7), while it demonstrated significant potassium ion release under acidic conditions (pH=4). To gain a deeper understanding of the adsorption process, we employed Langmuir and Freundlich isotherm models, as well as pseudo-first order and pseudo-second-order kinetic models, to conduct a comprehensive analysis. For pH=7 conditions, the Langmuir model provided a good fit to the experimental data with a correlation coefficient of 0.98, indicating its suitability for describing the adsorption of sodium ions. On the other hand, for pH=4 conditions, the Freundlich model exhibited a better fit with a correlation coefficient of 0.99, suggesting its appropriateness for describing the exchange of potassium ions. Thermodynamic analysis revealed that the standard free energy change ΔG^θ for sodium adsorption and potassium exchange by KMAA hydrogel was negative at both pH=4 and pH=7, indicating the spontaneity and feasibility of these processes. Upon introducing 2% hydrogel in soil, we observed a 26% reduction in sodium concentration and a 72% increase in potassium concentration in the filtrate. [27, 28].

Reference

1. Bobowski, Nuala, Aaron Rendahl, and Zata Vickers. "Preference for Salt in a Food May Be Alterable without a Low Sodium Diet." *Food Quality and Preference* 39 (2015): 40-45.
2. Shen, D., H. Song, T. Zou, A. Raza, P. Li, K. Li, and J. Xiong. "Reduction of Sodium Chloride: A Review." *J Sci Food Agric* 102, no. 10 (2022): 3931-39.

3. Albuquerque, T. G., J. Santos, M. A. Silva, Mbpp Oliveira, and H. S. Costa. "An Update on Processed Foods: Relationship between Salt, Saturated and Trans Fatty Acids Contents." *Food Chem* 267 (2018): 75-82.
4. Wang, Baoqiang Zhang and Na. "Study on the Harm of Saline Alkali Land and Its Improvement Technology in China." *IOP Conf. Series: Earth and Environmental Science* 692 (2021): 042053.
5. Li, Jianguo, Lijie Pu, Mingfang Han, Ming Zhu, Runsen Zhang, and Yangzhou Xiang. "Soil Salinization Research in China: Advances and Prospects." *Journal of Geographical Sciences* 24, no. 5 (2014): 943-60.
6. Awad, Mahmoud E., Amr M. Farrag, Ashraf A. El-Bindary, Mohamed A. El-Bindary, and Hala A. Kiwaan. "Photocatalytic Degradation of Rhodamine B Dye Using Low-Cost Pyrofabricated Titanium Dioxide Quantum Dots-Kaolinite Nanocomposite." *Applied Organometallic Chemistry* 37, no. 7 (2023).
7. Yu, Xiaoping, Wanjing Cui, Feng Zhang, Yafei Guo, and Tianlong Deng. "Removal of Iodine from the Salt Water Used for Caustic Soda Production by Ion-Exchange Resin Adsorption." *Desalination* 458 (2019): 76-83.
8. MRAZEK, S. D. HILL AND R. V. "Vacuum Evaporation of Salt from Titanium Sponge." *Metallurgical Transactions* 5 (1972): 1974-53.
9. Sedighi, Mehdi, Mohammad Mahdi Behvand Usefi, Ahmad Fauzi Ismail, and Mostafa Ghasemi. "Environmental Sustainability and Ions Removal through Electrodialysis Desalination: Operating Conditions and Process Parameters." *Desalination* 549 (2023).
10. Krasnopeeva, E. L., G. G. Panova, and A. V. Yakimansky. "Agricultural Applications of Superabsorbent Polymer Hydrogels." *Int J Mol Sci* 23, no. 23 (2022).
11. Zheng, F., L. Chen, P. Zhang, J. Zhou, X. Lu, and W. Tian. "Carbohydrate Polymers Exhibit Great Potential as Effective Elicitors in Organic Agriculture: A Review." *Carbohydr Polym* 230 (2020): 115637.
12. Kabiri, K., H. Omidian, M. J. Zohuriaan-Mehr, and S. Doroudiani. "Superabsorbent Hydrogel Composites and Nanocomposites: A Review." *Polymer Composites* 32, no. 2 (2011): 277-89.

13. Rashidi, Masoud, Anne Marit Blokhus, and Arne Skauge. "Viscosity Study of Salt Tolerant Polymers." *Journal of Applied Polymer Science* (2010): NA-NA.
14. Guo, Y., R. Guo, X. Shi, S. Lian, Q. Zhou, Y. Chen, W. Liu, and W. Li. "Synthesis of Cellulose-Based Superabsorbent Hydrogel with High Salt Tolerance for Soil Conditioning." *Int J Biol Macromol* 209, no. Pt A (2022): 1169-78.
15. Zhang, Cui, J. Viridiana García Meza, Keqiang Zhou, Jiazhi Liu, Shaoxian Song, Min Zhang, Delong Meng, Jinhui Chen, Ling Xia, and Hu Xiheng. "Superabsorbent Polymer Used for Saline-Alkali Soil Water Retention." *Journal of the Taiwan Institute of Chemical Engineers* 145 (2023).
16. Xiong, Hongran, Hui Peng, Xi'e Ye, Yanrong Kong, Na Wang, Fenghong Yang, Ben-Hur Meni, and Ziqiang Lei. "High Salt Tolerance Hydrogel Prepared of Hydroxyethyl Starch and Its Ability to Increase Soil Water Holding Capacity and Decrease Water Evaporation." *Soil and Tillage Research* 222 (2022).
17. Tian, Haizhou, Sha Cheng, Jianghong Zhen, and Ziqiang Lei. "Superabsorbent Polymer with Excellent Water/Salt Absorbency and Water Retention, and Fast Swelling Properties for Preventing Soil Water Evaporation." (2021).
18. Shi, Yong, Jing Li, Jie Shao, Shurong Deng, Ruigang Wang, Niya Li, Jian Sun, Hua Zhang, Huijuan Zhu, Yunxia Zhang, Xiaojiang Zheng, Dazhai Zhou, Aloys Hüttermann, and Shaoliang Chen. "Effects of Stockosorb and Luquasorb Polymers on Salt and Drought Tolerance of *Populus Popularis*." *Scientia Horticulturae* 124, no. 2 (2010): 268-73.
19. Islam, S., F. Mohammad, M. H. Siddiqui, and H. M. Kalaji. "Salicylic Acid and Trehalose Attenuate Salt Toxicity in *Brassica Juncea* L. By Activating the Stress Defense Mechanism." *Environ Pollut* 326 (2023): 121467.
20. Mahmoud Fathy, Th. Abdel Moghny, Ahmed E. Awadallah, Moaz M. Abdou1, and AbdelHameed A-A El-Bellihi. "Development of Sulfonated Nanocomposites Ion Exchange Resin for Removal of Sodium Ions from Saline Water." *International Journal of Organic Chemistry* 4, no. 1 (2015): 62-69.
21. Holback, H., Y. Yeo, and K. Park. "Hydrogel Swelling Behavior and Its Biomedical Applications." In *Biomedical Hydrogels*, 3-24, 2011.

22. Arens, L., F. Weissenfeld, C. O. Klein, K. Schlag, and M. Wilhelm. "Osmotic Engine: Translating Osmotic Pressure into Macroscopic Mechanical Force Via Poly(Acrylic Acid) Based Hydrogels." *Advanced Science* 4, no. 9 (2017): 1-8.
23. Tran, Hai Nguyen, Sheng-Jie You, and Huan-Ping Chao. "Thermodynamic Parameters of Cadmium Adsorption onto Orange Peel Calculated from Various Methods: A Comparison Study." *Journal of Environmental Chemical Engineering* 4, no. 3 (2016): 2671-82.
24. Revellame, Emmanuel D., Dhan Lord Fortela, Wayne Sharp, Rafael Hernandez, and Mark E. Zappi. "Adsorption Kinetic Modeling Using Pseudo-First Order and Pseudo-Second Order Rate Laws: A Review." *Cleaner Engineering and Technology* 1 (2020).
25. Babic Radic, M. M., V. V. Filipovic, J. S. Vukovic, M. Vukomanovic, T. Ilic-Tomic, J. Nikodinovic-Runic, and S. L. Tomic. "2-Hydroxyethyl Methacrylate/Gelatin/Alginate Scaffolds Reinforced with Nano TiO₂ as a Promising Curcumin Release Platform." *Polymers (Basel)* 15, no. 7 (2023).
26. El-Bindary, Mohamed A., Mohamed G. El-Desouky, and Ashraf A. El-Bindary. "Metal–Organic Frameworks Encapsulated with an Anticancer Compound as Drug Delivery System: Synthesis, Characterization, Antioxidant, Anticancer, Antibacterial, and Molecular Docking Investigation." *Applied Organometallic Chemistry* 36, no. 5 (2022).
27. Yamashita, M., K. Tomita-Yokotani, H. Hashimoto, N. Sawaki, and M. Notoya. "Sodium and Potassium Uptake of *Ulva* – Application of Marine Macro-Algae for Space Agriculture." *Advances in Space Research* 43, no. 8 (2009): 1220-23.
28. Liu, Y., J. Wang, H. Chen, and D. Cheng. "Environmentally Friendly Hydrogel: A Review of Classification, Preparation and Application in Agriculture." *Sci Total Environ* 846 (2022): 157303.

Chapter 5 Conclusion

The main goal of this study is to investigate the efficiency of DMAPAA/DMAPAAQ composite hydrogels in removing cadmium from aqueous solutions and assess their potential application in cadmium-contaminated soil. Additionally, a comparative analysis was conducted to evaluate the impact of two types of hydrogels ionic hydrogels DMAPAA/DMAPAAQ, and non-ionic hydrogel DMAA on plant growth when utilized in soil for vegetable cultivation. Lastly, the ion exchange behavior of KMAA hydrogel for potassium ions was studied to gain insights into its applicability in rice cultivation in saline-alkali soil.

During the experimental phase, DMAPAA/DMAPAAQ hydrogels were successfully synthesized using free radical polymerization, and their adsorption performance was comprehensively evaluated under varying pH values and cadmium concentrations. The results demonstrated excellent cadmium capture performance of the hydrogel under neutral conditions, with a high correlation coefficient of 0.97 when fitted to the Langmuir model. This underscores the suitability of the Langmuir model in describing the cadmium capture process in the hydrogel. The experiments also revealed that under neutral conditions, cadmium ions were encapsulated by the precipitation of cadmium hydroxide formed by OH⁻ on the hydrogel, with OH⁻ generated through the protonation of tertiary amine in water.

Furthermore, the growth of Swiss chard under different cadmium stress conditions was observed after introducing hydrogels into the soil. Under low cadmium concentrations, the addition of 4% hydrogel resulted in a dry weight of Swiss chard reaching 0.765g, which was 2.5 times higher than that without hydrogel. As the cadmium concentration increased, the dry weight of Swiss chard showed an increasing trend after the addition of hydrogel, with a maximum of 0.503g and a minimum of 0.145g. Under high cadmium concentrations, the addition of hydrogel significantly reduced cadmium absorption by Swiss chard to undetectable levels.

In addition, a comparative study was conducted to assess the effects of two types of hydrogels (non-ionic hydrogel DMAA and ionic hydrogels DMAPAA/DMAPAAQ) on vegetable growth in contaminated soil. The results showed that the ionic hydrogel

exhibited significant advantages over the non-ionic hydrogel in vegetable cultivation. The ionic hydrogel had the ability to absorb nutrients such as nitrate and phosphate ions in the soil that are not easily absorbed by the soil, and slowly release these nutrients through ion exchange, thereby promoting vegetable growth. In contrast, the incorporation of non-ionic hydrogel DMAA resulted in a decrease in vegetable dry weight.

Furthermore, the potassium polyacrylate (KMAA) hydrogel was also studied. The experimental results showed significant adsorption efficiency of the hydrogel for sodium ions under neutral conditions, and significant release of potassium ions under acidic conditions. Temperature analysis indicated that the adsorption and exchange processes of sodium and potassium by the hydrogel were spontaneous and feasible. After introducing 2% hydrogel into the soil, the sodium concentration decreased by 26%, while the potassium concentration increased by 72%.

Future research will primarily focus on two aspects. Firstly, we plan to select natural polymers and apply them to soil to investigate their effectiveness in removing heavy metal ions. In this study, we aim to induce flocculation of the hydrogel in soil-water solutions through agitation, followed by effective separation of soil and hydrogel through filtration. Secondly, we will concentrate on studying the effects of ionic hydrogels, non-ionic hydrogels, and amphoteric hydrogels on vegetable cultivation. We will evaluate the promoting effects of these hydrogels on plant growth and delve into the mechanisms of water molecules and elements within them. This will help determine whether water molecules or elements are more crucial under hydrogel application, thereby providing a strong scientific basis for further optimizing hydrogel application in cultivation.

List of publications

Journal Articles

1. Jin Huang, Takehiko Gotoh, Satoshi Nakai, Akihiro Ueda. A Novel Composite Hydrogel material for sodium removal and potassium provision. *Polymers*. 2023,28;15(17):3568
2. Jin Huang, Takehiko Gotoh, Satoshi Nakai and Akihiro Ueda, Dual benefits of hydrogel remediation of cadmium-contaminated water or soil and promotion of vegetable growth under cadmium stress. *Plants*. 2023, 12(24), 4115
3. Jin Huang, Takehiko Gotoh, Satoshi Nakai, and Akihiro Ueda, Functional hydrogel promotes vegetable growth in cadmium-contaminated soil. *Gels*. Under review

International Conferences

1. Jin Huang, Takehiko Gotoh, Satoshi Nakai, Akihiro Ueda. Functional hydrogel promotes vegetable growth in cadmium-contaminated soil. 20th Asian Pacific Confederation of Chemical Engineering (APCChE) 2023 Congress September 4-8, 2023 · SMX Convention Center Manila, Pasay City, Philippines (Chapter 3)

List of Figures

Chapter 1

Figure 1.1 Distribution data map of heavy metal content in agricultural soil in China

Figure 1.2 Comparison of different heavy metal contaminated soil remediation methods. Soil remediation methods can be broadly divided into three categories: physical, chemical, and biological.

Figure 1.3 Diagram of the adsorption mechanism of microorganisms

Figure 1.4 Different types of adsorption isotherm models.

Figure 1.5 Different methods for synthesizing hydrogels

Figure 1.6 Adsorption mechanism of heavy metals by functional groups containing N or O atoms.

Figure 1.7 The mechanism process based on the interaction between adsorbate and adsorbent.

Chapter 2

Figure 2.1 (a) Main elements contained in soil, (b) Swelling degree of hydrogel in water and soil.

Figure 2.2 Effect of hydrogel adsorption capacity on cadmium ions at different pH values.

Figure 2.3 Hydrogel isothermal adsorption curve for cadmium ions at pH=5.7, 7.3 (a) Langmuir simulation fitting curve (b) Freundlich simulation fitting curve.

Figure 2.4 adsorption isotherm fit curves of hydrogel at different temperatures (a) Cd^{2+} Adsorption Langmuir model simulated fit curve, (b) Cd^{2+} adsorption Freundlich model simulated fit curve.

Figure 2.5 Pseudo-first-order and pseudo-second-order dynamic model diagrams of cadmium adsorption by hydrogel; (b) Hydrogel adsorption and diffusion model

Figure 2.6 FTIR spectrum of hydrogel after adsorption at 600-4500

Figure 2.7 Physical image of vegetable growth, (a), (b), and (c); the addition of hydrogel is 0%, 2%, 4%. From left to right, the amount of cadmium added is 500, 50, 5 mg/kg, 0 mg/kg.

Figure 2.8 Dry weight of Swiss chard shoots.

Figure 2.9 Cadmium absorption by Swiss chard shoots.

Figure 2.10 Contents of various elements in vegetable leaves: (a) Potassium; (b) Phosphorus; (c) Magnesium; (d) Iron; (e) Manganese; (f) Zinc; (g) Copper; (h) Calcium; (i) Sodium.

Figure 2.11 Mechanism diagram of hydrogel adsorption of heavy metals.

Chapter 3

Figure 3.1 Elements in Soil.

Figure 3.2 pH value of soil.

Figure 3.3 Cadmium precipitation values of soil in different pH solutions.

Figure 3.4 Physical image of vegetable growth, (a), (b), and (c) the addition of hydrogel is 0%, 2%, 4%. From left to right, the amount of cadmium added is 0, 2mg/kg, 500mg/kg.

Figure 3.5 Physical image of vegetable growth, (a) from left to right the DMAPAA/DMAPAAQ hydrogel addition amount is 4%, 2%, 0%. (b) from left to right the DMAA hydrogel addition amount is 4%, 2%, 0%.

Figure 3.6 The amount of Cd absorbed by vegetables.

Figure 3.7 Contents of various trace elements in vegetable leaves: (a) Potassium; (b) Phosphorus; (c) Magnesium; (d) Iron; (e) Manganese; (f) Zinc; (g) Copper; (h) Calcium; (i) Sodium.

Figure 3.8 Dry weight of Swiss chard shoots.

Figure 3.9 The removal mechanism of heavy metal cadmium by DMAPAA/DMAPAAQ composite hydrogel.

Chapter 4

Figure 4.1 Schematic diagram of the mechanism of KMAA hydrogel to adsorb sodium and provide potassium in water and soil.

Figure 4.2 (a) water retention capability of hydrogel in soil, (b) swelling behavior of hydrogel in NaCl solution.

Figure 4.3 (a) Na⁺ removal efficiency and K⁺ exchange rate of hydrogel under various initial NaCl concentrations. (b) effect of different pH values on Na⁺ adsorption and K⁺ exchange capacity of hydrogel.

Figure 4.4 isothermal adsorption of Na^+ adsorption and K^+ exchange by hydrogel at pH=4 and 7 (a) Langmuir model simulated fit curve, (b) Freundlich model simulated fit curve.

Figure 4.5 adsorption isotherm fit curves of KMAA hydrogel at different temperatures (a) Na^+ Adsorption Langmuir model simulated fit curve, (b) Na^+ adsorption Freundlich model simulated fit curve, (c) K^+ exchange Langmuir model simulated fit curve, (d) K^+ exchange Freundlich model simulated fit curve.

Figure 4.6 (a) dynamic modeling of pseudo-first order and pseudo-second-order Na^+ Adsorption by KMAA hydrogel at Initial NaCl concentration of 100 mg/L; (b) dynamic modeling of pseudo-first-order and pseudo-second-order K^+ exchange by KMAA hydrogel at initial NaCl concentration of 100 mg/L

Figure 4.7 (a) Effect of different dosages of KMAA Hydrogel on Na^+ adsorption capacity and sodium removal efficiency. (b) effect of different dosages of KMAA hydrogel on K^+ exchange capacity and potassium exchange rate

Figure 4.8 (a) Na^+ leaching in soil solution at different pH levels. (b) K^+ leaching in soil solution at different pH levels.

Figure 4.9 (a) K^+ leaching in soil solution with varying gel amounts. (b) Na^+ leaching in soil solution with varying gel amounts.

Figure 4.10 FTIR spectrum of gels before and after adsorption at 600-4500

List of Tables

Table 1.1 Agricultural land soil pollution risk screening

Table 1.2 Heavy metal pollution standards

Table 2.1 Synthesis condition of the DMAPAA/DMAPAAQ hydrogel

Table 2.2 Parameters of Langmuir and Freundlich isotherm model by DMAPAA/DMAPAAQ gel at pH=5.7 and pH=7.3 cadmium adsorption capacity

Table 2.3 DMAPAA/DMAPAAQ hydrogel adsorption thermodynamic parameters for Cadmium

Table 2.4 Fit results of Cd^{2+} adsorption kinetics by DMAPAA/DMAPAAQ hydrogel.

Table 3.1 Synthesis condition of the DMAPAA/DMAPAAQ hydrogel.

Table 3.2 Synthesis condition of the DMAA hydrogel.

Table 4.1 Synthesis condition of the KMAA hydrogel

Table 4.2 Parameters of Langmuir and Freundlich isotherm model by KMAA gel at pH=4 and pH=7 sodium ion adsorption capacity

Table 4.3 Parameters of Langmuir and Freundlich isotherm model by KMAA gel at pH=4 and pH=7 potassium ion exchange capacity

Table 4.4 KMAA hydrogel adsorption thermodynamic parameters for sodium

Table 4.5 KMAA hydrogel exchange thermodynamic parameters for potassium.

Table 4.6 Fit results of Na^{+} adsorption kinetics by KMAA hydrogel.

Table 4.7 Fit results of K^{+} adsorption kinetics by KMAA hydrogel.

Acknowledgments

With immense gratitude, I write this letter to express my heartfelt appreciation for your dedicated guidance and support over the years.

Firstly, I would like to sincerely thank my mentors Professor Goto and Professor Nakai. You have always been a guiding light on my academic path, pointing me the way forward. Your profound knowledge, rigorous academic attitude, and passion for research have greatly benefited me. I am grateful to Mr. Ueda for teaching me experimental techniques, which have taught me how to grow vegetables, rice, and plant digestion methods.

Secondly, I would like to express my gratitude to all the experts of the evaluation committee. Your valuable opinions and suggestions have continuously improved and strengthened my research work. I will carefully listen to your feedback and strive to improve my academic level. I also want to thank all the students in the laboratory.

Thanks to Tatsuya FUNABIKI, for taking me to print the poster for the international academic conference. Thank you, Song Yu, for teaching me how to use the ICP instrument. Thank you, Tatsumi KAGAYAMA, for teaching me how to use the infrared instrument. Thank you, Yukine MITARAI, for teaching me how to use the freeze-drying machine. Thank you to the paper editing center for helping me revise my paper. Once again, I express my gratitude to everyone in the laboratory who has assisted me.

Lastly, I want to thank my family and friends. It is because of your endless care and encouragement during my time away from home that I have gained unwavering confidence and courage to face all difficulties and challenges. As I embark on a new phase of life, I will treasure your teachings and support, and strive to be a joyful researcher.

Huang jin
February 2024